Changes in belowground biodiversity during ecosystem development

Manuel Delgado-Baquerizo[a,b,1], Richard D. Bardgett[c], Peter M. Vitousek[d], Fernando T. Maestre[b], Mark A. Williams[e], David J. Eldridge[f], Hans Lambers[g], Sigrid Neuhauser[h], Antonio Gallardo[i], Laura García-Velázquez[b,i], Osvaldo E. Sala[j,k,l], Sebastián R. Abades[m], Fernando D. Alfaro[m], Asmeret A. Berhe[n], Matthew A. Bowker[o], Courtney M. Currier[j,k,l], Nick A. Cutler[p], Stephen C. Hart[n,q], Patrick E. Hayes[g,r,2], Zeng-Yei Hseu[s], Martin Kirchmair[h], Victor M. Peña-Ramírez[t], Cecilia A. Pérez[u], Sasha C. Reed[v], Fernanda Santos[n], Christina Siebe[t], Benjamin W. Sullivan[w], Luis Weber-Grullon[j,k,l], and Noah Fierer[a,x]

[a]Cooperative Institute for Research in Environmental Sciences, University of Colorado, Boulder, CO 80309; [b]Departamento de Biología y Geología, Física y Química Inorgánica, Escuela Superior de Ciencias Experimentales y Tecnología, Universidad Rey Juan Carlos, Calle Tulipán Sin Número, 28933 Móstoles, Spain; [c]School of Earth and Environmental Sciences, The University of Manchester, M13 9PT Manchester, United Kingdom; [d]Department of Biology, Stanford University, Stanford, CA 94305; [e]Department of Horticulture, Virginia Polytechnic Institute and State University, Blacksburg, VA 24061; [f]Centre for Ecosystem Studies, School of Biological, Earth and Environmental Sciences, University of New South Wales, Sydney, NSW 2052, Australia; [g]School of Biological Sciences, The University of Western Australia, Crawley (Perth), WA 6009, Australia; [h]Institute of Microbiology, University of Innsbruck, 6020 Innsbruck, Austria; [i]Departamento de Sistemas Físicos, Químicos y Naturales, Universidad Pablo de Olavide, 41013 Sevilla, Spain; [j]Global Drylands Center, Arizona State University, Tempe, AZ 85287; [k]School of Life Sciences, Arizona State University, Tempe, AZ 85287; [l]School of Sustainability, Arizona State University, Tempe, AZ 85287; [m]GEMA Center for Genomics, Ecology & Environment, Universidad Mayor, Huechuraba, Santiago 8580745, Chile; [n]Department of Life and Environmental Sciences, University of California, Merced, CA 95343; [o]School of Forestry, Northern Arizona University, Flagstaff, AZ 86011; [p]School of Geography, Politics and Sociology, Newcastle University, Newcastle upon Tyne NE1 7RU, United Kingdom; [q]Sierra Nevada Research Institute, University of California, Merced, CA 95343; [r]Centre for Microscopy, Characterisation and Analysis, The University of Western Australia, Perth, WA 6009, Australia; [s]Department of Agricultural Chemistry, National Taiwan University, 10617 Taipei, Taiwan; [t]Instituto de Geología, Universidad Nacional Autónoma de México, Ciudad Universitaria, México DF CP 04510, México; [u]Instituto de Ecología y Biodiversidad, Universidad de Chile, Las Palmeras 3425, Santiago, Chile; [v]Southwest Biological Science Center, US Geological Survey, Moab, UT 84532; [w]Department of Natural Resources and Environmental Science, University of Nevada, Reno, NV 89557; and [x]Department of Ecology and Evolutionary Biology, University of Colorado, Boulder, CO 80309

Edited by David Tilman, University of Minnesota, St. Paul, MN, and approved February 8, 2019 (received for review October 26, 2018)

Belowground organisms play critical roles in maintaining multiple ecosystem processes, including plant productivity, decomposition, and nutrient cycling. Despite their importance, however, we have a limited understanding of how and why belowground biodiversity (bacteria, fungi, protists, and invertebrates) may change as soils develop over centuries to millennia (pedogenesis). Moreover, it is unclear whether belowground biodiversity changes during pedogenesis are similar to the patterns observed for aboveground plant diversity. Here we evaluated the roles of resource availability, nutrient stoichiometry, and soil abiotic factors in driving belowground biodiversity across 16 soil chronosequences (from centuries to millennia) spanning a wide range of globally distributed ecosystem types. Changes in belowground biodiversity during pedogenesis followed two main patterns. In lower-productivity ecosystems (i.e., drier and colder), increases in belowground biodiversity tracked increases in plant cover. In more productive ecosystems (i.e., wetter and warmer), increased acidification during pedogenesis was associated with declines in belowground biodiversity. Changes in the diversity of bacteria, fungi, protists, and invertebrates with pedogenesis were strongly and positively correlated worldwide, highlighting that belowground biodiversity shares similar ecological drivers as soils and ecosystems develop. In general, temporal changes in aboveground plant diversity and belowground biodiversity were not correlated, challenging the common perception that belowground biodiversity should follow similar patterns to those of plant diversity during ecosystem development. Taken together, our findings provide evidence that ecological patterns in belowground biodiversity are predictable across major globally distributed ecosystem types and suggest that shifts in plant cover and soil acidification during ecosystem development are associated with changes in belowground biodiversity over centuries to millennia.

soil biodiversity | ecosystem development | global scale | acidification | soil chronosequences

Belowground organisms play critical roles in maintaining the rates and stability of multiple ecosystem processes, including plant productivity, decomposition, and nutrient cycling (1–3). Complementary ecological theories have been proposed to explain belowground biodiversity patterns, including theories related to aboveground and belowground resource availability, nutrient stoichiometry, and abiotic environmental factors (1–12) (*SI Appendix*, Table S1). However, and despite a longstanding interest in the topic (4–8), the patterns in belowground biodiversity as soils develop over centuries to millennia (pedogenesis), as well as the

Significance

We do not know how and why belowground biodiversity may change as soils develop over centuries to millennia, hampering our ability to predict the myriad of ecosystem processes regulated by belowground organisms under changing environments. We conducted a global survey of 16 soil chronosequences spanning a wide range of ecosystem types and found that in less productive ecosystems, increases in belowground biodiversity followed increases in plant cover, but in more productive ecosystems, acidification during soil development was often associated with declines in belowground biodiversity. The biodiversity of multiple soil organisms exhibited similar patterns over time, but in contrast to expectations, changes in plant diversity were not associated with corresponding changes in belowground biodiversity.

Author contributions: M.D.-B. and N.F. designed research; M.D.-B., R.D.B., P.M.V., F.T.M., M.A.W., D.J.E., H.L., S.N., A.G., L.G.-V., O.E.S., S.R.A., F.D.A., A.A.B., M.A.B., C.M.C., N.A.C., S.C.H., P.E.H., Z.-Y.H., M.K., V.M.P.-R., C.A.P., S.C.R., F.S., C.S., B.W.S., L.W.-G., and N.F. performed research; M.D.-B., F.T.M., A.G., L.G.-V., and N.F. contributed new reagents/analytic tools; M.D.-B., R.D.B., P.M.V., F.T.M., M.A.W., D.J.E., H.L., S.N., A.G., O.E.S., and N.F. analyzed data; and M.D.-B. and N.F. wrote the paper, with all authors contributing to the drafts.

The authors declare no conflict of interest.

This article is a PNAS Direct Submission.

Data deposition: The primary data used in this paper have been deposited in Figshare: https://figshare.com/s/0dc27c87f09d0a1c6ca3 (doi: 10.6084/m9.figshare.7556675).

[1]To whom correspondence should be addressed. Email: m.delgadobaquerizo@gmail.com.

[2]Present address: Crop, Livestock, and Environment Division, Japan International Research Center for Agricultural Sciences, Tsukuba, 305-8656 Ibaraki, Japan.

This article contains supporting information online at www.pnas.org/lookup/suppl/doi:10.1073/pnas.1818400116/-/DCSupplemental.

environmental factors responsible for those patterns, remain largely unresolved. It is also unclear whether belowground biodiversity follows a similar trend to that of plant diversity during pedogenesis (4–6), which often exhibits a positive or hump-shaped relationship attributed to changes in abiotic environmental factors (e.g., acidification) and soil resource availability (e.g., soil phosphorus) as soils develop (4–6). Improving our knowledge of the mechanisms driving changes in belowground biodiversity during pedogenesis is critical for predicting both global ecological patterns and the many ecosystem processes regulated by belowground organisms (1–3).

There are two main reasons why we lack a mechanistic understanding of how belowground biodiversity changes during pedogenesis. First, studies of belowground biodiversity patterns with pedogenesis have mostly been conducted on a few individual soil chronosequences (13–17), with such work focusing mainly on a single group of belowground organisms, such as bacteria (16), fungi (18) or protists (19), or on changes in microbial biomass and community structure (17). Although such studies provide valuable information, pedogenesis often follows different trajectories depending on such factors as soil parent material and climate (7, 8, 19–21). Moreover, multiple taxa should be considered in concert to achieve a holistic understanding of how belowground biodiversity changes during pedogenesis. Second, most studies reported to date have focused on changes in belowground biodiversity during initial stages of primary succession (i.e., years to centuries) (13, 22), with few studies evaluating effects over much longer time scales (i.e., from centuries to thousands or millions of years) (13, 15, 16). The fate of belowground biodiversity is expected to differ between early and late stages of pedogenesis, because older ecosystems may enter a retrogressive phase (19, 23–25). This stage of ecosystem development is typically characterized by reduced resource availability [e.g., soil phosphorus (P), carbon (C), plant biomass], altered soil nutrient stoichiometry [e.g., increased nitrogen (N):P ratios], and soil acidification (19, 23–26), which could change the long-term development of belowground biodiversity.

Here we considered multiple complementary ecological theories, based on aboveground and belowground resource availability, nutrient stoichiometry, and abiotic environmental factors (*SI Appendix*, Table S1), to identify the predominant mechanisms driving the changes in belowground biodiversity during pedogenesis across ecosystem types (*SI Appendix*, *Materials and Methods*). Toward this aim, we conducted soil and vegetation surveys across 16 globally distributed chronosequences ranging in age from hundreds to millions of years and encompassing a wide range of climatic conditions (tropical, temperate, continental, polar, and arid), vegetation types (grasslands, shrublands, forests, and croplands), and chronosequence origins (volcanic, sedimentary, dunes, and glaciers) (Fig. 1*A* and *SI Appendix*, Tables S2 and S3). The diversity of soil organisms (bacteria, fungi, protists, and invertebrates) was measured via marker gene amplicon sequencing. Data on the dominant bacterial, fungal, protist, and invertebrate taxa detected are provided in *SI Appendix*, Table S4.

Results and Discussion

Species richness (i.e., number of phylotypes) and Shannon diversity of soil bacteria, fungi, protists, and invertebrates were highly correlated (*SI Appendix*, Figs. S1–S4). Consequently, we used richness as our metric of diversity in further analyses. Importantly, we found that the richness ("diversity" hereinafter) of soil bacteria, fungi, protists, and invertebrates across each chronosequence was generally well correlated over time (*SI Appendix*, Tables S5 and S6), and so we used an integrated index of belowground biodiversity to evaluate changes in diversity with pedogenesis (*SI Appendix*, *Material and Methods*). This index was positively and significantly correlated with the biodiversity of the major groups of organisms in >92% of the cases (59 out of 64 cases; *SI Appendix*, Table S6). The strong positive correlations among soil bacteria, fungi, protists, and invertebrates suggest that the changes in the biodiversity of multiple soil organisms during pedogenesis are driven by similar ecological factors.

We then identified the form of the relationship between chronosequence stage and belowground biodiversity within each chronosequence. For this, we considered the three most common regression models used to evaluate changes in soil attributes during pedogenesis: linear, quadratic, and cubic (4–6, 17, 27) (*SI Appendix*, *Material and Methods* and Table S7). We found a high degree of variation in the observed patterns across the 16 soil chronosequences (Fig. 2). In most cases, belowground biodiversity took thousands to millions of years to reach its maximum as it followed either a positive (linear or cubic: seven cases) or hump-shaped (quadratic; five cases) relationship with chronosequence stage (Fig. 2 and *SI Appendix*, Figs. S5–S8 and Table S7). Changes in belowground biodiversity during pedogenesis were not influenced by including chronosequences of very different age ranges (from thousands to millions of years), as several patterns were found within each soil age range (Fig. 2). We found similar results when evaluating the relationships between chronosequence stage and the diversity of soil bacteria, fungi, protists, and invertebrates individually (*SI Appendix*, Figs. S5–S8 and Table S7). In support of this, the dissimilarity in belowground community composition consistently increased with chronosequence stage (*SI Appendix*, Figs. S9–S13 and Table S8), which suggests that belowground communities become more dissimilar as pedogenesis proceeds. Further discussions about the changes in belowground community composition during ecosystem development, based on the results reported below, are available in *SI Appendix*, *Extended Discussion*.

Perennial plant diversity ("plant diversity" hereinafter) was not correlated with belowground biodiversity in 75% of the studied soil chronosequences (12 out of 16 cases; *SI Appendix*, Fig. S14). Furthermore, and unlike previously reported positive relationships between chronosequence stage and plant diversity (4–6), we detected a high degree of variation in the responses of plant diversity to pedogenesis (*SI Appendix*, Fig. S15; *SI Appendix*, Table S9 presents the most important environmental factors associated with perennial plant diversity). In particular, we found positive (25% of cases), negative (18% of cases), and neutral (57% of cases) relationships between the diversity of plants and belowground communities. Matching patterns of plant and soil biodiversity were not associated with any particular type of ecosystem (*SI Appendix*, Table S9). In contrast to expectations (4–6), which have developed largely from work on individual soil chronosequences typically located in temperate environments, the observed changes in plant diversity during pedogenesis were highly variable. We acknowledge that directly comparing patterns in the diversity of plants and soil organisms is not straightforward, due to differences in spatial scales, organism sizes, and taxonomic resolution; however, despite this important caveat, we still compared soil and plant diversity patterns during pedogenesis (*SI Appendix*, Figs. S14 and S15; compare with Fig. 2). Our findings challenge the common expectation that belowground biodiversity mirrors aboveground diversity during pedogenesis (4, 9, 16).

We then sought to identify the most important environmental factors associated with belowground biodiversity across the 16 chronosequences studied (*Materials and Methods*). We first used random forest modeling to identify those environmental factors that change during pedogenesis related to each chronosequence (*SI Appendix*, Fig. S16). Environmental factors included aboveground (plant cover) and belowground (soil total organic C and available P) resource availability, nutrient stoichiometry (soil C:N and N:P ratios, calculated from soil total organic C, total N, and total P) and other soil abiotic factors (soil salinity, pH, and texture: % clay + silt). These factors were then selected as potential predictors of changes in belowground biodiversity and the diversity of individual taxonomic groups during pedogenesis. Statistical modeling was conducted independently for each of the 16 soil chronosequences. The rationale for including soil

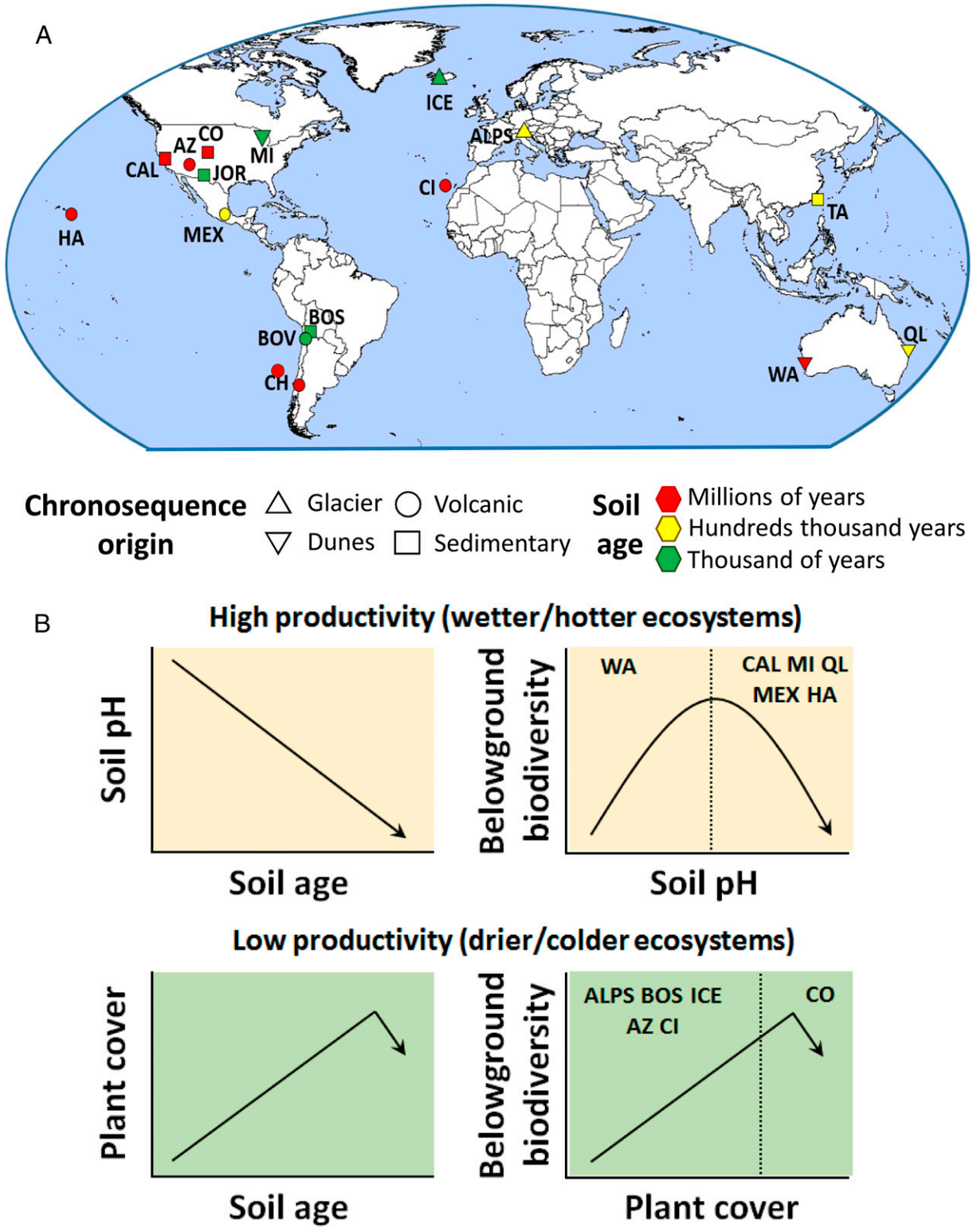

Fig. 1. Geographical distribution and major patterns showing the fate of belowground biodiversity during pedogenesis. Belowground biodiversity is defined as the standardized average of the diversity of soil bacteria, fungi, protists, and invertebrates. (*A*) Locations of the 16 soil chronosequences (87 plots) included in this study. (*B*) A conceptual figure summarizing the major ecological patterns observed (data provided in Figs. 2 and 3). Acronyms for each chronosequence are listed in *SI Appendix*, Table S2. Correlations between pH and plant cover with belowground diversity across sites are shown in *SI Appendix*, Fig. S26.

available P and plant cover in our models is provided in *SI Appendix*, *Environmental Predictors of Belowground Biodiversity During Pedogenesis*.

Our random forest analyses provided evidence that plant cover and soil pH are the most important statistical predictors of changes in belowground biodiversity during pedogenesis (Fig. 3

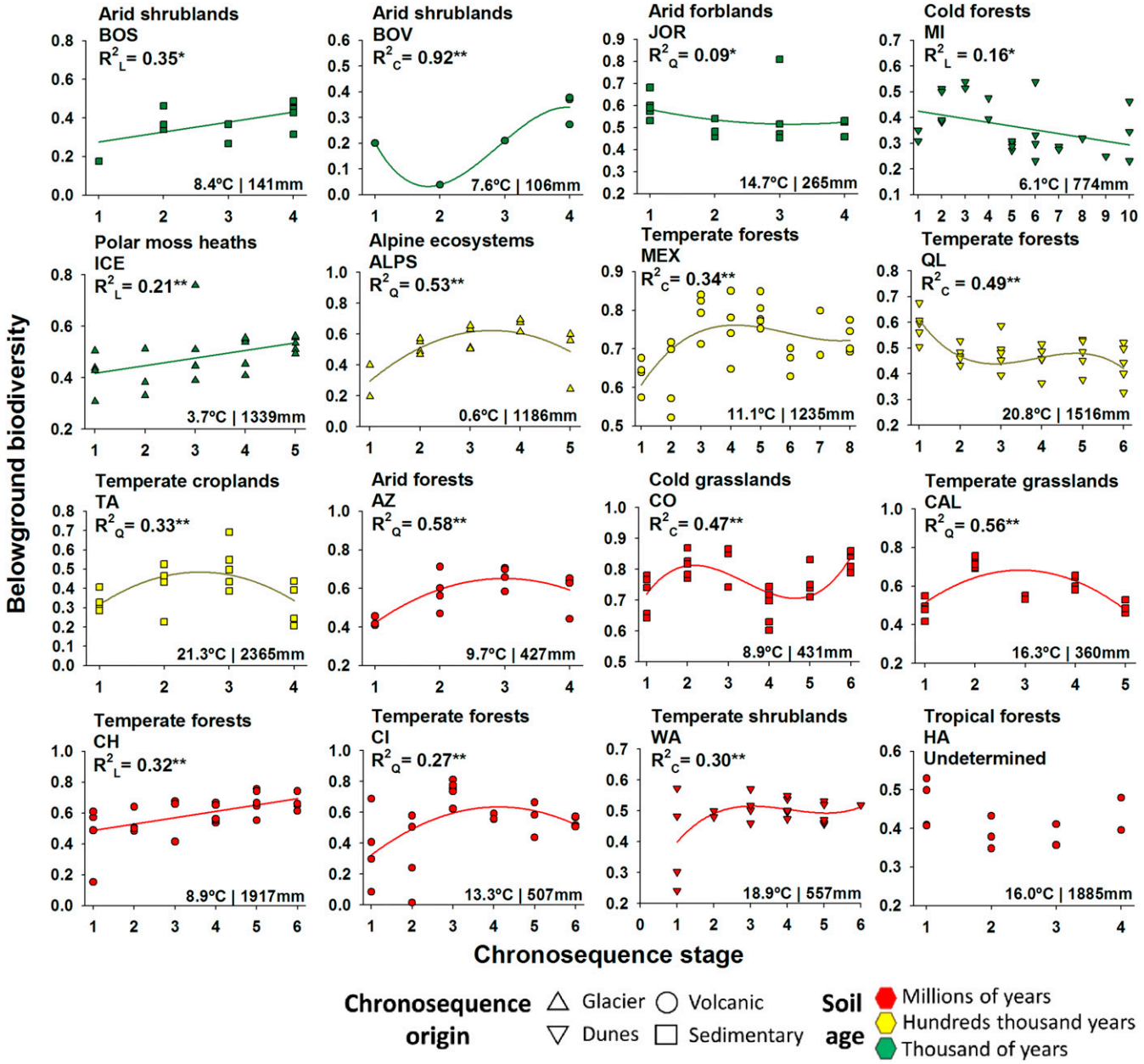

Fig. 2. Changes in belowground biodiversity during pedogenesis. Shown are the relationships between chronosequence stage and belowground biodiversity across 16 globally distributed soil chronosequences. $*P \leq 0.05$; $**P < 0.01$.

and *SI Appendix*, Figs. S17–S23). We then used hierarchical clustering to test the importance of environmental factors in predicting belowground biodiversity (from random forest modeling) and to classify our 16 soil chronosequences by the major ecological patterns associated with the observed changes in belowground biodiversity during pedogenesis. Most chronosequences were clustered by either soil pH or plant cover (6 out of 16 in both cases) as the major factors associated with the changes in belowground biodiversity during pedogenesis (Fig. 3 and *SI Appendix*, Fig. S24). Interestingly, on average, locations for chronosequences in which belowground biodiversity was associated with plant cover also had significantly lower ecosystem productivity and harsher climatic conditions (i.e., lower temperature and precipitation) compared with those in which belowground biodiversity was associated with soil pH (*SI Appendix*, Fig. S25). In other words, soil chronosequences in which belowground biodiversity was positively correlated with plant cover had lower ecosystem productivity and corresponded with colder and drier ecosystems (*SI Appendix*, Figs. S24 and S25). In these ecosystems, increases in plant cover during pedogenesis were typically associated with increases in belowground biodiversity (Figs. 1*B* and 3 and *SI Appendix*, Tables S10 and S11). The sole exception to this pattern was a very old (millions of years) chronosequence located in semiarid grasslands in Colorado, in which a reduction in plant cover late in pedogenesis was associated with reductions in belowground biodiversity (Figs. 1*B* and 3).

Conversely, our findings indicate that on average, chronosequences in which soil pH was strongly correlated with changes in belowground biodiversity during pedogenesis had higher ecosystem productivity, corresponding with warmer and wetter ecosystems (*SI Appendix*, Figs. S24 and S25). In these ecosystems, a drop in soil pH during pedogenesis was associated (Fig. 3*A*) with a reduced number of soil taxa in most cases (Figs. 1*B* and 3 and *SI*

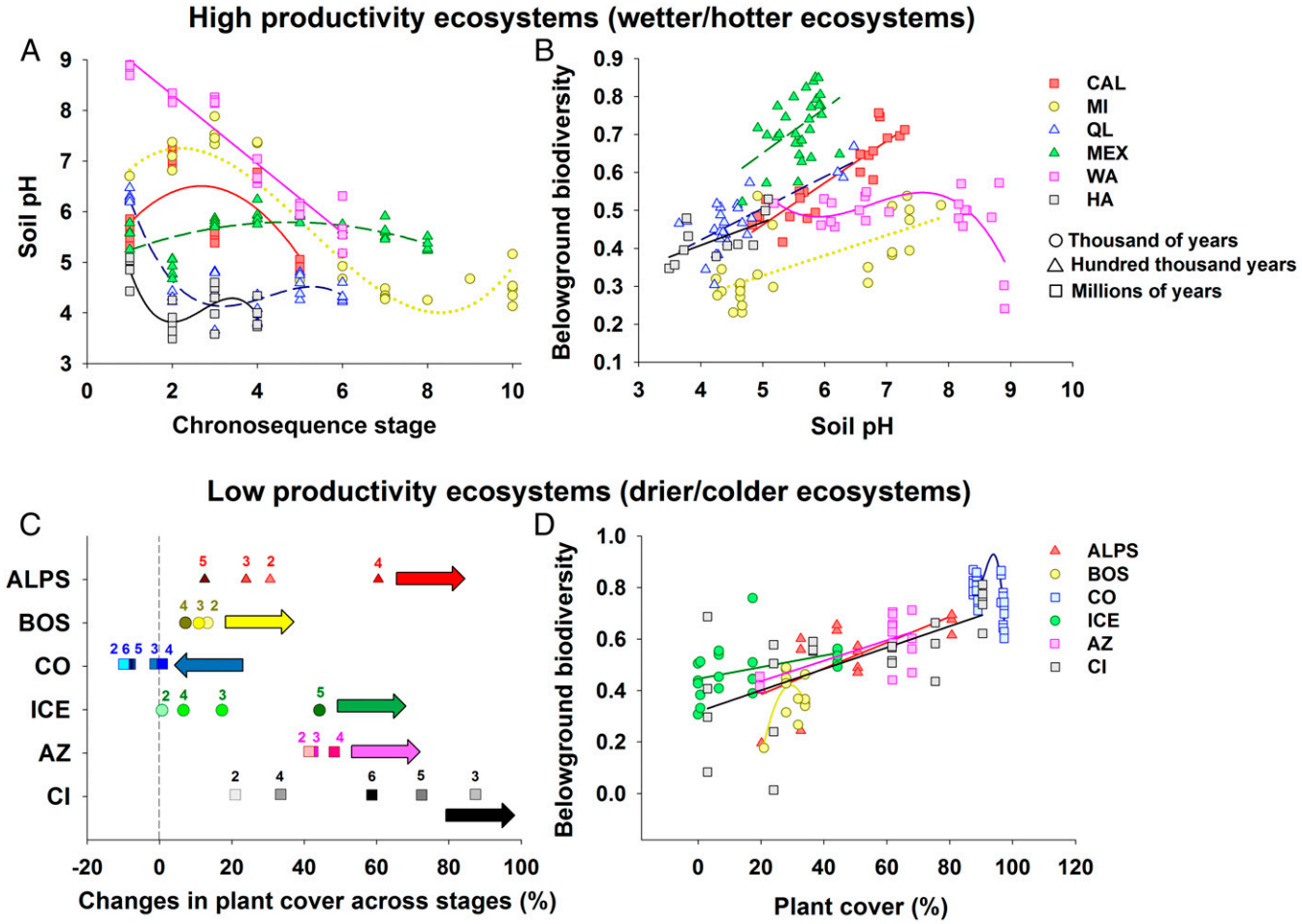

Fig. 3. Major ecological drivers of the fate of belowground biodiversity during pedogenesis. (*A* and *B*) High-productivity ecosystems. (*C* and *D*) Low-productivity ecosystems. Statistical support for these patterns is provided in *SI Appendix*, Tables S10 and S11. In *C*, the numbers indicate the chronosequence stage, and the arrows indicate the overall directions for the changes in plant cover across stages. Changes in plant cover across chronosequence stages are calculated from stage 1 in each chronosequence.

Appendix, Tables S10 and S11). This pattern likely can be attributed to environmental filtering linked to soil acidification, which is a result of intense weathering (Figs. 1*B* and 3 and *SI Appendix*, Figs. S25 and S26). Such a pattern has been reported for another highly productive and wet chronosequence from New Zealand not included in our study (16). The sole exception to this pattern was observed in an ecosystem with very high initial soil pH located in warm Mediterranean shrublands from Western Australia. Alkaline soils in young sand dunes (pH ~9) from this chronosequence support low belowground biodiversity, explaining the increase in belowground biodiversity as pH declines during pedogenesis (*SI Appendix*, Fig. S26). Thus, our results suggest that pH deviations away from neutral are associated with decreased belowground biodiversity during ecosystem development, supporting an overall hump-shaped relationship between soil pH and belowground diversity (Fig. 1*B* and *SI Appendix*, Fig. S26). Taken together, these findings reveal the prevalent patterns associated with the changes in belowground biodiversity during pedogenesis and across resource gradients worldwide, and suggest that changes in belowground biodiversity during pedogenesis are predictable across major ecosystem types. We note that the observed soil biodiversity patterns associated with changes in plant cover and pH can be found in soil chronosequences with very different age ranges (Figs. 2 and 3), suggesting that the extent of changes in these key factors, rather than soil age per se, drives soil biodiversity during pedogenesis.

Our findings indicate that the fate of belowground biodiversity during pedogenesis is associated with two major ecological factors across a wide range of globally distributed ecosystem types and environmental conditions: plant cover in less productive systems and acidification in more productive systems. These results are valid for soil chronosequences with very different age ranges (thousands to millions of years). Our results suggest that more productive, wetter, and hotter ecosystems can potentially limit the development of belowground biodiversity as a consequence of the soil acidification associated with pedogenesis. Conversely, in low-productivity, colder, and drier ecosystems, plant cover is positively correlated with the changes in belowground biodiversity during ecosystem development across multiple chronosequences with very different age ranges. Of course, plants not only are a source of C for soil organisms (via litter and root exudates), but also improve microclimatic conditions, especially in the low productivity ecosystems often found in low-temperature and/or arid climates (*SI Appendix*, Fig. S25). This could explain, for instance, the reduction in belowground biodiversity at the Colorado chronosequence as plant cover declined with soil age in this relatively dry and cold region. In more productive ecosystems (*SI Appendix*, Fig. S25), acidification can potentially constrain the diversity of soil organisms (*SI Appendix*, Fig. S26) via multiple interactive mechanisms, including metal toxicity, solubility of essential nutrients, enzyme stability, and internal cell pH regulation.

We also found two other, less common patterns of the changes in belowground biodiversity during pedogenesis. For instance, soil salinity was identified as the most important environmental factor associated with the changes in belowground diversity during pedogenesis in a nonsaline (0.01–0.29 dS m^{-1}) temperate forest from Chile (*SI Appendix*, Table S2). In addition, soil texture was identified as the most important environmental factor associated with the changes in belowground diversity during ecosystem development in a temperate cropland ecosystem with very high levels of silt and clay (79.5–86.4%) and very high potential weathering rates (i.e., high levels of precipitation and temperature) (*SI Appendix*, Fig. S25).

The observed correlation between soil pH and belowground biodiversity could be an indirect consequence of reductions in soil P availability as soil develops (23, 24), but our results suggest otherwise. In fact, we expected to identify soil C, N, and P concentrations (or their stoichiometric ratios) as important factors associated with belowground biodiversity during pedogenesis, because soil C is a major energy source for heterotrophic microbes and because resource quality (i.e., C:N and N:P) and soil P concentrations are commonly considered limiting factors for belowground biodiversity during pedogenesis (16, 23, 24). However, in our models, soil N:P ratio, soil total organic C concentration, and soil P availability were never identified as the most important factors associated with observed changes in belowground diversity (*SI Appendix*, Figs. S17 and S18), and soil C:N ratio was identified as the most important environmental factor only in a volcanic arid chronosequence (*SI Appendix*, Fig. S27 and Table S2). More importantly, a survey conducted in a 27-y N and P fertilization experiment (24) showed that nutrient additions did not increase belowground biodiversity in very young (0.3 ky; stage 1 in our study) and very old (4,100 ky; stage 4 in our study) soils from Hawaii (*SI Appendix*, Fig. S28).

In summary, we found that plant cover and soil pH were the most important environmental factors associated with changes in belowground biodiversity during pedogenesis across a wide range of globally distributed ecosystem types. In less productive, drier, and colder ecosystems increases in plant cover during pedogenesis were related to increases in belowground biodiversity, whereas in more productive ecosystems, which are also warmer and wetter, declines in soil pH during pedogenesis were associated with declines in belowground diversity. Moreover, our results suggest that the temporal changes in aboveground plant diversity and belowground biodiversity are not correlated, challenging the common perception that belowground biodiversity should follow similar patterns to those of plant diversity during ecosystem development. Our results also indicate that we need to consider multiple soil chronosequences simultaneously to identify consistent ecological patterns. Taken together, our findings provide insight into the fate of belowground biodiversity during pedogenesis, and ultimately suggest that plant cover and soil acidification drive belowground biodiversity over centuries to millennia on a global scale.

Materials and Methods

Complete documentation of the study sites, field survey, sample collection, and laboratory procedures, as well as additional details on the statistical analyses, are provided in *SI Appendix, Materials and Methods*. Field data were collected between 2016 and 2017 from 16 soil age chronosequences located in nine countries from six continents (Fig. 1*A*). Each of the 16 chronosequences studied included between 4 and 10 chronosequence age-based stages (*SI Appendix*, Tables S2 and S3). At each stage, we conducted a vegetation survey and collected five composite samples of mineral soil (five soil cores 0–10 cm deep, a total of 435 soil samples) and obtained information on aboveground and belowground resource availability, nutrient stoichiometry, and other abiotic factors. The diversity of soil organisms was measured via marker gene amplicon sequencing. Belowground biodiversity was calculated as the standardized average of the diversity (i.e., richness; number of phylotypes) of soil bacteria, fungi, protists, and invertebrates. Detailed information on our regression, random forest, and hierarchical clustering analyses is provided in *SI Appendix, Materials and Methods*.

ACKNOWLEDGMENTS. This project received funding from the European Union's Horizon 2020 research and innovation program under Marie Sklodowska-Curie Grant Agreement 702057. N.F. was supported through grants from the US National Science Foundation (EAR1331828, DEB 1556090). Any use of trade, product, or firm names is for descriptive purposes only and does not imply endorsement by the US Government. An extended version of the acknowledgments is provided in *SI Appendix*.

1. Bardgett RD, van der Putten WH (2014) Belowground biodiversity and ecosystem functioning. *Nature* 515:505–511.
2. Wagg C, Bender SF, Widmer F, van der Heijden MG (2014) Soil biodiversity and soil community composition determine ecosystem multifunctionality. *Proc Natl Acad Sci USA* 111:5266–5270.
3. Delgado-Baquerizo M, et al. (2017) Soil microbial communities drive the resistance of ecosystem multifunctionality to global change in drylands across the globe. *Ecol Lett* 20:1295–1305.
4. Wardle DA, et al. (2008) The response of plant diversity to ecosystem retrogression: Evidence from contrasting long-term chronosequences. *Oikos* 117:93–103.
5. Laliberté E, et al. (2013) How does pedogenesis drive plant diversity? *Trends Ecol Evol* 28:331–340.
6. Laliberté E, Zemunik G, Turner BL (2014) Environmental filtering explains variation in plant diversity along resource gradients. *Science* 345:1602–1605.
7. Jenny H (1941) *Factors of Soil Formation: A System of Quantitative Pedology* (Dover, New York).
8. Crews TE, et al. (1995) Changes in soil phosphorus fractions and ecosystem dynamics across a long chronosequence in Hawaii. *Ecology* 76:1407–1424.
9. De Deyn GB, Van der Putten WH (2005) Linking aboveground and belowground diversity. *Trends Ecol Evol* 20:625–633.
10. Wu T, Ayres E, Bardgett RD, Wall DH, Garey JR (2011) Molecular study of worldwide distribution and diversity of soil animals. *Proc Natl Acad Sci USA* 108:17720–17725.
11. Tedersoo L, et al. (2014) Fungal biogeography: Global diversity and geography of soil fungi. *Science* 346:1256688.
12. Fierer N (2017) Embracing the unknown: Disentangling the complexities of the soil microbiome. *Nat Rev Microbiol* 15:579–590.
13. Tripathi BM, et al. (2018) Soil pH mediates the balance between stochastic and deterministic assembly of bacteria. *ISME J* 12:1072–1083.
14. Rillig MC, et al. (2001) Large contribution of arbuscular mycorrhizal fungi to soil carbon pools in tropical forest soils. *Plant Soil* 233:167–177.
15. Tarlera S, Jangid K, Ivester AH, Whitman WB, Williams MA (2008) Microbial community succession and bacterial diversity in soils during 77,000 years of ecosystem development. *FEMS Microbiol Ecol* 64:129–140.
16. Jangid K, et al. (2013) Progressive and retrogressive ecosystem development coincide with soil bacterial community change in a dune system under lowland temperate rainforest in New Zealand. *Plant Soil* 367:235–247.
17. Wardle DA, Walker LR, Bardgett RD (2004) Ecosystem properties and forest decline in contrasting long-term chronosequences. *Science* 305:509–513.
18. Roy-Bolduc A, Laliberté E, Hijri M (2015) High richness of ectomycorrhizal fungi and low host specificity in a coastal sand dune ecosystem revealed by network analysis. *Ecol Evol* 6:349–362.
19. Carlson ML, et al. (2010) Community development along a proglacial chronosequence: Are above-ground and below-ground community structure controlled more by biotic than abiotic factors? *J Ecol* 98:1084–1095.
20. Walker LR, et al. (2010) The use of chronosequences in studies of ecological succession and soil development. *J Ecol* 98:725–736.
21. Alfaro FD, et al. (2017) Microbial communities in soil chronosequences with distinct parent material: The effect of soil pH and litter quality. *J Ecol* 105:1709–1722.
22. Ortiz-Álvarez R, Fierer N, de Los Ríos A, Casamayor EO, Barberán A (2018) Consistent changes in the taxonomic structure and functional attributes of bacterial communities during primary succession. *ISME J* 12:1658–1667.
23. Walker TW, Syers JK (1976) The fate of phosphorus during pedogenesis. *Geoderma* 15:1–19.
24. Vitousek PM (2004) *Nutrient Cycling and Limitation: Hawai'i as a Model System* (Princeton Univ Press, Princeton, NJ).
25. Peltzet DA, et al. (2010) Understanding ecosystem retrogression. *Ecol Monogr* 80: 509–529.
26. McGill WB, Cole CV (1981) Comparative aspects of cycling organic C, N, S, and P through soil organic matter. *Geoderma* 26:267–286.
27. Wardle DA, et al. (2009) Among- and within-species variation in plant litter decomposition in contrasting long-term chronosequences. *Funct Ecol* 23:442–453.

Supporting Information

Changes in belowground biodiversity during ecosystem development

Manuel Delgado-Baquerizo, Richard D. Bardgett, Peter M. Vitousek, Fernando T. Maestre, Mark A. Williams, David J. Eldridge, Hans Lambers, Antonio Gallardo, Laura García-Velázquez, Osvaldo E. Sala, Sebastián R. Abades, Fernando D. Alfaro, Asmeret A. Berhe, Matthew A. Bowker, Courtney M. Currier, Nick A. Cutler, Stephen C. Hart, Patrick E. Hayes, Zeng-Yei Hseu, Martin Kirchmair, Sigrid Neuhauser, Victor M. Peña, Cecilia A. Pérez, Sasha C. Reed, Fernanda Santos, Christina Siebe, Benjamin W. Sullivan, Luis Weber-Grullon, Noah Fierer.

Author for correspondence:
Manuel Delgado-Baquerizo. E-mail: M.DelgadoBaquerizo@gmail.com

This PDF file includes:
Extended Discussion
Extended Acknowledgements
Material and Methods
Figures S1-S32
Tables S1-S15

www.pnas.org/cgi/doi/10.1073/pnas.1818400116

Extended discussion

Belowground community composition. Plant cover and soil pH were also significantly associated with belowground community composition (SI Appendix, Fig. S29; Tables S12-S13). Further, we detected some shared patterns for taxa within those chronosequences where belowground biodiversity was predicted by either pH or plant cover (see Methods). For example, we found that the relative abundance of the classes Acidobacteria group 6, Opitutae, Acidimicrobiia and Saprospirae were positively correlated with soil pH across five chronosequences (see SI Appendix, Table S14 for a complete list of taxa). Dominant taxa within these classes have previously been reported to be positively related to soil pH across the globe (1). Similarly, the relative abundances of, among others, Anaerolineae, Blastocladiomycetes and Glomeromycetes (SI Appendix, Table S14) followed a positive correlation with plant cover in chronosequences driven by this environmental factor (SI Appendix, Table S14). The fungal classes included taxa associated with plants, such as arbuscular mycorrhizal fungi (Glomeromycetes) and potential plant parasites (Blastocladiomycetes). Moreover, Anaerolineae have previously been reported to be abundant in the rhizosphere (2). These results suggest that major groups of belowground taxa follow similar temporal patterns worldwide despite the large differences in their composition across chronosequences (SI Appendix, Fig. S30 and Table S4).

Extended acknowledgements

M.D-B. is supported by a Large Research Grant from the British Ecological Society (grant agreement n° LRA17\1193, MUSGONET). We would like to thank Matt Gebert, Jessica Henley, Victoria Ochoa and Beatriz Gozalo for their help with lab analyses. We also want to thank Lynn Riedel, Julie Larson, Katy Waechter and Drs. David Buckner and Brian Anacker for their help with soil sampling in the chronosequence from Colorado, and to the City of Boulder Open Space and Mountain Parks for allowing us to conduct these collections. S.A. and F.D.A. were funded by FONDECYT 1170995, IAI-CRN 3005, PFB-23 (from CONICYT) and P05-002 (from Millennium Scientific Initiative) to the Institute of Ecology and Biodiversity, Chile. N.A.C. acknowledges Churchill College, University of Cambridge, for financial support and Dr. Vicki Parry for fieldwork assistance. M.W. acknowledges support from the Wilderness State Park, MI for access to sample soil and conduct an ecosystem survey. O.S. acknowledges support from NSF grants DEB 1754106, DEB 1354732, DEB 1456597. S.C.R. acknowledges support from the U.S. Department of Energy Office of Science (DE-SC-0008168, DE-SC-0011806) and the U.S. Geological Survey Ecosystems Mission Area. The Arizona research sites were established with the support of an EPA‐STAR Graduate Fellowship (U‐916251), a Merriam‐Powell Center for Environmental Research Graduate Fellowship, an Achievement Rewards for College Scientists (ARCS) Foundation of Arizona Scholarship, and McIntire‐Stennis appropriations to Northern Arizona University and the State of Arizona. A.G., F.T.M and M.D-B. acknowledge support from the Spanish Ministry (project CGL2017-88124-R). SN was funded by the Austrian Science Fund: grant Y0801-B16. F.T.M. is supported by the European Research Council (Consolidator Grant Agreement No 647038, BIODESERT). A.A.B. and F.S. acknowledge support from Jennifer Harden and Sebastian Doetterl for prior works and information about sites along the Merced Chronosequence and from Benjamin Sulman for help during sampling. N.F. was supported through grants from the U.S. National Science Foundation (EAR1331828, DEB 1556090).

Material and Methods

Field survey. Field data were collected between 2016 and 2017 from 16 soil age chronosequences located in nine countries from six continents (Fig. 1; SI Appendix, Tables S2-S3). The selected chronosequences ranged from hundreds to millions of years (SI Appendix, Tables S2-S3), representing changes in soil and plant conditions during pedogenesis. These chronosequences cover a wide variety of globally distributed vegetation types (including grasslands, shrublands, forests, and croplands; see SI Appendix, Tables S2-S3 for the dominant vegetation at each chronosequence), chronosequence origins (volcanic, sedimentary, dunes, and glacier) and climatic (tropical, temperate, continental, polar and arid) types (SI Appendix, Fig. S1 and Tables S2-S3). Field surveys were conducted according to a standardized sampling protocol (3). We surveyed a 50 m × 50 m plot within each chronosequence stage. Three parallel transects of 50 m length, spaced 25 m apart, formed the basis of the plot. The size of the plot was chosen to account for the spatial heterogeneity within the selected terrestrial ecosystem including different plant sizes from grasslands to forest ecosystems. The total plant cover and the number of perennial plant species (plant diversity) were measured from data collected in each transect using the line-intercept method (3). Plant cover has also been shown to be a good predictor for tree basal area (4), a variable that is commonly used in chronosequence studies (5-6).

Soil sampling. Five composite soil samples (five soil cores/sample; 0-10 cm depth) were collected under the dominant ecosystem vegetation type (e.g., trees, shrubs, grasses). We selected 0-10 cm for three reasons. First, this is the most commonly-used depth in comparable studies. Second, and more importantly, most of the belowground microbial and soil animal biomass is in the top 10 cm, a critical point given the focus on soil biodiversity of our study. Finally, because some sites have very shallow soils, sampling more deeply may not even have been possible at a number of the sites, and more importantly, would have not allowed to compare the same depth increment across all chronosequences.

Following field sampling, soils were sieved (2 mm) and separated into two portions. One portion was air-dried and used for biochemical analyses and the other immediately frozen at -20 ºC for molecular analyses. These storage approaches have been used widely in global field surveys (3,7-8). Sampling was conducted during the same days within each soil chronosequence. Moreover, we know that short-term climatic influences (e.g., seasonality) on soil biodiversity and community composition are much lower than that one from spatial variability associated with soil properties and perennial vegetation (9). This should be especially noticeable in locations ranging given that each of our chronosequence include locations ranging from hundreds to millions of years. Therefore, we do not expect any seasonality influence within each chronosequence.

Soil physical and chemical analyses. For all soil samples, we measured pH, electrical conductivity (salinity), texture (% of clay+silt), total organic carbon (C) and soil available P (Olsen inorganic P). We selected these soil variables because, together with plant cover (10), are known to be important environmental predictors of belowground biodiversity (8,11-12; Appendix S1, Table S1 for further details), and, have been reported to change predictably during pedogenesis (13-15). To avoid biases associated with having multiple laboratories analysing soils from different sites, and to facilitate the comparison of results among them, all dried soil samples were shipped to the Universidad Rey Juan Carlos (Spain) for laboratory analyses. Soil properties were determined using standardized protocols (3). Soil pH was measured in a 1:2.5 suspensions of dry soil mass to deionized water volume with a pH meter. Electrical conductivity (salinity hereafter) was measured as described in ref. 3. Texture (%

clay + silt) was determined on a composite sample per chronosequence stage according to ref. 16. The concentration of soil total organic C (soil C hereafter) was determined by colorimetry after oxidation with a mixture of potassium dichromate and sulfuric acid (17). Total N in these samples was measured with a CN analyzer (LECO CHN628 Series, LECO Corporation, St Joseph, MI, USA). Olsen P (soil P hereafter) was determined from bicarbonate extracts as described in ref. 18. Total P was obtained using a SKALAR San++ Analyzer (Skalar, Breda, The Netherlands) after digestion with sulfuric acid (3h at 415ºC; 3). The collected soils represent a wide range in soil properties. In brief, pH ranged from 3.19 to 9.45, salinity ranged from 0.00217 to 1.971 dS m^{-1}, C from 0.3 to 473.6 g C kg^{-1}, P from <0.01 to 90.69 mg P kg^{-1} soil and % clay + silt from 0.27 to 86.4 %.

Soil molecular analyses. The diversity of soil bacteria, fungi, protists and invertebrates was measured via amplicon sequencing using the Illumina MiSeq platform. Ten grams of frozen soil/sample (from composite soil samples as explained above) were ground using a mortar and liquid N aiming to homogenize soils and obtain a representative sample. Soil DNA was extracted using the Powersoil® DNA Isolation Kit (MoBio Laboratories, Carlsbad, CA, USA) according to the manufacturer's instructions. A portion of the bacterial 16S and eukaryotic 18S rRNA genes were sequenced using the 515F/806R and Euk1391f/EukBr primer sets (12,19), respectively. Bioinformatic processing was performed using a combination of QIIME (20), USEARCH (21) and UNOISE3 (22). Phylotypes (i.e. Operational Taxonomic Units; OTUs) were identified at the 100% identity level. The OTU abundance tables were rarefied at 5000 (bacteria via 16S rRNA gene), 2000 (fungi via 18S rRNA gene), 800 (protists via 18S rRNA gene) and 300 (invertebrates via 18S rRNA gene) sequences/sample, respectively, to ensure even sampling depth within each belowground group of organisms. Protists are defined as all eukaryotic taxa, except fungi, invertebrates (Metazoa) and vascular plants (Streptophyta). Note that not all samples passed our rarefaction cut-off. The total number of samples included in statistical modelling for each chronosequence stage and group of belowground organisms can be found in SI Appendix, Table S15.

The diversity (richness, i.e., number of phylotypes, and Shannon diversity) of soil bacteria, fungi, protists and invertebrates was determined from rarefied OTU abundance tables. Before conducting statistical modelling, we also ensured that our choice of rarefaction level, taken to maximize the number of samples in our study, was not obscuring our results. Thus, using the samples with the highest sequence/sample yield, we tested for the impact of different levels of rarefaction on belowground diversity. Importantly, we found highly statistically significant correlations between the diversities and community compositions of soil bacteria (rarefied at 5000 vs. 18,000 sequences/sample), fungi (rarefied at 2,000 vs. 10,000 sequences/sample), protists (rarefied at 800 vs. 4,000 sequences/sample), and invertebrates (rarefied at 300 vs. 1,800 sequences/sample), providing evidence that our choice of rarefaction level did not affect our results or conclusions (SI Appendix, Figs S31-S32).

Belowground biodiversity index. To obtain a quantitative index of belowground biodiversity for each sample, the diversity of soil bacteria, fungi, protists and invertebrates were standardized using the following equation: ((rawDiversity-min(rawDiversity)/(max(rawDiversity)- min(rawDiversity)), where min = minimum diversity value and max = maximum diversity (richness) value across all samples. The standardized samples were then averaged across organism groups. This is a common approach used to calculate integrated biodiversity indices for belowground (2) and aboveground (23) communities (often called multidiversity indices). For this index, we used only those soil

samples for which information on diversity for all soil bacteria, fungi, protists and invertebrates was available (SI Appendix, Table S15). The only exception was the chronosequence from Hawaii (HA; SI Appendix, Table S1), for which we had insufficient resolution (sequences/sample) to calculate the diversity of protists. In this chronosequence, belowground biodiversity only includes the diversity of soil bacteria, fungi and invertebrates. A similar approach was used in the analyses included in SI Appendix, Fig. S28.

Changes in belowground biodiversity during pedogenesis. We first identified the shape of the relationship between soil chronosequence stage and belowground biodiversity using the three most common regression models used to evaluate changes in soil attributes during pedogenesis: linear, quadratic and cubic (5-6, 24-27). Additionally, we also identified the shape of the relationship between perennial plant diversity and chronosequence stage. Separate analyses were carried out for each of the 16 chronosequences. Moreover, analyses were carried out for belowground biodiversity and for the diversity of individual belowground groups of organisms. As used in previous studies (5-6, 24-27), we used chronosequence stage as our surrogate of time. The use of rank values for chronosequence stage is justified, because of the high level of uncertainty in assigning precise ages for many of the chronosequences studied (5). We identified the best model for the regression between chronosequence stage and belowground biodiversity using the next set of three hierarchical rules:

(1) *Models need to be significant* ($P \leq 0.05$)(5). If only, one (out of three) models is significant, the significant model is selected by default. We used P-values from robust regressions (28-29) to avoid misinterpretation of our data resulting from outliers. We conducted these analyses using the R package rlm (28-29).
(2) *Akaike information criterion*. For those significant models, best model fits were selected using Akaike Information Criteria (AICc)(30-31) where a lower AICc value represents a model with a better fit. AICc is a corrected version of AIC, which is recommended when dealing with small sample sizes, as in our case (30-31). We further used a difference in AICc values of 2 (ΔAICc > 2) to determine substantial differences between models (30-31). If a single model had a ΔAICc > 2 compared with the rest of the models, that model was selected as our best model. These analyses were performed using the R package MuMIn (32).
(3) *Parsimony criterion*. If two or more models showed a difference in AICc values lower than 2 (ΔAICc < 2), we then selected the simplest model (linear > quadratic > cubic) as the best model.

Environmental predictors of belowground biodiversity during pedogenesis. We aimed to identify the best environmental variables, including aboveground (plant cover) and belowground (soil C and available P) resource availability, nutrient stoichiometry (soil N:P and C:N ratios) and soil abiotic factors (salinity, pH and % of clay+silt) as predictors of the changes in belowground biodiversity during pedogenesis at each soil chronosequence. Note that the concentrations of total organic C (referred above as soil C) were strongly correlated with those of total N ($\rho = 0.90$; $P < 0.001$, n = 435) and dissolved inorganic N ($\rho = 0.72$, $P < 0.001$, n = 435) across samples, so we kept only soil C for statistical modeling. We used plant cover data, collected *in situ* for each location, as an integrated index of plant productivity and the availability of plant C inputs, which are major resources for soil organisms. Plant cover data was positively and significantly correlated with mean annual plant productivity (2008-2017 period) estimated using remote sensing at 250m resolution ($\rho = 0.55$; $P < 0.001$). Moreover, plant cover was positively correlated with rates of microbial respiration based on

laboratory incubations across locations ($\rho = 0.32$; $P < 0.001$, see Methods for details). In addition, we used Olsen P (Soil P) concentrations in our analyses as a surrogate of P availability. We expected this measure of labile P pool size to have a stronger influence on belowground communities than total P, which includes occluded and mineral-bound P. Soil P concentrations (Olsen P) were positively correlated with soil total P concentration across our samples ($\rho = 0.73$, $P < 0.001$, n = 435), and to other commonly-used methods for estimating available P pool sizes (resin-P; $\rho = 0.72$, $P < 0.001$, n = 87; 33). This suggests that the analytical approach used here provides a reasonable estimate of P availability across the samples included in this study.

In order to identify the environmental predictors of belowground biodiversity during pedogenesis, we used a three step approach:

(1) *Identifying environmental predictors of pedogenesis*. As we were particularly interested in those environmental predictors that shift during pedogenesis, we first identified significant environmental predictors ($P \leq 0.05$) for changes in chronosequence stages. To do this, we used Random Forest modelling as explained in ref. 34. Random Forest was chosen for these analyses because it works well with response variables with different response types, i.e. it does not require linearity. Random Forest generates a collection of classification trees with binary divisions. The fit of each tree is assessed using randomly selected cases (1/3 of the data), which are withheld during its construction (out-of-bag or OOB cases). The importance of each predictor variable was determined by evaluating the reduction in prediction accuracy (i.e. increase in the mean square error between observations and OOB predictions) when the data for that predictor were randomly permuted. This reduction was averaged over all trees to produce the final measure of importance. Notably, unlike multi-model inference using linear regressions or regression tree analyses, Random Forest alleviates multicolinearity problems in multivariate analyses by building bagged tree ensembles and including a random subset of features for each tree (9999 trees here). These analyses were conducted using the rfPermute R package (35).

(2) *Identifying environmental predictors of belowground diversity*. Once we had identified those key environmental factors (Step 1) predicting changes in environmental conditions during pedogenesis, we then used these variables and Random Forest modelling to identify the most important predictors of changes in belowground diversity. Environmental predictors were allowed to differ for each chronosequence according to Step (1). A predictor was considered significant when $P \leq 0.05$.

(3) *Clustering major belowground biodiversity patterns during pedogenesis.* Using the derived information on the importance of each significant predictor from Random Forest in Step 2, we clustered the sixteen chronosequences by their major environmental predictors (See SI Appendix, Fig. S24). To do so, we used hierarchical cluster analysis, as implemented in the "hclust" function in the R package "stats". This analysis aimed to identify major types of ecosystem development (ecological clusters) valid across multiple soil chronosequences. Before conducting hierarchical clustering, the importance (from Random Forest) of all significant predictors within each chronosequence was standardized between 0 and 1 to allow the direct comparison of predictor importance across chronosequences in our clustering analyses. We then identified the shape of the relationships between the top significant predictor across all chronosequences from Random Forest analyses and belowground

biodiversity following the three hierarchical rules explained above (significance, AIC and parsimony).

(4) *Chronosequence ecosystem productivity and climate as regulators of the fate of belowground biodiversity during pedogenesis.* Using information from step 3, we compared the ecosystem productivity and climate (precipitation and temperature) across chronosequence belonging to different ecological clusters (SI Appendix, Fig. S24). For ecosystem productivity, we used the Normalized Difference Vegetation Index (NDVI). This index provides a global measure of the "greenness" of vegetation across Earth's landscapes for a given composite period, and thus acts as a proxy of photosynthetic activity and large-scale vegetation distribution. The NDVI data were obtained from the Moderate Resolution Imaging Spectroradiometer (MODIS) aboard NASA's Terra satellites (http://neo.sci.gsfc.nasa.gov/). We calculated the monthly average value for this variable between the 2008-2017 period. We also calculated a "climatic index" as the standardized average of mean temperature and precipitation at each chronosequences using climatic data from www.worldclim.org/. We used PERMANOVA analyses (36) to test for significant differences in ecosystem productivity and climatic index for those chronosequence belonging to different ecological clusters.

Changes in belowground community composition dissimilarity during pedogenesis. We evaluated the relationship between chronosequence stage and belowground community composition dissimilarity. We first calculated Bray–Curtis dissimilarity matrices for the community of soil bacteria, fungi, protists and invertebrates at the OTU level. All these distance matrices were then averaged within each chronosequence to generate a belowground community dissimilarity matrix. Note that as Bray–Curtis dissimilarities are already standardized, no further standardization was needed prior to matrix averaging. See SI Appendix, Table S15 for the number of samples within each chronosequence stage. We then used the Euclidean distance to create a matrix of environmental distance (based on plant cover, soil pH, texture, salinity, soil C, soil P, N:P and C:N ratios) across stages within each chronosequence. After this, we correlated the matrix of chronosequence stage dissimilarity to that one of belowground communities using Mantel test correlations (Spearman). Finally, we used Mantel test correlation to evaluate the correlation between belowground community dissimilarity and environmental distance.

Environmental predictors of belowground taxa. We conducted additional analyses to identify groups of taxa following similar environmental patterns to those reported in Fig. 3 for belowground diversity. We conducted these analyses for those chronosequences following the exact environmental pattern within the two dominant environmental predictors (pH: CAL, HA, MI, QL and MEX, and plant cover: AZ, ALPS, CI, ICE and BOS). We used Spearman correlation to identify taxa associated with either pH or plant cover. Because of the high variability in community composition at the phylotype level found for belowground community composition (SI Appendix, Fig. S30), we conducted these analyses at the class level. We retained taxa that were always positively correlated with either pH or plant cover in all five selected chronosequences.

Table S1. Conceptual information on complementary ecological theories and associated environmental factors potentially driving belowground biodiversity during pedogenesis.

Ecological theory	Above and belowground resource availability	Soil nutrient stoichiometry	Abiotic factors
Environmental factors	Plant cover, and soil C, N and P.	Soil N:P and C:N ratios.	Salinity, pH and texture.
Theory	Belowground communities often obtain their energy from aboveground litter inputs and soil organic matter (soil C) and nutrients (soil N and P). Several prominent ecological theories emphasize the important role of aboveground and belowground resource supply and competition in regulating the diversity of plants and soil organisms in terrestrial ecosystems (14,37). Belowground biodiversity is expected to increase as resource availability increases (increasing species co-existence); however, situations with very high levels of resources often lead to high levels of biomass declining biodiversity via competitive exclusion (38). Very old soil chronosequences are known to enter a retrogressive phase, exceptionally reducing resource availability. This could potentially drive the long-term development of belowground biodiversity. Resource availability could be especially critical for low productivity ecosystems.	Soil nutrient stoichiometry is often associated with resource quality and its control of the relative abundance of elements in soil (14,37). Soil nutrient stoichiometry affects biotically-driven processes such as litter decomposition, mineralization and nutrient immobilization. Because, plants and belowground organisms maintain a highly conserved elemental stoichiometry driven by the relative availability of C, N and P (39), locations where one of these elements is comparatively lacking might result in a reduction of the species capable of surviving in such conditions. For example, soils with very high C:N ratios often lead to reduced mineralization and promoted nutrient immobilization, limiting the access to resources (40). Moreover, nutrient stoichiometry can potentially regulate belowground biodiversity by regulating the relative abundance of N vs. P in soils. Very old soils often lead to large reductions in P relative to N (27,40). The reason is that P is only available from the bedrock, while N can also be obtained from the atmosphere. Very low soil N:P ratio are hypothesized to reduce the number of co-existing species and processes by limiting the access to energy sources.	Soil salinity, very low or high pH and very low or very high fine texture content are major abiotic factors limiting the growth and biodiversity of plants and soil organisms worldwide (10) (e.g., see Appendix S1, Fig. S26). Soils are expected to become more acid, accumulate more soil fine grain sizes and increase their salinity during pedogenesis. Locations with very high levels of weathering might result in strong abiotic stresses limiting the diversity of soil organisms. Abiotic stress could be especially important during pedogenesis in highly productive environments, where plant productivity is likely to contribute to greater reductions in soil pH, and increases in salinity and fine texture.
Examples	Soil P has been postulated for years as one of the major limiting factors for belowground biodiversity during pedogenesis (27,39-40).	Nutrient stoichiometry has been reported to be a good predictor of bacterial diversity in highly weathered soils from Scotland (41).	Soil pH has been reported to be a major driver of biodiversity across resource gradients (25,44).

Table S2. **Vegetation type and age for sixteen soil chronosequences**. Vegetation community composition for each chronosequence stage is available in Appendix S1, Table S3. See Fig. 1A for the location of these chronosequences. Chronosequence origin describe the major causal agent of each chronosequence. For example, the chronosequence from ICE takes place on volcanic soils, but it is classified as a glacier chronosequence. Biome classification followed the Köppen climate classification and the major vegetation types found in our database. Aridity classification followed the Aridity Index (AI) classification: arid (0.05 > AI < 0.20), semiarid (0.20 > AI < 0.50), dry-subhumid (0.50 > AI < 0.65) and mesic (AI > 0.65).

Label	Country	Name	Age	Chronosequence origin	Aridity classification	Biome	MAT (°C)	MAP (mm)
ALPS	Austria	Alps	0.01-120ky	Glacier	Mesic	Alpine ecosystems	0.60	1182
AZ	USA	SAGA	0.9-3000ky	Volcanic	Semiarid	Arid forests	9.68	427
BOS	Bolivia	Cojiri	0.025-20ky	Sedimentary	Arid	Arid shrublands	8.40	141
BOV	Bolivia	Chiar Kkollu	0.025-20ky	Volcanic	Arid	Arid shrublands	7.55	106
CAL	USA	Merced	0.1-3000ky	Sedimentary	Semiarid	Temperate grasslands	16.32	360
CH	Chile	Conguillio	0.06-5000ky	Volcanic	Mesic	Temperate forests	8.95	1917
CI	Spain	La Palma	0.5-1700ky	Volcanic	Dry-subhumid	Temperate forests	13.27	507
CO	USA	Coal creek	5-2000ky	Sedimentary	Semiarid	Cold grasslands	8.95	431
HA	USA	Hawaii	0.3-4100ky	Volcanic	Mesic	Tropical forests	16.03	1885
ICE	Iceland	Mt Hekla	0.1-0.9ky	Glacier	Mesic	Polar moss heaths	3.70	1339
JOR	USA	Jornada Desert	1.1-25ky	Sedimentary	Arid	Arid forblands	14.65	265
MEX	Mexico	Chichinautzin	1-100ky	Volcanic	Mesic	Temperate forests	11.06	1235
MI	USA	Lake Michigan	0.7-4ky	Sand dunes	Mesic	Cold forests	6.10	774
QL	Australia	Cooloola	3.6-716ky	Sand dunes	Mesic	Temperate forests	20.77	1516
TA	Taiwan	Taiwan	28-399ky	Sedimentary	Mesic	Temperate croplands	21.33	2365
WA	Australia	Jurien Bay	0.1-2000ky	Sand dunes	Semiarid	Temperate shrublands	18.97	557

Table S3. Dominant vegetation community composition in each of the stages for the 16 soil chronosequences included in this study. See Appendix S1, Fig. 1A for the location of these chronosequences.

Name	Stage	Age (years)	Dominant vegetation
ALPS	1	10	*Saxifraga azoides, Saxifraga oppositifolia, Poa alpina, Linaria alpina, Artemisia gentipi*
	2	45	*Trifolium pallescens, Campanula scheuchzeri, Saxifraga oppositiolia, Saxifraga aizoides*
	3	125	*Kobresia myosuroides, Agrostis alpina, Alchemilla fissa, Trifolium pratense spp., Nivale*
	4	10000	*Avenula versicolor, Carex sempervirens, Festuca halleri, Anthoxanthum alpinum*
	5	120000	*Fagus sylvatica, Abies alba, Acer pseudoplatanus, Picea abies, Quercus robur*
AZ	1	900	*Juniperus monosperma, Pinus edulis, Bouteloua gracilis*
	2	55000	*Juniperus monosperma, Pinus edulis, Bouteloua gracilis*
	3	750000	*Juniperus monosperma, Pinus edulis, Bouteloua gracilis*
	4	3000000	*Juniperus monosperma, Pinus edulis, Bouteloua gracilis*
BOS	1	25	*Astragalus pusillus, Atriplex imbricata, Baccharis boliviensis, Baccharis tola, Ephedra breana, Haplopappus rigidus, Junellia seriphioides, Lycium chanar, Opuntia boliviensis*
	2	11400	*Fabiana densa, Atriplex imbricata, Baccharis boliviensis, Lycium chanar, Baccharis tola, Haplopappus rigidus, Hoffmannseggia minor, Junellia seriphioides, Mutisia ledifolia, Nassella curviseta*
	3	14100	*Atriplex imbricata, Baccharis boliviensis, Haplopappus rigidus, Junellia seriphioides, Lycium chanar, Mutisia ledifolia, Nassella curviseta, Trichocereus atacamensis*
	4	20000	*Atriplex imbricata, Baccharis boliviensis, Cheilanthes ternifolia, Diplostephium cinereum, Ephedra breana, Fabiana densa, Lycium chanar, Mutisia ledifolia, Senecio dryophyllus, Senecio nutans, Stevia sp., Trichocereus atacamensis*
BOV	1	25	*Adesmia spinosa, Atriplex imbricata, Chuquiraga atacamensis. Frankenia triandra, Sisymbrium sp., Nassella curviseta*
	2	11400	*Opuntia boliviensis, Acantholippia punensis, Atriplex imbricata, Chuquiraga atacamensis, Ephedra breana, Senecio dryophyllus, Sisymbrium sp.*
	3	14100	*Acantholippia punensis, Adesmia spinosa, Atriplex imbricata, Chuquiraga atacamensis, Nassella curviseta*
	4	20000	*Acantholippia punensis, Atriplex imbricata, Chuquiraga atacamensis, Senecio dryophyllus*
CAL	1	100	*Populus fremontii, Helianthus annuus, Amaranthus albus*
	2	3000	*Quercus lobata, Silybum marianum, Hordeum murinum L*
	3	30000	*Festuca californica*
	5	600000	*Rytidosperma penicillatum*
	6	3000000	*Festuca bromoides, F. myuros, Bromus hordaceous, B. diandrus*
CH	1	60	*Gaultheria pumila, Racomitrium lanuginosum*
	2	266	*Lomatia hirsuta, Austrocedrus chilensis*
	3	776	*Araucaria araucana, Nothofagus antarctica*
	4	3470	*Nothofagus dombeyi, Araucaria araucana*

	5	60000	*Nothofagus dombeyi, N. obliqua, N. alpina*
	6	5000000	*Nothofagus dombeyi, N. alpina*
CI	2	525	*Pinus canariensis*
	3	6000	*Pinus canariensis, Erica arborea, Pterocephalus porphyranthus*
	4	40000	*Pinus canariensis, Adenocarpus viscosus, Chamaecytisus proliferus, Erica arborea*
	5	600000	*Pinus canariensis, Adenocarpus viscosus*
	6	1100000	*Pinus canariensis, Cistus symphytifolius*
	7	1700000	*Pinus canariensis, Cistus symphytifolius*
CO	1	5000	*Juncus arcticus, Andropogon gerardii, Panicum virgatum*
	2	140000	*Andropogon gerardii, Panicum virgatum*
	3	240000	*Panicum virgatum, Poa compresa, Andropogon gerardii*
	4	640000	*Chrysopsis sp, Andropogon gerardii, L. cinquefoil*
	5	1000000	*Andropogon gerardii, M. Burgia, Poa compresa,*
	6	2000000	*Andropogon gerardii, Poa compresa, M. Burgia*
HA	1	300	*Metrosideros polymorpha, Morella faya, Vaccinium calycinum, Ilex anomala, Cheirodendron trigynum, Cibotium glaucom, Hedychium gardnerianum, Isoetes sp. (grass), Coprosma sp., Myrsine lessertiana, Dicranopteris linearis, Machaerina angustifolia, Anemone hupehensis, , ,*
	2	20000	*Metrosideros polymorpha, Cheirodendron trigynum, Cibotium glaucom, Cibotium menziesii, Ilex anomala, Freycinetia arborea, Astelia menziesii, Melicope clusiifolia, Vaccinium calycinum, Nephrolepis sp., Asplenium spp. (multi), Athyrium microphyllum, Ilex myrtifolia, Peperomia sp., Polypodium sp.,*
	3	150000	*Metrosideros polymorpha, Cibotium glaucom, Cibotium menziesii, Hedychium gardnerianum, Vaccinium calycinum, Cheirodendron trigynum, Psidium cattleianum, Dicranopteris linearis, Asplenium sp., Melicope clusiifolia, Myrsine sandwicensis, Elaphoglossum sp, Polygonum punctatum (sic?) (water smartweed), Tibouchina herbacea, Peperomia sp., Psilotum nudum*
	4	4100000	*Metrosideros polymorpha, Hedychium gardnerianum, Dicranopteris linearis, Pittosporum gayanum, Psidium cattleianum, Astelia menziesiana, Morella faya, Vaccinium meyenianum, Smilax hawaiensis, Elaphoglossum spp, Elaeocarpus bifidus, Clerodendrum sp, Alyxia oliviformis,*
ICE	1	172	*Racomitrium lanuginosum; Empetrum nigrum; Stereocaulon vesuvianum*
	2	463	*Racomitrium lanuginosum; Empetrum nigrum; Arctostaphylos uva-ursi*
	3	628	*Racomitrium lanuginosum; Betula nana; Hylocomium splendens; Empetrum nigrum; Arctostaphylos uva-ursi*
	4	717	*Racomitrium lanuginosum; Salix phylicifolia; Empetrum nigrum; Hylocomium splendens*
	5	859	*Racomitrium lanuginosum; Empetrum nigrum; Betula nana; Hylocomium splendens*
JOR	1	1100-2200	*Opuntia phaeacantha Engelm. var., Boerhavia spp., Eragrostis Lehmanniana Ness.*
	2	2200-7000	*Sporobolus contractus Hitchc., Muhlenbergia Porteri Scribn., Larrea tridentata Cov., Ephedra trifurca Torr.*
	3	8000-15000	*Boerhavia spp., Larrea tridentata Cov.*
	4	25000-75000	*Boerhavia spp., Ephedra trifurca Torr., Erioneuron pulchellum*

MEX	1	1000	*Pinus montezumae, Bacharis conferta, Alnus firmifolia, Penstemon sp.*
	2	1835	*Abies religiosa, Arbutus xalapensis, Pinus herrerae, Bacharis conferta, Pinus montezumae, Penstemon sp., Bacharis conferta, Buddleja sp.,*
	3	3800	*Alnus firmifolia, Quercus laurina, Pinus montezumae, Pinus pseudostrobus*
	4	6200	*Pinus montezumae, Alnus firmifolia*
	5	8000	*Pinus montezumae, Bacharis conferta, Buddleja parviflora*
	6	10000	*Pinus patula, Alnus firmifolia, Pinus montezumae, Senecio sp*
	7	30500	*Pinus ayacahuite, Pinus pseudostrobus, Pinus montezumae*
	8	100000	*Pinus montezumae, Abies religiosa, Quercus laurina, Penstemos sp., Bacharis conferta*
MI	1	73	*Amophilous breviligulata, Agropyron dasystachium, Cerisium pitheri, Arctostaphylos uva-ursi*
	2	113	*Amophilous breviligulata, Agropyron dasystachium, Cerisium pitheri, Arctostaphylos uva-ursi, Schizachyrium scoparium*
	3	163	*Arctostaphylos uva-ursi, Juniperus communis, Pinus strobus*
	4	243	*Pteridium aquilinum, Pinus resinosa, Abies sp*
	5	485	*Gaultheria procumbens, Pinus resinosa, Betula papyrifera*
	6	863	*Abies balsamea, Pinus resinosa, Juniperus communis*
	7	1400	*Abies balsamea, Pinus resinosa, Pinus strobus*
	8	2500	*Pinus resinosa, Vaccinium myrtilloides, Gaultheria procumbens*
	9	3200	*Pinus resinosa, Vaccinium myrtilloides, Gaultheria procumbens*
	10	4000	*Pinus resinosa, Pinus strobus, Gaultheria procumbens*
QL	1	3600	*Eucalyptus tessellaris, Angophora costata, Eucalyptus intermedia, Casuarina littoralis, Melaleuca quinquenerva, Banksia integrifolia, Banksia serrata, Macrozamia spp., Acacia aulacocarpa, Acacia flavescens, Groundstorey, Cassytha paniculata, Gahnia sieberiana, Hardenbergia violacea*
	2	6700	*Eucalyptus tessellaris, Angophora costata, Eucalyptus intermedia, Casuarina littoralis, Melaleuca quinquenerva, Banksia integrifolia, Banksia serrata, Macrozamia spp., Acacia aulacocarpa, Acacia flavescens, Groundstorey, Cassytha paniculata, Gahnia sieberiana, Hardenbergia violacea*
	3	134000	*Eucalyptus tessellaris, Angophora costata, Eucalyptus intermedia, Casuarina littoralis, Melaleuca quinquenerva, Banksia integrifolia, Banksia serrata, Macrozamia spp., Acacia aulacocarpa, Acacia flavescens, Groundstorey, Cassytha paniculata, Gahnia sieberiana, Hardenbergia violacea*
	4	176000	*Eucalyptus tessellaris, Angophora costata, Eucalyptus intermedia, Casuarina littoralis, Melaleuca quinquenerva, Banksia integrifolia, Banksia serrata, Macrozamia spp., Acacia aulacocarpa, Acacia flavescens, Groundstorey, Cassytha paniculata, Gahnia sieberiana, Hardenbergia violacea*
	5	324000	*Eucalyptus tessellaris, Angophora costata, Eucalyptus intermedia, Casuarina littoralis, Melaleuca quinquenerva, Banksia integrifolia, Banksia serrata, Macrozamia spp., Acacia aulacocarpa, Acacia flavescens, Groundstorey, Cassytha paniculata, Gahnia sieberiana, Hardenbergia violacea*
	6	716000	*Eucalyptus tessellaris, Angophora costata, Eucalyptus intermedia, Casuarina littoralis, Melaleuca quinquenerva, Banksia integrifolia, Banksia serrata, Macrozamia spp., Acacia aulacocarpa, Acacia flavescens, Groundstorey, Cassytha paniculata, Gahnia sieberiana, Hardenbergia violacea*
TA	1	28000	*Tea camellia*

	2	105000	*Tea camellia*
	3	322000	*Tea camellia*
	4	399000	*Tea camellia*
WA	1	100	*Acacia cyclops, Acacia rostellifera, Scaevola crassifolia, Olearia axillaris, Spyridium globulosum*
	2	1000	*Melaleuca systena, Acacia lasiocarpa, Acacia rostellifera*
	3	6500	*Melaleuca systena, Acacia lasiocarpa, Acacia rostellifera*
	4	120000	*Melaleuca systena, Banksia leptophylla, Calothamnus quadrifidus*
	5	480000	*Banksia menziesii, Banksia attenuata, Mesomelaena pseudostygia, Hibbertia hypericoides*
	6	2000000	*Banksia menziesii, Jacksonia floribunda, Banksia leptophylla*

Table S4. Mean values (%) for the relative abundance of main taxonomic groups within bacteria, fungi, protists and soil invertebrates in each of the stages for 16 soil chronosequences included in this study. A "-" symbol indicates no data.

		Bacteria			Fungi			Invertebrates			Protists		
Name	Stage	Acidobacteria	Actino bacteria	Proteo bacteria	Asco mycota	Basidio mycota	Mucoro mycota	Arthropoda	Nematoda	Rotifera	Cercozoa	Ciliophora	Lobosa
ALPS	1	10.09	8.28	40.20	39.80	31.48	18.00	37.17	45.00	14.92	29.23	11.05	0.50
	2	10.94	16.47	37.35	38.11	40.00	14.04	0.60	80.87	6.33	24.70	18.45	0.65
	3	11.75	16.35	37.07	40.94	33.65	16.05	5.33	77.33	7.73	42.60	15.88	0.85
	4	13.79	14.38	32.13	40.45	36.96	17.23	4.73	72.53	4.20	28.40	17.48	2.50
	5	33.89	11.47	30.35	26.60	46.45	24.60	5.44	68.22	6.00	39.96	18.75	5.71
AZ	1	14.72	20.07	33.82	59.55	33.29	2.73	3.89	79.89	6.89	16.09	51.53	9.59
	2	12.31	26.29	30.45	58.01	26.05	4.99	37.67	22.83	23.58	28.16	39.09	6.22
	3	15.28	25.32	25.95	68.54	27.35	0.35	41.67	46.20	6.40	22.93	48.45	7.33
	4	18.56	24.33	25.57	54.21	36.48	1.19	14.83	55.67	12.92	23.38	47.03	6.38
BOS	1	11.38	31.49	23.76	67.56	11.48	3.02	2.33	96.33	0.00	14.58	54.18	15.33
	2	16.56	22.74	23.52	63.30	18.15	1.93	16.25	77.00	6.42	17.31	45.72	8.75
	3	8.89	26.43	27.12	59.68	6.63	2.81	0.50	95.67	0.00	13.41	55.00	8.41
	4	18.37	22.45	22.78	63.07	19.86	5.30	24.13	58.40	5.13	31.05	36.28	6.60
BOV	1	27.45	18.63	36.10	26.15	10.05	63.35	20.00	14.67	1.33	9.56	73.63	10.63
	2	12.06	13.04	40.86	99.95	0.05	0.00	100.00	0.00	0.00	0.00	100.00	0.00
	3	9.24	20.53	32.28	81.48	5.87	2.22	0.00	44.67	54.33	14.81	29.00	7.44
	4	12.37	18.38	31.95	62.85	16.75	0.17	24.11	25.44	50.33	25.54	47.92	4.21
CAL	1	9.90	16.92	29.58	34.38	50.81	4.14	68.80	1.60	8.07	13.53	13.78	6.08
	2	12.35	17.89	34.09	54.94	33.32	8.30	8.20	64.73	1.40	40.63	23.73	6.90
	3	14.78	20.88	33.59	50.32	29.35	11.52	42.58	8.25	21.50	17.90	15.35	7.98
	4	11.36	21.11	35.03	74.47	13.85	1.95	12.20	66.73	4.40	33.83	41.40	3.95
	5	13.04	15.84	28.36	80.05	13.75	0.63	25.93	52.80	11.53	31.15	38.53	2.83
CH	1	13.07	21.57	23.68	41.81	49.27	2.85	21.92	21.67	22.58	44.00	12.47	5.88
	2	16.71	11.97	31.80	64.60	17.46	12.62	15.75	43.08	10.33	39.00	8.28	11.06
	3	16.60	14.97	33.16	29.68	47.08	19.30	19.27	27.07	26.93	41.13	11.05	7.95
	4	18.16	10.90	40.78	18.13	59.53	18.16	21.13	43.20	6.33	43.88	12.53	3.58
	5	13.11	18.22	40.08	35.31	39.72	19.26	12.27	62.27	7.93	47.20	11.25	3.00
	6	16.55	12.45	42.45	27.33	46.31	22.95	24.08	45.17	10.50	46.97	8.38	3.84
CI	1	14.97	25.50	27.64	56.22	28.47	4.79	17.00	42.25	33.92	33.83	23.78	4.48
	2	14.95	18.85	24.23	61.04	25.08	2.67	3.25	44.50	5.08	33.28	11.70	12.40
	3	13.78	19.64	32.68	51.20	30.19	10.48	21.00	61.73	11.33	31.30	36.90	5.33

	4	12.31	19.55	30.79	41.22	47.99	7.56	47.73	41.33	1.87	34.17	42.71	2.88
	5	12.44	19.84	41.23	44.75	44.28	8.84	36.33	50.75	8.00	27.56	42.13	12.06
	6	13.50	21.92	32.40	41.96	51.02	3.01	17.75	64.00	6.75	37.95	29.45	7.78
CO	1	12.06	23.50	28.29	47.00	24.12	17.85	29.80	47.00	5.60	40.28	14.30	7.90
	2	11.18	27.39	26.30	61.04	19.47	7.30	14.93	40.07	24.13	29.78	24.80	6.90
	3	11.44	25.77	24.19	55.23	14.94	9.39	19.67	47.40	18.53	36.58	23.73	7.85
	4	11.90	27.71	27.45	67.01	15.31	8.89	11.53	62.27	8.67	32.20	26.23	6.75
	5	10.23	24.03	28.11	61.92	20.16	3.28	27.42	42.33	24.92	30.43	20.08	7.60
	6	11.86	26.36	28.28	63.87	13.80	9.81	13.60	52.87	13.60	28.08	29.83	4.43
HA	1	23.64	7.48	38.20	61.13	30.46	7.33	27.75	43.08	1.75	-	-	-
	2	33.13	10.62	35.09	68.99	18.68	8.80	35.08	22.00	8.42	-	-	-
	3	27.41	13.85	29.79	65.73	22.88	5.13	39.33	23.67	17.17	-	-	-
	4	21.68	12.02	32.85	61.28	22.88	11.38	49.17	28.33	8.33	-	-	-
ICE	1	20.70	6.39	31.28	58.99	34.19	5.12	4.67	28.73	24.13	27.55	28.30	11.83
	2	20.87	9.57	33.81	29.32	60.95	4.02	11.07	58.20	12.67	24.88	25.78	4.53
	3	15.16	10.07	33.27	35.19	46.42	13.97	7.00	59.93	12.47	36.65	18.60	7.73
	4	18.50	8.92	31.32	31.02	60.94	4.99	11.00	78.07	3.40	29.75	20.78	4.13
	5	15.38	10.16	35.04	22.77	62.06	13.56	30.13	55.07	4.53	36.35	28.70	8.25
JOR	1	9.76	24.68	30.01	59.15	19.48	11.10	24.67	59.20	5.53	15.58	65.08	3.90
	2	10.73	23.50	33.02	76.95	13.69	3.95	3.92	89.58	1.25	10.13	74.69	4.75
	3	11.31	25.61	28.36	61.07	20.61	3.46	20.33	67.33	5.33	13.33	66.63	4.43
	4	12.12	24.51	28.25	67.21	18.45	5.05	13.89	50.56	9.44	13.63	63.55	6.90
MEX	1	18.08	10.77	41.67	20.69	64.49	11.45	28.27	51.07	7.27	43.81	11.28	13.41
	2	14.84	14.00	31.40	26.69	59.72	9.84	40.60	37.13	7.27	45.22	10.78	5.00
	3	15.91	13.52	32.11	23.05	53.22	17.02	21.33	62.60	3.33	42.40	10.15	6.35
	4	14.98	14.45	31.84	25.73	51.91	16.53	16.73	65.80	3.00	47.34	14.72	5.47
	5	15.83	13.98	33.82	19.69	56.21	15.56	20.13	53.13	2.27	44.20	13.70	8.08
	6	16.35	12.60	33.96	17.87	57.96	21.07	5.00	78.07	1.60	44.00	8.42	7.25
	7	15.94	13.64	32.18	24.39	57.48	12.25	1.83	66.00	3.33	44.75	8.81	10.56
	8	18.22	13.81	31.69	21.34	55.73	18.02	6.40	66.00	6.33	46.69	9.50	11.13
MI	1	5.57	24.58	34.91	57.71	32.45	0.97	0.17	74.33	18.67	21.68	22.70	13.53
	2	6.15	15.60	42.19	62.13	31.25	2.90	9.33	41.00	43.25	17.83	47.53	13.58
	3	10.01	21.04	34.47	60.63	24.00	14.06	12.22	69.11	16.67	19.75	32.03	9.34
	4	8.23	18.80	42.05	48.07	30.21	19.06	0.67	5.83	9.83	20.13	50.48	9.00
	5	21.48	16.24	38.31	42.60	22.07	34.26	49.93	33.93	11.67	39.25	7.97	22.03

	6	23.51	9.37	43.08	16.27	48.65	34.60	42.33	21.92	20.25	40.59	20.59	19.56
	7	23.44	16.29	41.36	33.13	16.33	50.41	66.44	23.00	8.78	30.00	12.75	40.06
	8	26.58	15.27	46.33	40.82	7.36	51.82	84.83	8.83	4.17	25.38	14.88	29.88
	9	20.30	17.42	41.54	30.57	20.75	48.56	65.92	15.42	3.83	33.38	14.38	38.00
	10	20.37	13.95	42.79	33.90	28.26	37.50	51.58	17.17	17.42	22.16	19.94	36.75
QL	1	15.24	13.84	35.21	36.90	49.98	11.53	32.80	50.00	14.93	48.17	22.71	6.00
	2	14.60	19.18	35.86	52.73	45.24	0.85	33.08	48.67	8.67	42.56	20.19	17.50
	3	15.13	18.13	36.09	73.53	21.46	3.01	40.27	22.07	33.20	35.00	20.43	13.50
	4	15.96	20.03	32.39	53.94	43.73	1.09	28.75	56.25	11.92	24.50	15.78	14.22
	5	12.38	22.79	36.56	54.07	42.14	2.32	30.25	52.08	14.75	43.83	15.23	8.70
	6	13.99	16.05	35.19	74.80	21.67	1.42	32.07	44.73	12.20	45.35	9.33	15.68
TA	1	19.95	15.00	24.06	49.00	30.01	12.77	24.67	36.58	34.58	27.78	20.35	20.90
	2	12.54	16.82	38.52	48.95	39.11	4.30	27.25	13.33	48.17	24.58	27.65	3.88
	3	19.38	11.25	26.41	27.59	34.48	20.83	22.53	28.27	24.40	44.95	15.73	15.05
	4	17.47	12.88	50.38	57.50	18.09	14.78	7.73	20.80	46.60	36.83	27.65	5.98
WA	1	10.37	18.26	37.02	52.69	31.56	2.04	2.92	71.00	19.08	10.03	24.53	6.88
	2	8.19	35.06	32.79	48.73	14.00	8.63	3.67	86.44	7.22	16.33	53.83	3.96
	3	7.88	24.90	37.48	66.02	10.42	1.22	0.93	75.33	11.07	27.15	32.85	5.43
	4	8.78	25.74	35.38	71.59	11.86	6.60	3.33	39.67	30.00	28.68	38.23	4.73
	5	11.44	21.90	41.12	60.74	29.27	6.85	15.27	14.93	15.93	46.00	24.93	3.18
	6	13.41	25.32	37.22	82.88	10.72	3.54	23.67	52.67	12.33	45.60	20.43	3.53

Table S5. Correlations (Pearson) between the diversity of bacteria, fungi, protists and soil invertebrates across stages within each of the 16 studied chronosequences. See Appendix S1, Table S15 for the number of samples used within each chronosequence stage. Red and blue shading indicate significant ($P \leq 0.05$) positive and negative correlations, respectively.

Site	Group	Parameter	Invertebrates	Protists	Fungi
ALPS	**Protists**	**r**	0.651		
		P value	0.001		
		n	22		
	Fungi	**r**	0.468	0.802	
		P value	0.058	<0.001	
		n	17	17	
	Bacteria	**r**	0.263	0.658	0.761
		P value	0.249	0.001	0.001
		n	21	22	16
AZ	**Protists**	**r**	0.693		
		P value	0.003		
		n	16		
	Fungi	**r**	0.549	0.657	
		P value	0.028	0.004	
		n	16	17	
	Bacteria	**r**	0.593	0.601	0.204
		P value	0.02	0.014	0.448
		n	15	16	16
BOS	**Protists**	**r**	0.336		
		P value	0.285		
		n	12		
	Fungi	**r**	0.388	0.869	
		P value	0.212	<0.001	
		n	12	18	
	Bacteria	**r**	0.324	0.256	0.481
		P value	0.305	0.305	0.043
		n	12	18	18
BOV	**Protists**	**r**	0.289		
		P value	0.579		
		n	6		
	Fungi	**r**	0.402	0.951	
		P value	0.429	0.001	
		n	6	7	
	Bacteria	**r**	-0.185	0.53	0.279
		P value	0.725	0.177	0.503
		n	6	8	8
CAL	**Protists**	**r**	0.602		

		P value	0.002		
		n	24		
	Fungi	**r**	0.587	0.827	
		P value	0.004	<0.001	
		n	22	23	
	Bacteria	**r**	0.642	0.679	0.534
		P value	0.001	<0.001	0.009
		n	24	25	23
CH	**Protists**	**r**	0.736		
		P value	<0.001		
		n	27		
	Fungi	**r**	0.407	0.591	
		P value	0.035	0.001	
		n	27	27	
	Bacteria	**r**	0.351	0.581	0.525
		P value	0.073	0.001	0.003
		n	27	27	29
CI	**Protists**	**r**	0.641		
		P value	0.001		
		n	24		
	Fungi	**r**	0.792	0.831	
		P value	<0.001	<0.001	
		n	26	27	
	Bacteria	**r**	0.743	0.722	0.778
		P value	<0.001	<0.001	<0.001
		n	25	26	28
CO	**Protists**	**r**	0.401		
		P value	0.031		
		n	29		
	Fungi	**r**	0.156	0.422	
		P value	0.427	0.022	
		n	28	29	
	Bacteria	**r**	0.198	0.183	0.303
		P value	0.313	0.343	0.117
		n	28	29	28
HA	**Protists**	**r**			
		P value			
		n			
	Fungi	**r**	0.388		
		P value	0.212		
		n	12		
	Bacteria	**r**	0.34		0.702
		P value	0.307		0.016

		n	11		11
ICE	**Protists**	**r**	0.51		
		P value	0.009		
		n	25		
	Fungi	**r**	0.737	0.712	
		P value	<0.001	<0.001	
		n	23	23	
	Bacteria	**r**	0.376	0.341	0.497
		P value	0.064	0.095	0.016
		n	25	25	23
JOR	**Protists**	**r**	0.671		
		P value	0.004		
		n	16		
	Fungi	**r**	0.716	0.629	
		P value	0.002	0.004	
		n	16	19	
	Bacteria	**r**	0.538	0.699	0.734
		P value	0.031	0.001	<0.001
		n	16	19	19
MEX	**Protists**	**r**	0.43		
		P value	0.016		
		n	31		
	Fungi	**r**	0.368	0.643	
		P value	0.021	<0.001	
		n	39	31	
	Bacteria	**r**	0.351	0.714	0.73
		P value	0.031	<0.001	<0.001
		n	38	30	39
MI	**Protists**	**r**	0.011		
		P value	0.956		
		n	26		
	Fungi	**r**	0.133	0.658	
		P value	0.462	<0.001	
		n	33	35	
	Bacteria	**r**	-0.448	0.541	0.526
		P value	0.011	0.001	<0.001
		n	31	34	46
QL	**Protists**	**r**	0.499		
		P value	0.011		
		n	25		
	Fungi	**r**	0.232	0.41	
		P value	0.254	0.038	
		n	26	26	

	Bacteria	**r**	-0.103	0.229	0.053
		P value	0.61	0.26	0.793
		n	27	26	27
TA	**Protists**	**r**	0.405		
		P value	0.096		
		n	18		
	Fungi	**r**	0.732	0.738	
		P value	0.001	<0.001	
		n	17	18	
	Bacteria	**r**	0.524	0.51	0.633
		P value	0.026	0.026	0.005
		n	18	19	18
WA	**Protists**	**r**	0.251		
		P value	0.248		
		n	23		
	Fungi	**r**	0.579	0.674	
		P value	0.005	<0.001	
		n	22	26	
	Bacteria	**r**	-0.029	0.835	0.281
		P value	0.9	<0.001	0.173
		n	22	27	25

Table S6. Correlations (Spearman) between the diversity of soil bacteria, fungi, protists and invertebrates with environmental predictors and belowground biodiversity within each of the 16 studied chronosequences included in this study. See Appendix S1, Table S15 for number of samples within each chronosequence stage. Red and blue shading indicate significant ($P \leq 0.05$) positive and negative correlations, respectively.

	Group	Parameter	Belowground diversity	Plant cover	pH	Salinity	Clay+silt	Soil C	Soil P	CN	NP
ALPS	Bacteria	ρ	0.635	0.497	-0.005	-0.342	0.173	-0.049	-0.002	-0.320	0.003
		P-value	0.008	0.019	0.984	0.119	0.442	0.828	.992	0.146	0.988
		n	16	22	22	22	22	22	22	22	22
	Fungi	ρ	0.829	0.448	0.118	0.203	-0.14	-0.067	0.203	-0.483	-0.044
		P-value	<0.001	0.071	0.653	0.434	0.591	0.797	0.434	0.050	.866
		n	16	17	17	17	17	17	22	17	17
	Protists	ρ	0.941	0.63	-0.282	-0.095	-0.134	0.358	0.452	-0.388	0.425
		P-value	<0.001	0.001	0.192	0.665	0.541	0.093	0.031	0.067	0.043
		n	16	23	23	23	23	23	22	23	23
	Invertebrates	ρ	0.798	0.474	-0.549	0.096	0.122	0.639	0.659	-0.542	0.692
		P-value	<0.001	0.026	0.008	0.672	0.587	0.001	0.001	0.009	<0.001
		n	16	22	22	22	22	22	22	22	22
AZ	Bacteria	ρ	0.564	0.396	-0.019	0.53	0.396	0.489	0.421	-0.011	0.553
		P-value	0.028	0.094	0.937	0.02	0.094	0.033	0.073	0.966	0.014
		n	15	19	19	19	19	19	19	19	19
	Fungi	ρ	0.575	0.524	0.056	0.191	0.25	0.127	0.137	-0.255	0.140
		P-value	0.025	0.031	0.830	0.462	0.332	0.626	0.599	0.323	0.593
		n	15	17	17	17	17	17	17	17	17
	Protists	ρ	0.786	0.422	0.096	0.712	0.57	0.703	0.758	0.224	0.704
		P-value	0.001	0.092	0.714	0.001	0.017	0.002	0	0.388	0.002
		n	15	17	17	17	17	17	17	17	17
	Soil invertebrates	ρ	0.941	0.427	0.209	0.597	0.523	0.562	0.42	0.209	0.637
		P-value	<0.001	0.099	0.436	0.015	0.037	0.024	0.105	0.437	0.008
		n	15	16	16	16	16	16	16	16	16
BOS	Bacteria	ρ	0.678	0.337	0.105	-0.133	0.027	-0.125	0.125	-0.509	-0.032
		P-value	0.015	0.146	0.661	0.576	0.91	0.6	0.6	0.022	0.895
		n	12	20	20	20	20	20	20	20	20
	Fungi	ρ	0.883	0.381	-0.477	-0.376	0.338	0.537	0.463	-0.310	0.491
		P-value	<0.001	0.119	0.045	0.124	0.17	0.022	0.053	0.211	0.038
		n	12	18	18	18	18	18	18	18	18
	Protists	ρ	0.86	0.369	-0.511	-0.444	0.365	0.607	0.381	-0.125	0.518
		P-value	<0.001	0.131	0.03	0.065	0.136	0.008	0.119	0.621	0.028
		n	12	18	18	18	18	18	18	18	18
	Soil invertebrates	ρ	0.575	-0.121	-0.395	-0.425	-0.329	0.007	0.414	0.158	0.281
		P-value	0.05	0.709	0.203	0.169	0.297	0.983	0.181	0.624	0.377

		n	12	12	12	12	12	12	12	12	12
BOV	Bacteria	ρ	0.886	-0.719	-0.067	0.4	-0.546	-0.433	-0.55	-0.800	-0.283
		P-value	0.019	0.029	0.865	0.286	0.128	0.244	0.125	0.010	0.460
		n	6	9	9	9	9	9	9	9	9
	Fungi	ρ	0.754	-0.353	-0.539	0.371	0.113	-0.743	-0.287	-0.431	-0.060
		P-value	0.084	0.392	0.168	0.365	0.789	0.035	0.49	0.286	0.888
		n	6	8	8	8	8	8	8	8	8
	Protists	ρ	0.886	-0.704	-0.524	0.333	-0.309	-0.714	-0.476	-0.595	-0.357
		P-value	0.019	0.051	0.183	0.420	0.457	0.047	0.233	0.120	0.385
		n	6	8	8	8	8	8	8	8	8
	Soil invertebrates	ρ	0.334	0.097	-0.482	0.00	-0.447	-0.704	0.037	0.037	-0.927
		P-value	0.518	0.836	0.274	1.00	0.315	0.077	0.937	0.937	0.003
		n	6	7	7	7	7	7	7	7	7
CAL	Bacteria	ρ	0.955	0.139	0.861	-0.115	-0.184	0.273	0.493	0.312	0.052
		P-value	<0.001	0.509	<0.001	0.585	0.378	0.186	0.012	0.129	0.804
		n	21	25	25	25	25	25	25	25	25
	Fungi	ρ	0.645	0.214	0.734	0.307	0.077	0.272	0.693	0.328	-0.177
		P-value	0.002	0.327	<0.001	0.154	0.728	0.209	<0.001	0.127	0.418
		n	21	23	23	23	23	23	23	23	23
	Protists	ρ	0.848	0.042	0.732	0.17	0.051	0.266	0.546	0.241	-0.047
		P-value	<0.001	0.843	<0.001	0.415	0.809	0.199	0.005	0.245	0.825
		n	21	25	25	25	25	25	25	25	25
	Soil invertebrates	ρ	0.774	-0.121	0.591	-0.204	-0.243	0.382	0.231	0.039	0.301
		P-value	<0.001	0.572	0.002	0.338	0.252	0.065	0.278	0.856	0.152
		n	21	24	24	24	24	24	24	24	24
CH	Bacteria	ρ	0.668	0.363	-0.08	0.31	0.131	0.141	0.175	-0.303	0.287
		P-value	<0.001	0.053	0.68	0.102	0.497	0.466	0.364	0.110	0.132
		n	27	29	29	29	29	29	29	29	29
	Fungi	ρ	0.733	0.414	-0.368	0.439	-0.039	0.398	0.369	-0.222	0.468
		P-value	<0.001	0.025	0.049	0.017	0.84	0.032	0.049	0.248	0.011
		n	27	29	29	29	29	29	29	29	29
	Protists	ρ	0.845	0.431	-0.581	0.544	0.003	0.458	0.446	-0.337	0.413
		P-value	<0.001	0.025	0.001	0.003	0.989	0.016	0.02	0.085	0.032
		n	27	27	27	27	27	27	27	27	27
	Soil invertebrates	ρ	0.715	0.584	-0.554	0.593	-0.067	0.55	0.505	-0.204	0.480
		P-value	<0.001	0.001	0.003	0.001	0.74	0.003	0.007	0.307	0.011
		n	27	27	27	27	27	27	27	27	27
CI	Bacteria	ρ	0.897	0.577	-0.098	0.509	0.036	0.306	0.298	-0.190	0.273
		P-value	<0.001	0.001	0.614	0.005	0.854	0.107	0.117	0.323	0.152
		n	23	29	29	29	29	29	29	29	29
	Fungi	ρ	0.89	0.613	-0.225	0.482	-0.006	0.397	0.343	-0.350	0.394
		P-value	<0.001	<0.001	0.241	0.008	0.976	0.033	0.068	0.063	0.034

		n	23	29	29	29	29	29	29	29	29
	Protists	ρ	0.778	0.766	-0.361	0.784	0.325	0.674	0.536	-0.312	0.636
		P-value	<0.001	<0.001	0.064	0	0.098	0	0.004	0.113	<0.001
		n	23	27	27	27	27	27	27	27	27
	Soil invertebrates	ρ	0.846	0.466	-0.029	0.42	-0.154	0.251	0.232	-0.161	0.127
		P-value	<0.001	0.016	0.887	0.033	0.454	0.215	0.255	0.432	0.535
		n	23	26	26	26	26	26	26	26	26
CO	Bacteria	ρ	0.477	-0.303	0.217	0.115	0.387	-0.074	-0.125	0.094	0.081
		P-value	0.012	0.11	0.259	0.552	0.038	0.704	0.518	0.629	0.675
		n	27	29	29	29	29	29	29	29	29
	Fungi	ρ	0.609	-0.402	0.052	-0.076	-0.125	-0.244	-0.229	-0.136	-0.125
		P-value	0.001	0.031	0.788	0.694	0.518	0.201	0.232	0.481	0.518
		n	27	29	29	29	29	29	29	29	29
	Protists	ρ	0.803	-0.55	-0.253	0.093	-0.042	0.085	-0.036	0.011	0.244
		P-value	<0.001	0.002	0.177	0.627	0.827	0.656	0.849	0.953	0.194
		n	27	30	30	30	30	30	30	30	30
	Soil invertebrates	ρ	0.825	-0.477	-0.101	0.075	-0.266	0.194	-0.109	-0.044	0.264
		P-value	<0.001	0.009	0.601	0.698	0.162	0.312	0.575	0.821	0.167
		n	27	29	29	29	29	29	29	29	29
HA	Bacteria	ρ	0.809	-0.198	0.61	-0.522	-0.57	-0.512	-0.593	-0.297	-0.198
		P-value	0.003	0.518	0.027	0.067	0.042	0.074	0.033	0.325	0.517
		n	11	13	13	13	13	13	13	13	13
	Fungi	ρ	0.527	-0.349	0.503	-0.266	-0.524	-0.49	-0.594	-0.462	0.119
		P-value	0.096	0.266	0.095	0.404	0.080	0.106	0.042	0.131	0.713
		n	11	12	12	12	12	12	12	12	12
	Soil invertebrates	ρ	0.465	0.242	-0.106	0.155	-0.022	0.067	0.12	0.303	0.514
		P-value	0.15	0.449	0.744	0.631	0.946	0.836	0.711	0.339	0.087
		n	11	12	12	12	12	12	12	12	12
ICE	Bacteria	ρ	0.758	0.541	0.108	0.272	0.047	-0.14	-0.197	-0.333	0.278
		P-value	<0.001	0.005	0.607	0.189	0.823	0.504	0.345	0.104	0.179
		n	23	25	25	25	25	25	25	25	25
	Fungi	ρ	0.914	0.565	0.123	0.304	0.169	0.009	-0.089	-0.291	0.377
		P-value	<0.001	0.005	0.575	0.159	0.442	0.968	0.686	0.178	0.076
		n	23	23	23	23	23	23	23	23	23
	Protists	ρ	0.677	0.292	0.102	0.261	0.292	-0.005	0.002	-0.144	0.358
		P-value	<0.001	0.156	0.629	0.208	0.156	0.983	0.994	0.492	0.079
		n	23	25	25	25	25	25	25	25	25
	Soil invertebrates	ρ	0.773	0.367	-0.01	0.37	0.092	-0.191	0.303	-0.501	0.337
		P-value	<0.001	0.071	0.962	0.068	0.661	0.361	0.141	0.011	0.100
		n	23	25	25	25	25	25	25	25	25
JOR	Bacteria	ρ	0.603	-0.558	-0.258	-0.153	0.558	0.105	-0.095	0.179	-0.129
		P-value	0.013	0.01	0.271	0.519	0.01	0.658	0.691	0.450	0.587

		n	16	20	20	20	20	20	20	20	20
	Fungi	ρ	0.765	-0.322	-0.425	-0.514	0.322	-0.061	-0.058	0.526	-0.423
		P-value	0.001	0.178	0.07	0.024	0.178	0.805	0.813	0.021	0.071
		n	16	19	19	19	19	19	19	19	19
	Protists	ρ	0.709	-0.122	-0.431	-0.085	0.122	0.113	0.183	0.259	-0.186
		P-value	0.002	0.618	0.065	0.729	0.618	0.646	0.452	0.285	0.446
		n	16	19	19	19	19	19	19	19	19
	Soil invertebrates	ρ	0.871	-0.26	-0.426	-0.227	0.26	0.221	0.141	0.357	-0.278
		P-value	0	0.331	0.1	0.397	0.331	0.411	0.602	0.175	0.297
		n	16	16	16	16	16	16	16	16	16
MEX	Bacteria	ρ	0.791	0.259	0.405	0.348	0.147	0.177	0.523	-0.163	-0.113
		P-value	0	0.112	0.011	0.03	0.37	0.28	0.001	0.322	0.492
		n	30	39	39	39	39	39	39	39	39
	Fungi	ρ	0.778	0.154	0.408	0.215	0.122	0.096	0.229	-0.089	-0.103
		P-value	0	0.342	0.009	0.183	0.452	0.554	0.155	0.586	0.527
		n	30	40	40	40	40	40	40	40	40
	Protists	ρ	0.784	0.571	0.511	0.276	0.332	0.275	0.486	0.049	-0.269
		P-value	0	0.001	0.003	0.134	0.068	0.134	0.006	0.794	0.144
		n	30	31	31	31	31	31	31	31	31
	Soil invertebrates	ρ	0.718	-0.189	0.127	0.098	0.063	0.005	0.238	-0.196	-0.015
		P-value	0	0.248	0.442	0.553	0.702	0.978	0.144	0.231	0.930
		n	30	39	39	39	39	39	39	39	39
MI	Bacteria	ρ	0.816	-0.432	0.698	0.431	-0.159	-0.409	-0.359	-0.507	-0.341
		P-value	0	0.002	0	0.002	0.282	0.004	0.120	<0.001	0.018
		n	25	48	48	48	48	48	48	48	48
	Fungi	ρ	0.827	-0.323	0.672	0.495	-0.341	-0.401	-0.298	-0.535	-0.446
		P-value	0	0.025	0	0	0.018	0.005	0.040	<0.001	0.002
		n	25	48	48	48	48	48	48	48	48
	Protists	ρ	0.791	-0.016	0.335	0.159	-0.045	0.003	0.141	-0.048	-0.243
		P-value	0	0.926	0.049	0.363	0.798	0.988	0.419	0.786	0.159
		n	25	35	35	35	35	35	35	35	35
	Soil invertebrates	ρ	0.014	-0.01	-0.248	-0.526	0.112	0.235	0.169	0.329	-0.243
		P-value	0.946	0.956	0.165	0.002	0.536	0.188	0.347	0.061	0.159
		n	25	33	33	33	33	33	33	33	33
QL	Bacteria	ρ	0.595	0.02	0.672	-0.222	0.529	-0.41	-0.280	-0.221	-0.668
		P-value	0.002	0.919	0	0.247	0.003	0.027	0.141	0.249	<0.001
		n	25	29	29	29	29	29	29	29	29
	Fungi	ρ	0.599	-0.111	0.157	-0.147	0.147	-0.08	-0.067	0.170	-0.201
		P-value	0.002	0.58	0.436	0.463	0.465	0.693	0.738	0.397	0.316
		n	25	27	27	27	27	27	29	27	27
	Protists	ρ	0.667	-0.134	0.463	-0.036	0.336	0.019	-0.065	0.014	-0.323
		P-value	0	0.515	0.017	0.86	0.093	0.925	0.754	0.947	0.108

		n	25	26	26	26	26	26	26	26	26
	Soil invertebrates	ρ	0.59	0.105	0.114	0.111	0.108	0.375	0.070	-0.04	0.113
		P-value	0.002	0.601	0.573	0.581	0.591	0.054	0.730	0.867	0.575
		n	25	27	27	27	27	27	27	27	27
TA	Bacteria	ρ	0.922	0.00	0.568	-0.391	-0.41	-0.343	-0.468	-0.047	0.174
		P-value	0	1.00	0.011	0.098	0.081	0.151	0.043	0.847	0.477
		n	17	19	19	19	19	19	19	19	19
	Fungi	ρ	0.856	0.00	0.482	0.01	-0.427	0.064	-0.285	0.069	0.445
		P-value	0	1.00	0.043	0.968	0.077	0.800	0.251	0.785	0.064
		n	17	18	18	18	18	18	18	18	18
	Protists	ρ	0.855	0.00	0.605	-0.328	-0.194	-0.066	-0.477	0.344	0.414
		P-value	0	1.00	0.005	0.158	0.413	0.781	0.034	0.137	0.070
		n	17	20	20	20	20	20	20	20	20
	Soil invertebrates	ρ	0.632	0.00	0.484	-0.264	-0.593	-0.309	-0.168	-0.270	-0.248
		P-value	0.006	1.00	0.042	0.29	0.009	0.212	504	0.278	0.320
		n	17	18	18	18	18	18	18	18	18
WA	Bacteria	ρ	0.43	0.456	-0.309	0	0.516	0.246	-0.272	0.052	0.264
		P-value	0.052	0.017	0.116	0.999	0.006	0.216	0.170	0.797	0.184
		n	21	27	27	27	27	27	27	27	27
	Fungi	ρ	0.656	-0.004	0.056	-0.006	0.195	-0.17	-0.064	-0.293	-0.018
		P-value	0.001	0.983	0.785	0.975	0.34	0.406	0.755	0.146	0.929
		n	21	26	26	26	26	26	26	26	26
	Protists	ρ	0.665	0.337	-0.244	-0.162	0.456	0.112	-0.372	-0.002	0.273
		P-value	0.001	0.079	0.21	0.409	0.015	0.571	0.052	0.991	0.159
		n	21	28	28	28	28	28	28	28	28
	Soil invertebrates	ρ	0.607	0.068	-0.046	0.068	0.035	0.177	0.002	-0.189	0.091
		P-value	0.004	0.757	0.836	0.759	0.874	0.419	0.993	0.388	0.679
		n	21	23	23	23	23	23	23	23	23

Table S7. Summary for the best models predicting the relationship between selected stage and belowground biodiversity for 16 studied chronosequences. Models are ranked by significance, AICc and parsimony. AIC_c measures the relative goodness of fit of a given model; the lower its value, the more likely the model is correct. ΔAIC_c denotes the difference between the AIC_c of each model and that of the best model.

Diversity	Soil	Model	R^2	P value	AICc	DeltaAICc	Selected Model
Belowground biodiversity	**ALPS**	**Linear**	0.12	0.031	-12.00	6.46	
		Quadratic	0.53	0.001	-18.46	0.00	✓
		Cubic	0.54	0.006	-14.44	4.02	
	AZ	**Linear**	0.28	0.012	-21.56	4.15	
		Quadratic	0.58	0.001	-25.71	0.00	✓
		Cubic	0.58	0.002	-21.19	4.51	
	BOS	**Linear**	0.35	0.038	-19.92	0.00	✓
		Quadratic	0.39	0.078			
		Cubic	0.65	0.035	-16.17	3.76	
	BOV	**Linear**	0.53	0.154			
		Quadratic	0.82	0.074			
		Cubic	0.92	<0.001			✓
	CAL	**Linear**	0.01	0.737			
		Quadratic	0.56	0.000	-43.80	1.24	✓
		Cubic	0.65	<0.001	-45.04	0.00	
	CH	**Linear**	0.32	0.003	-41.16	0.00	✓
		Quadratic	0.35	0.010	-39.34	1.82	
		Cubic	0.35	0.031	-36.39	4.78	
	CI	**Linear**	0.10	0.401			
		Quadratic	0.27	0.017	-5.70	0.00	✓
		Cubic	0.27	0.013	-2.40	3.31	
	CO	**Linear**	0.04	0.273			
		Quadratic	0.07	0.510			
		Cubic	0.47	0.004			✓
	HA	**Linear**	0.06	0.504			
		Quadratic	0.39	0.135			**Undetermined**
		Cubic	0.39	0.291			

	ICE	**Linear**	0.21	0.013	-42.73	0.00	✓
		Quadratic	0.22	0.027	-39.86	2.88	
		Cubic	0.22	0.050	-36.69	6.04	
	JOR	**Linear**	0.07	0.070			
		Quadratic	0.09	0.018	-21.03	0.00	✓
		Cubic	0.24	0.031	-19.45	1.58	
	MEX	**Linear**	0.10	0.121			
		Quadratic	0.30	0.073			
		Cubic	0.34	0.006			✓
	MI	**Linear**	0.16	0.033	-42.31	1.34	✓
		Quadratic	0.18	0.113			
		Cubic	0.38	0.006	-43.66	0.00	
	QL	**Linear**	0.22	0.033	-55.10	4.68	
		Quadratic	0.31	0.020	-55.33	4.45	
		Cubic	0.49	0.000	-59.78	0.00	✓
	TA	**Linear**	0.01	0.708			
		Quadratic	0.33	0.028			✓
		Cubic	0.41	0.093			
	WA	**Linear**	0.15	0.350			
		Quadratic	0.25	0.138			
		Cubic	0.30	0.047			✓
Bacteria	**ALPS**	**Linear**	0.01	0.343			
		Quadratic	0.49	0.002	313.92	0.00	✓
		Cubic	0.49	0.006	317.19	3.27	
	AZ	**Linear**	0.05	0.040	284.93	0.00	✓
		Quadratic	0.19	0.000	284.98	0.05	
		Cubic	0.25	0.001	287.27	2.34	
	BOS	**Linear**	0.00	0.733			
		Quadratic	0.00	0.799			Undetermined
		Cubic	0.35	0.245			
	BOV	**Linear**	0.75	0.003	141.83	0.00	✓
		Quadratic	0.75	0.020	148.89	7.06	
		Cubic	0.78	0.073			
	CAL	**Linear**	0.35	0.351			

		Quadratic	0.37	0.005	350.26	0.00	✓
		Cubic	0.44	0.004	350.41	0.15	
	CH	**Linear**	0.10	0.231			
		Quadratic	0.10	0.347			Undetermined
		Cubic	0.11	0.602			
	CI	**Linear**	0.13	0.127			
		Quadratic	0.19	0.034	443.56	0.00	✓
		Cubic	0.19	0.045	446.49	2.93	
	CO	**Linear**	0.19	0.039	365.35	4.42	
		Quadratic	0.19	0.152			
		Cubic	0.43	0.002	360.93	0.00	✓
	HA	**Linear**	0.01	0.715			
		Quadratic	0.55	0.002			✓
		Cubic	0.57	0.089			
	ICE	**Linear**	0.22	0.023	352.73	0.00	✓
		Quadratic	0.24	0.065			
		Cubic	0.26	0.173			
	JOR	**Linear**	0.02	0.293			
		Quadratic	0.03	0.506			Undetermined
		Cubic	0.33	0.176			
	MEX	**Linear**	0.01	0.817			
		Quadratic	0.29	0.006	521.24	2.52	
		Cubic	0.37	0.000	518.72	0.00	✓
	MI	**Linear**	0.19	0.001	730.17	8.65	
		Quadratic	0.20	0.003	732.08	10.55	
		Cubic	0.39	<0.001	721.52	0.00	✓
	QL	**Linear**	0.25	0.005	421.03	1.44	✓
		Quadratic	0.31	0.006	421.22	1.63	
		Cubic	0.41	0.001	419.59	0.00	
	TA	**Linear**	0.02	0.946			
		Quadratic	0.25	0.052			✓
		Cubic	0.26	0.078			
	WA	**Linear**	0.12	0.152			
		Quadratic	0.37	0.001	395.18	0.00	✓

		Cubic	0.38	0.003	397.73	2.55	
Fungi	**ALPS**	**Linear**	0.04	0.524			
		Quadratic	0.32	0.070			Undetermined
		Cubic	0.32	0.156			
	AZ	**Linear**	0.12	0.231			
		Quadratic	0.31	0.195			Undetermined
		Cubic	0.36	0.171			
	BOS	**Linear**	0.49	0.000	175.29	0.00	✓
		Quadratic	0.49	0.002	178.49	3.20	
		Cubic	0.59	0.001	178.57	3.28	
	BOV	**Linear**	0.21	0.439			
		Quadratic	0.54	0.145			Undetermined
		Cubic	0.71	0.246			
	CAL	**Linear**	0.22	0.049	231.83	3.33	
		Quadratic	0.41	0.008	228.50	0.00	✓
		Cubic	0.44	0.000	230.41	1.91	
	CH	**Linear**	0.21	0.073			
		Quadratic	0.32	0.038			✓
		Cubic	0.35	0.061			
	CI	**Linear**	0.05	0.417			
		Quadratic	0.20	0.022	304.99	0.00	✓
		Cubic	0.21	0.006	307.57	2.58	
	CO	**Linear**	0.00	0.946			
		Quadratic	0.00	0.994			Undetermined
		Cubic	0.13	0.206			
	HA	**Linear**	0.16	0.201			
		Quadratic	0.79	0.001	94.92	0.00	✓
		Cubic	0.79	0.028	101.20	6.29	
	ICE	**Linear**	0.18	0.016	224.90	0.00	✓
		Quadratic	0.20	0.061			
		Cubic	0.20	0.150	230.64	5.74	
	JOR	**Linear**	0.16	0.010	195.70	0.00	✓
		Quadratic	0.16	0.018	198.96	3.26	
		Cubic	0.31	0.039	199.05	3.35	

	MEX	**Linear**	0.01	0.518			
		Quadratic	0.16	0.073			
		Cubic	0.25	0.052	405.05	0.00	✓
	MI	**Linear**	0.31	<0.001	483.30	9.10	
		Quadratic	0.31	<0.001	485.23	11.03	
		Cubic	0.48	<0.001	474.20	0.00	✓
	QL	**Linear**	0.00	0.856			
		Quadratic	0.00	0.756			Undetermined
		Cubic	0.00	0.916			
	TA	**Linear**	0.14	0.126			
		Quadratic	0.35	0.042			✓
		Cubic	0.39	0.134			
	WA	**Linear**	0.01	0.779			
		Quadratic	0.08	0.383			Undetermined
		Cubic	0.08	0.377			
Protists	**ALPS**	**Linear**	0.13	0.004	250.19	4.11	
		Quadratic	0.36	0.002	246.07	0.00	✓
		Cubic	0.40	0.006	247.95	1.87	
	AZ	**Linear**	0.29	0.030	187.12	5.02	
		Quadratic	0.57	0.004	182.10	0.00	✓
		Cubic	0.57	0.020	186.22	4.12	
	BOS	**Linear**	0.35	0.002	197.81	0.00	✓
		Quadratic	0.36	0.009	200.89	3.09	
		Cubic	0.45	0.008	202.28	4.47	
	BOV	**Linear**	0.41	0.060			
		Quadratic	0.64	0.075			Undetermined
		Cubic	0.65	0.312			
	CAL	**Linear**	0.14	0.034	273.49	3.95	
		Quadratic	0.35	0.000	269.55	0.00	✓
		Cubic	0.35	0.001	272.71	3.16	
	CH	**Linear**	0.21	0.018			✓
		Quadratic	0.25	0.062			
		Cubic	0.26	0.132			
	CI	**Linear**	0.30	0.002	311.32	6.56	

		Quadratic	0.50	0.000	304.77	0.00	✓
		Cubic	0.51	0.000	307.33	2.57	
	CO	**Linear**	0.08	0.152			
		Quadratic	0.08	0.355			
		Cubic	0.29	0.054			✓
	ICE	**Linear**	0.09	0.039			✓
		Quadratic	0.10	0.118			
		Cubic	0.10	0.266			
	JOR	**Linear**	0.11	0.099			
		Quadratic	0.11	0.082			Undetermined
		Cubic	0.16	0.158			
	MEX	**Linear**	0.21	0.039	307.25	16.26	
		Quadratic	0.57	<0.001	290.99	0.00	✓
		Cubic	0.58	<0.001	293.03	2.05	
	MI	**Linear**	0.01	0.505			
		Quadratic	0.02	0.809			
		Cubic	0.07	0.810			
	QL	**Linear**	0.19	0.032	269.60	3.93	
		Quadratic	0.37	0.006	266.03	0.37	✓
		Cubic	0.44	<0.001	265.67	0.00	
	TA	**Linear**	0.05	0.350			
		Quadratic	0.17	0.199			Undetermined
		Cubic	0.32	0.079			
	WA	**Linear**	0.22	0.135			
		Quadratic	0.45	<0.001	286.43	0.00	✓
		Cubic	0.47	<0.001	288.52	2.09	
Invertebrates	**ALPS**	**Linear**	0.50	<0.001	158.39	3.04	
		Quadratic	0.62	<0.001	155.35	0.00	✓
		Cubic	0.62	<0.001	158.42	3.07	
	AZ	**Linear**	0.29	0.018	122.47	3.32	
		Quadratic	0.54	0.009	119.15	0.00	✓
		Cubic	0.57	0.006	122.51	3.36	
	BOS	**Linear**	0.45	0.018	75.09	0.00	✓
		Quadratic	0.47	0.060			

		Cubic	0.68	0.057	79.41	4.32	
	BOV	**Linear**	0.04	0.312			
		Quadratic	0.71	0.001	61.24	0.00	✓
		Cubic	0.99	0.002	77.32	16.08	
	CAL	**Linear**	0.00	0.476			
		Quadratic	0.53	0.000	171.65	0.00	✓
		Cubic	0.54	0.002	174.54	2.88	
	CH	**Linear**	0.36	0.001	209.28	0.00	✓
		Quadratic	0.36	0.004	212.03	2.75	
		Cubic	0.40	0.015	213.55	4.27	
	CI	**Linear**	0.00	1.000			
		Quadratic	0.04	0.577			Undetermined
		Cubic	0.04	0.703			
	CO	**Linear**	0.00	0.900			
		Quadratic	0.12	0.219			
		Cubic	0.31	0.036			✓
	HA	**Linear**	0.26	0.156			
		Quadratic	0.30	0.289			Undetermined
		Cubic	0.38	0.381			
	ICE	**Linear**	0.12	0.063			
		Quadratic	0.12	0.188			Undetermined
		Cubic	0.14	0.175			
	JOR	**Linear**	0.14	0.097			
		Quadratic	0.19	0.169			Undetermined
		Cubic	0.26	0.406			
	MEX	**Linear**	0.02	0.452			
		Quadratic	0.02	0.736			Undetermined
		Cubic	0.08	0.369			
	MI	**Linear**	0.10	0.036			✓
		Quadratic	0.12	0.094			
		Cubic	0.12	0.202			
	QL	**Linear**	0.01	0.378			
		Quadratic	0.03	0.635			Undetermined
		Cubic	0.03	0.832			

	TA	**Linear**	0.00	0.710			
		Quadratic	0.38	0.004	128.66	0.00	✓
		Cubic	0.47	0.002	129.54	0.88	
	WA	**Linear**	0.00	0.835			
		Quadratic	0.01	0.658			Undetermined
		Cubic	0.05	0.561			
Plants	**ALPS**	**Linear**	0.06	0.692			
		Quadratic	0.96	0.009			✓
		Cubic	0.99	0.120			
	AZ	**Linear**	0.18	0.037			✓
		Quadratic	0.50	0.706			
		Cubic	Undetermined	Undetermined			
	BOS	**Linear**	0.89	0.056			✓
		Quadratic	0.98	0.135			
		Cubic	NC	NC			
	BOV	**Linear**	0.97	0.017			✓
		Quadratic	0.99	0.076			
		Cubic	NC	NC			
	CAL	**Linear**	0.75	0.122			
		Quadratic	0.81	0.001			✓
		Cubic	0.89	0.409			
	CH	**Linear**	0.77	0.022			✓
		Quadratic	0.84	0.066			
		Cubic	0.84	0.229			
	CI	**Linear**	0.05	0.709			
		Quadratic	0.31	0.704			Undetermined
		Cubic	0.88	0.173			
	CO	**Linear**	0.02	0.864			
		Quadratic	0.02	0.967			Undetermined
		Cubic	0.03	0.937			
	HA	**Linear**	0.01	0.914			
		Quadratic	0.93	0.258			Undetermined
		Cubic	Undetermined	Undetermined			
	ICE	**Linear**	0.63	<0.001			✓

		Quadratic	0.68	0.003			
		Cubic	0.71	0.647			
	JOR	**Linear**	0.03	0.833			
		Quadratic	0.97	0.167			✓
		Cubic	Undetermined	Undetermined			
	MEX	**Linear**	0.00	0.923			
		Quadratic	0.02	0.781			Undetermined
		Cubic	0.02	0.768			
	MI	**Linear**	0.07	0.175			
		Quadratic	0.21	0.497			Undetermined
		Cubic	0.35	0.209			
	QL	**Linear**	0.09	0.610			
		Quadratic	0.13	0.889			Undetermined
		Cubic	0.16	0.351			
	TA	**Linear**	0.00	1.000			
		Quadratic	0.00	1.000			Undetermined
		Cubic	0.00	1.000			
	WA	**Linear**	0.88	0.006			✓
		Quadratic	0.88	0.040			
		Cubic	0.89	0.301			

Table S8. Correlations (Pearson) between the community composition of soil bacteria, fungi, invertebrates and protists for all the studied soil chronosequences. See Appendix S1, Table S15 for the number of samples used within each chronosequence stage. Red shading indicate significant ($P \leq 0.05$) positive correlations.

Site	Group	Parameter	Invertebrates	Protists	Fungi
ALPS	Protists	r	.590		
		P value	<.001		
	Fungi	r	.646	.748	
		P value	<.001	<.001	
	Bacteria	r	.636	.802	.850
		P value	<.001	<.001	<.001
AZ	Protists	r	.518		
		P value	<.001		
	Fungi	r	.318	.530	
		P value	.004	<.001	
	Bacteria	r	.333	.595	.403
		P value	.002	<.001	.001
BOS	Protists	r	.274		
		P value	.035		
	Fungi	r	.200	.486	
		P value	.070	<.001	
	Bacteria	r	.268	.652	.586
		P value	.030	<.001	<.001
BOV	Protists	r	.513		
		P value	.056		
	Fungi	r	.545	.867	
		P value	.047	.002	
	Bacteria	r	.687	.818	.909
		P value	.016	.019	.004
CAL	Protists	r	.398		
		P value	<.001		
	Fungi	r	.659	.467	
		P value	<.001	<.001	
	Bacteria	r	.577	.434	.827
		P value	<.001	<.001	<.001
CH	Protists	r	.721		
		P value	<.001		
	Fungi	r	.625	.764	
		P value	<.001	<.001	
	Bacteria	r	.618	.753	.657
		P value	<.001	<.001	<.001
CI	Protists	r	.615		

		P value	<.001		
	Fungi	r	.585	.867	
		P value	<.001	<.001	
	Bacteria	r	.654	.902	.869
		P value	<.001	<.001	<.001
CO	Protists	r	.403		
		P value	<.001		
	Fungi	r	.461	.742	
		P value	<.001	<.001	
	Bacteria	r	.389	.672	.683
		P value	<.001	<.001	<.001
HA	Fungi	r	.284		
		P value	.024		
	Bacteria	r	.186		.656
		P value	.111		<.001
ICE	Protists	r	.252		
		P value	.003		
	Fungi	r	.241	.390	
		P value	.001	<.001	
	Bacteria	r	.122	.239	.426
		P value	.141	.062	<.001
JOR	Protists	r	.063		
		P value	.223		
	Fungi	r	.101	.644	
		P value	.129	<.001	
	Bacteria	r	.055	.523	.496
		P value	.259	<.001	<.001
MEX	Protists	r	.380		
		P value	<.001		
	Fungi	r	.269	.667	
		P value	<.001	<.001	
	Bacteria	r	.296	.717	.652
		P value	<.001	<.001	<.001
MI	Protists	r	.594		
		P value	<.001		
	Fungi	r	.647	.783	
		P value	<.001	<.001	
	Bacteria	r	.682	.871	.871
		P value	<.001	<.001	<.001
QL	Protists	r	.296		
		P value	.004		
	Fungi	r	.191	.455	
		P value	.077	<.001	

	Bacteria	**r**	.485	.505	.571
		P value	<.001	<.001	<.001
TA	**Protists**	**r**	.349		
		P value	<.001		
	Fungi	**r**	.349	1.00	
		P value	<.001	<.001	
	Bacteria	**r**	.285	.711	.711
		P value	.005	<.001	<.001
WA	**Protists**	**r**	.400		
		P value	<.001		
	Fungi	**r**	.376	.841	
		P value	<.001	<.001	
	Bacteria	**r**	.438	.831	.780
		P value	<.001	<.001	<.001

Table S9. Correlations (Spearman) between the plant diversity (perennial plant richness; number of species) with environmental predictors within each of the 16 soil chronosequences studied. Red and blue shading indicate significant ($P \leq 0.05$) positive and negative correlations, respectively.

Chronosequence	Parameter	Plant cover	Soil C	Soil aP	Clay+silt	pH	Salinity	Soil C:N	Soil N:P	Shared pattern with belowground diversity
ALPS	ρ	0.900	0.361	0.357	-0.3	-0.333	-0.369	-0.671	0.384	
	P-value	<0.001	0.076	0.080	0.145	0.103	0.07	<0.001	0.058	✓
	n	25	25	25	25	25	25	25	25	
AZ	ρ	0.00	0.24	-0.256	-0.4	0.012	-0.039	0.628	0.209	
	P-value	1.00	0.307	0.276	0.081	0.961	0.871	0.003	0.376	
	n	20	20	20	20	20	20	20	20	
BOS	ρ	-0.105	0.515	0.458	0.211	-0.722	-0.405	0.119	0.515	
	P-value	0.658	0.02	0.042	0.372	<0.001	0.077	0.619	0.02	
	n	20	20	20	20	20	20	20	20	
BOV	ρ	0.800	0.14	0.481	0.6	0.186	-0.473	0.768	-0.279	
	P-value	<0.001	0.557	0.032	0.005	0.431	0.035	<0.001	0.233	
	n	20	20	20	20	20	20	20	20	
CAL	ρ	0.612	-0.266	0.566	-0.289	0.748	0.023	0.034	-0.453	
	P-value	0.001	0.198	0.003	0.162	<0.001	0.914	0.872	0.023	✓
	n	25	25	25	25	25	25	25	25	
CH	ρ	0.943	0.626	0.502	-0.143	-0.452	0.696	-0.098	0.639	
	P-value	<0.001	<0.001	0.005	0.451	0.012	<0.001	0.606	<0.001	✓
	n	30	30	30	30	30	30	30	30	
CI	ρ	0.334	0.114	0.116	0.03	-0.274	0.093	-0.78	0.212	
	P-value	0.071	0.549	0.541	0.873	0.142	0.623	<0.001	0.261	
	n	30	30	30	30	30	30	30	30	
CO	ρ	0.086	0.185	0.035	0.543	0.112	-0.08	0.369	0.152	
	P-value	0.652	0.328	0.855	0.002	0.557	0.674	0.045	0.422	
	n	30	30	30	30	30	30	30	30	
HA	ρ	-0.316	0.399	0.544	0.949	-0.29	0.278	0.00	-0.139	
	P-value	0.174	0.082	0.013	<0.001	0.215	0.235	1.00	0.559	
	n	20	20	20	20	20	20	20	20	
ICE	ρ	0.975	-0.495	0.225	0.154	0.205	0.423	-0.543	0.32	
	P-value	<0.001	0.012	0.279	0.463	0.325	0.035	0.005	0.119	✓
	n	25	25	25	25	25	25	25	25	
JOR	ρ	0.4	0.012	-0.209	-0.4	0.404	0.527	-0.411	0.45	
	P-value	0.081	0.961	0.376	0.081	0.077	0.017	0.072	0.047	
	n	20	20	20	20	20	20	20	20	
MEX	ρ	-0.229	-0.123	-0.516	-0.639	-0.277	-0.071	0.068	0.405	
	P-value	0.155	0.45	0.001	<0.001	0.083	0.664	0.677	0.01	

	n	40	40	40	40	40	40	40	40
MI	ρ	0.414	0.23	0.469	-0.037	-0.572	-0.369	0.362	0.18
	P-value	0.003	0.108	0.001	0.798	<0.001	0.008	0.01	0.21
	n	50	50	50	50	50	50	50	50
QL	ρ	0.348	0.023	0.282	-0.257	-0.404	0.267	0.071	0.134
	P-value	0.06	0.906	0.131	0.17	0.027	0.153	0.709	0.48
	n	30	30	30	30	30	30	30	30
TA	ρ	0.00	0.00	0.00	0.00	0.00	0.00	0.00	0.00
	P-value	1.00	1.00	1.00	1.00	1.00	1.00	1.00	1.00
	n	20	20	20	20	20	20	20	20
WA	ρ	0.600	0.403	-0.736	-0.143	-0.873	-0.626	0.781	0.883
	P-value	<0.001	0.027	<0.001	0.451	<0.001	<0.001	<0.001	<0.001
	n	30	30	30	30	30	30	30	30

Table S10. Summary for the best models predicting the relationship between stage and selected environmental factors for the 16 soil chronosequences studied. Models are ranked by significance, AIC and parsimony. AICc measures the relative goodness of fit of a given model; the lower its value, the more likely the model is correct. ΔAICc are difference between the AICc of each model and that of the best model.

Response variable	Soil	Model	R^2	P value	AICc	DeltaAICc	Selected Model
pH	**CAL**	**Linear**	0.09	0.148			
		Quadratic	0.39	0.006	57.44	0.00	✓
		Cubic	0.39	0.020	60.59	3.15	
	HA	**Linear**	0.28	0.017	28.60	8.93	
		Quadratic	0.46	0.012	26.18	6.50	
		Cubic	0.67	0.001	19.67	0.00	✓
	MEX	**Linear**	0.01	0.834			
		Quadratic	0.30	<0.001	22.40	1.10	✓
		Cubic	0.36	0.000	21.30	0.00	
	MI	**Linear**	0.67	<0.001	120.75	28.31	
		Quadratic	0.68	<0.001	120.90	28.46	
		Cubic	0.83	<0.001	92.44	0.00	✓
	QL	**Linear**	0.39	<0.001	61.74	39.71	
		Quadratic	0.74	<0.001	38.87	16.85	
		Cubic	0.86	<0.001	22.02	0.00	✓
	WA	**Linear**	0.93	<0.001	24.90	4.41	
		Quadratic	0.93	<0.001	26.23	5.74	
		Cubic	0.95	<0.001	20.50	0.00	✓
Salinity	**CH**	**Linear**	0.47	<0.001	324.98	4.54	
		Quadratic	0.54	<0.001	323.78	3.34	
		Cubic	0.62	<0.001	320.44	0.00	✓
Soil C:N	**BOV**	**Linear**	0.53	<0.001	115.21	0.00	✓
		Quadratic	0.54	<0.001	118.19	2.98	
		Cubic	0.59	0.007	119.11	3.90	

Table S11. Summary for the best models predicting the relationship between selected environmental variables and belowground biodiversity. Models are ranked by significance, AIC and parsimony. AICc measures the relative goodness of fit of a given model; the lower its value, the more likely the model is correct. ΔAICc are differences between the AICc of each model and that of the best model.

Predictor variable	Soil	Model	R^2	P value	AICc	DeltaAICc	Selected Model
pH	**CAL**	**Linear**	0.798	<0.001	-63.213	0.000	✓
		Quadratic	0.824	<0.001	-63.002	0.211	
		Cubic	0.834	<0.001	-60.764	2.449	
	HA	**Linear**	0.395	0.032	-28.502	0.893	✓
		Quadratic	0.455	0.060			
		Cubic	0.822	0.006	-29.395	0.000	
	MEX	**Linear**	0.240	0.005	-65.380	0.000	✓
		Quadratic	0.275	0.018	-64.120	1.260	
		Cubic	0.279	0.047	-61.380	4.000	
	MI	**Linear**	0.478	<0.001	-54.050	0.000	✓
		Quadratic	0.482	<0.001	-51.371	2.678	
		Cubic	0.514	<0.001	-49.818	4.232	
	QL	**Linear**	0.539	<0.001	-68.278	0.000	✓
		Quadratic	0.552	<0.001	-66.143	2.135	
		Cubic	0.577	0.001	-64.373	3.905	
	WA	**Linear**	0.110	0.042	-43.360	2.114	
		Quadratic	0.226	0.396			
		Cubic	0.412	0.004	-45.474	0.000	✓
Plant cover	**ALPS**	**Linear**	0.455	0.015	-19.678	0.000	✓
		Quadratic	0.517	0.011	-17.946	1.732	
		Cubic	0.560	0.002	-15.085	4.594	
	AZ	**Linear**	0.454	0.005	-25.757	0.000	✓
		Quadratic	0.518	<0.001	-23.807	1.950	
		Cubic	0.579	<0.001	-21.194	4.562	
	BOS	**Linear**	0.774	0.559			
		Quadratic	0.449	0.019	-17.132	0.000	✓
		Cubic	0.646	0.035	-16.165	0.966	
	CI	**Linear**	0.423	0.000	-14.072	0.000	✓

		Quadratic	0.436	0.002	-11.624	2.448	
		Cubic	0.439	<0.001	-8.445	5.628	
	CO	**Linear**	0.322	0.002	-67.095	4.058	
		Quadratic	0.349	0.010	-65.402	5.752	
		Cubic	0.530	<0.001	-71.154	0.000	✓
	ICE	**Linear**	0.167	0.049			✓
		Quadratic	0.232	0.096			
		Cubic	0.260	0.110			
Texture	**TA**	**Linear**	0.110	0.066			
		Quadratic	0.128	0.165			
		Cubic	0.414	0.066			✓
Salinity	**CH**	**Linear**	0.289	0.005	-39.902	0.672	✓
		Quadratic	0.374	0.008	-40.574	0.000	
		Cubic	0.385	0.023	-38.009	2.565	
Soil C:N	**BOV**	**Linear**	0.3089	0.053	6.87	0	✓
		Quadratic	0.7557	0.004	30.63	23.76	
		Cubic	0.8136	0.252			

Table S12. Mantel test correlations (Spearman) between number of chronosequence stage dissimilarity (Euclidean) and environmental factors dissimilarity (Euclidean). Red shading indicate significant ($P \leq 0.05$) positive correlations.

	Plant cover	Soil C	Soil P	pH	Salinity	Clay+silt	CN	NP
ALPS	.338	.511	.468	.616		.609	.227	.681
AZ	.659		.332		.387	.964		.262
BOS	.659		.193	.340		.659		.261
BOV	.746		.143			.616	.405	
CAL			.704	.201	.393	.292		.365
CH	.726	.305	.236	.396	.404	.469		.489
CI	.566	.358	.535		.473	.845	.151	.237
CO	.285	.151	.178	.125		.485		
HA	.181		.160	.249		.355		.225
ICE	.681				.131	.259	.299	.203
JOR	.210			.457	.234	.210	.254	.341
MEX	.443	.282		.216	.186	.377		.255
MI	.263	.210	.124	.606	.441	.652	.275	.321
QL	.507			.304		.645		.457
TA		.214	.152			.659		.133
WA	.418	.386	.748	.892	.322	.452	.557	.763

Table S13. Mantel test correlations (Spearman) between environmental factors dissimilarity (Euclidean) and soil belowground community dissimilarity (Bray-Curtis). Red shading indicate significant ($P \leq 0.05$) positive correlations.

	Plant cover	C	aP	pH	Salinity	Clay+silt	CN	NP
ALPS	.387	.574	.439	.711		.632		.672
AZ	.483		.360		.235	.367		
BOS	.613			.328		.661		
BOV	.732		.639					
CAL			.612	.507	649	.319		.267
CH	.706	.205	.323	.510	.338			.508
CI	.298						.318	.194
CO	.182			.459		.371		
HA	.331		.423	.646		.559		
ICE	.299				.252	.319	.320	.315
JOR					.471			
MEX	.207	.292		.501	.365	.364		
MI	.155		.260	.596	.518	.561		
QL	.139			.537		.587		.472
TA		.432	.399			.195		
WA	.595	.576	.682	.684	.410	.587		.527

Table S14. Correlation (Spearman) between the relative abundance of soil bacteria, fungi, protists and invertebrates at the class level. Only positive correlations between abundance of taxa and pH or plant cover are shown. A "-" symbol indicates that this taxon was not found in this chronosequence. $^{b}P < 0.10$; $^{a}P = 0.06$; $*P \leq 0.05$; $**P < 0.01$. Red shading indicate positive correlations.

Environmental cluster	Group	Taxa	ICE	CI	BOS	AZ	ALPS
Plant cover	Bacteria	Anaerolineae	0.10	**0.41***	**0.53^{b}**	0.09	0.40
	Bacteria	Betaproteobacteria	**0.62****	0.10	0.16	0.03	0.20
	Bacteria	Planctomycetia	0.04	0.35	**0.51^{b}**	0.36	0.38
	Fungi	Blastocladiomycetes	0.07	0.22	0.27	**0.62***	**0.47^{a}**
	Fungi	Glomeromycetes	0.00	0.34	**0.55^{a}**	0.42	**0.43^{b}**
	Protists	Raphidpennate	-	0.33	**0.70***	0.29	0.10
	Protists	Sandonidae	0.22	0.12	0.39	**0.46^{b}**	0.17
	Protists	Sorogenidae	0.15	**0.39^{a}**	0.08	0.20	**0.59***
	Protists	Urostylidae	0.18	0.02	**0.55^{a}**	0.35	**0.54***
Environmental cluster	**Group**	**Taxa**	**QL**	**MI**	**MEX**	**HA**	**CAL**
pH	Bacteria	Acidobacteria.6	**0.40***	**0.85****	**0.39***	**0.55^{b}**	**0.95****
	Bacteria	Opitutae	0.33	**0.68****	0.11	0.32	**0.67****
	Bacteria	Acidimicrobiia	0.26	**0.84****	0.17	**0.61***	**0.85****
	Bacteria	Anaerolineae	0.32	**0.79****	**0.35^{a}**	**0.55^{b}**	0.02
	Bacteria	Cytophagia	0.30	**0.68****	**0.65****	**0.65***	**0.82****
	Bacteria	Saprospirae	**0.60****	**0.75****	0.19	0.37	0.16
	Protists	Mb5C lineage	0.06	**0.54****	**0.72****	-	0.19
	Protists	Filamoebidae	**0.38***	**0.48***	**0.54****	-	0.37
	Protists	Sorogenidae	**0.40***	0.06	0.26	-	0.05
	Protists	Thaumatomonadidae	**0.52****	**0.58****	**0.51****	-	**0.77****
	Protists	Chrysophyceae Clade C	0.20	**0.66****	**0.80****	-	**0.67****

Table S15. Number of soil samples that passed the cut-off after rarefaction for single groups of belowground organisms and for belowground biodiversity in each stage and soil chronosequence. These data were used for statistical modelling out of five possible. A "-" symbol indicates no data.

Chronosequence	Stage	Bacteria	Fungi	Protists	Invertebrates	Belowground diversity
ALPS	1	5	2	5	4	2
	2	5	4	5	5	4
	3	5	4	5	5	4
	4	4	4	5	5	3
	5	3	3	3	3	3
AZ	1	5	4	4	3	3
	2	5	4	4	4	4
	3	4	5	5	5	4
	4	5	4	4	4	4
BOS	1	5	5	5	1	1
	2	5	4	4	4	4
	3	5	4	4	2	2
	4	5	5	5	5	5
BOV	1	2	1	2	1	1
	2	1	1	1	2	1
	3	3	3	2	1	1
	4	3	3	3	3	3
CAL	1	5	5	5	5	5
	2	5	5	5	5	5
	3	5	3	5	4	2
	4	5	5	5	5	5
	5	5	5	5	5	4
CH	1	5	5	4	4	4
	2	5	5	4	4	4
	3	5	5	5	5	5
	4	5	5	5	5	5
	5	5	5	5	5	5
	6	4	4	4	4	4
CI	1	5	5	5	4	4
	2	5	5	5	4	4

	3	5	5	5	5	5
	4	5	5	3	5	3
	5	4	4	4	4	3
	6	5	5	5	4	4
CO	1	5	5	5	5	5
	2	5	5	5	5	5
	3	4	4	5	5	3
	4	5	5	5	5	5
	5	5	5	5	4	4
	6	5	5	5	5	5
HA	1	5	4	-	4	4
	2	3	4	-	4	3
	3	3	2	-	2	2
	4	2	2	-	2	2
ICE	1	5	5	5	5	5
	2	5	3	5	5	3
	3	5	5	5	5	5
	4	5	5	5	5	5
	5	5	5	5	5	5
JOR	1	5	5	5	5	5
	2	5	4	4	4	4
	3	5	5	5	4	4
	4	5	5	5	3	3
MEX	1	5	5	4	5	4
	2	5	5	4	5	4
	3	4	5	5	5	4
	4	5	5	4	5	4
	5	5	5	5	5	5
	6	5	5	3	5	3
	7	5	5	2	4	2
	8	5	5	4	5	4
MI	1	5	5	5	2	2
	2	5	5	5	4	4
	3	4	4	4	3	2
	4	5	5	5	2	2

	5	5	5	4	5	4
	6	5	5	4	4	4
	7	5	4	2	3	2
	8	4	5	1	2	1
	9	5	5	1	4	1
	10	5	5	4	4	3
QL	1	5	4	3	5	3
	2	5	4	4	4	4
	3	5	5	5	5	5
	4	4	4	4	4	4
	5	5	5	5	4	4
	6	5	5	5	5	5
TA	1	5	5	5	4	4
	2	4	4	5	4	4
	3	5	5	5	5	5
	4	5	4	5	5	4
WA	1	5	4	5	4	4
	2	3	2	3	3	2
	3	4	5	5	5	4
	4	5	5	5	5	5
	5	5	5	5	5	5
	6	5	5	5	1	1

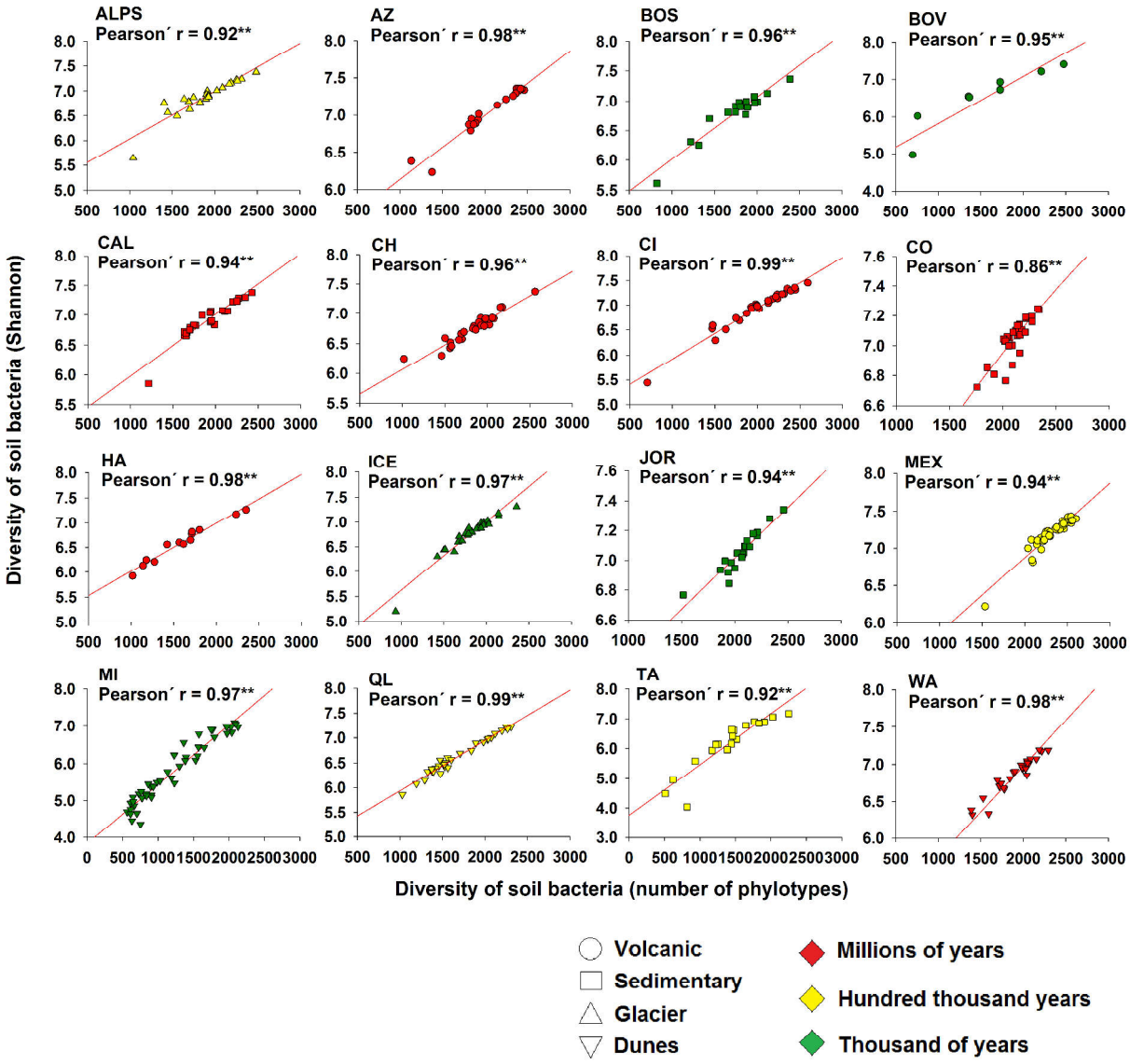

Figure S1. Relationships between number of phylotypes and Shannon diversity of soil bacteria in 16 globally distributed soil chronosequences.

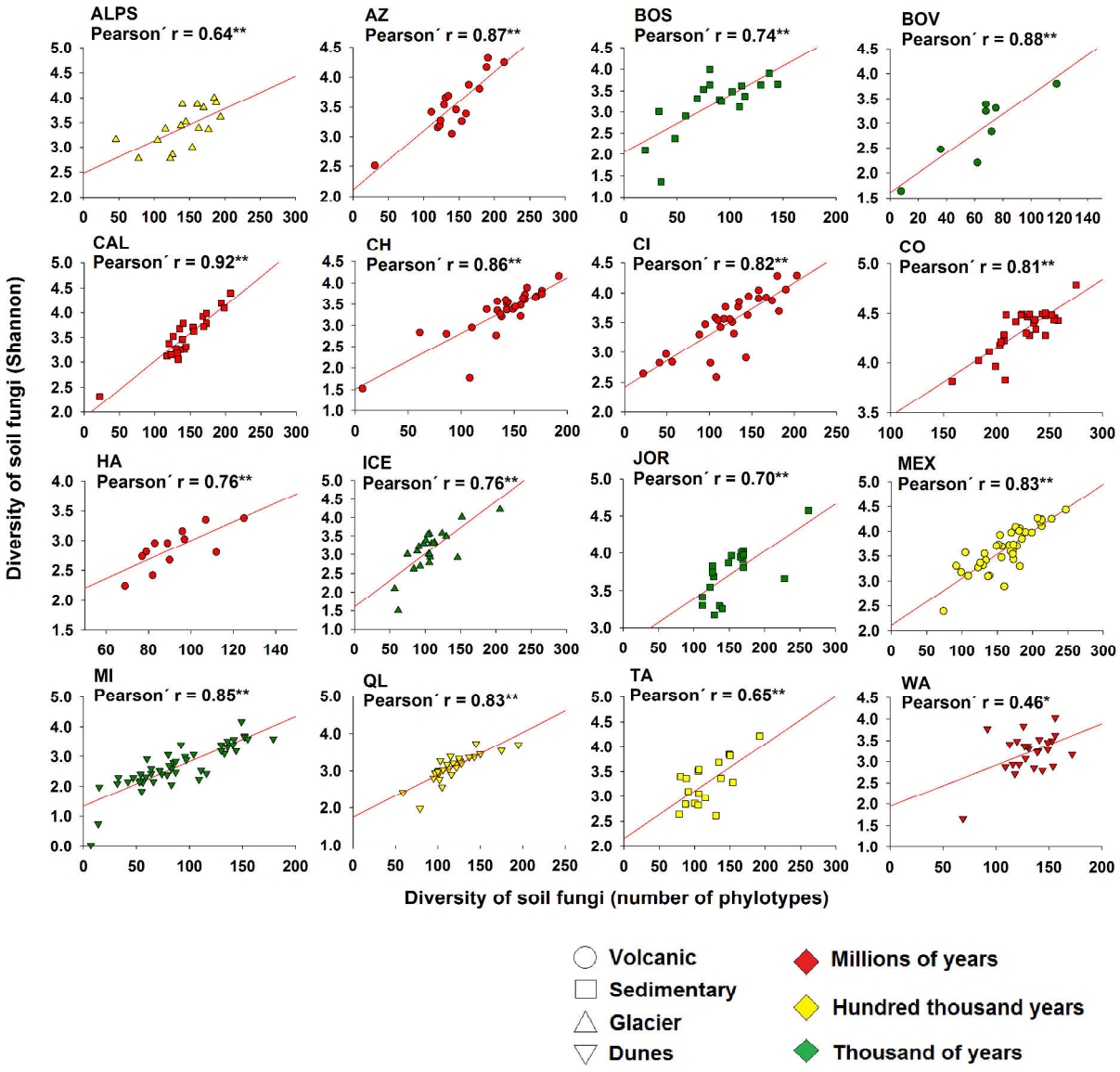

Figure S2. Relationships between number of phylotypes and Shannon diversity of soil fungi in 16 globally distributed soil chronosequences.

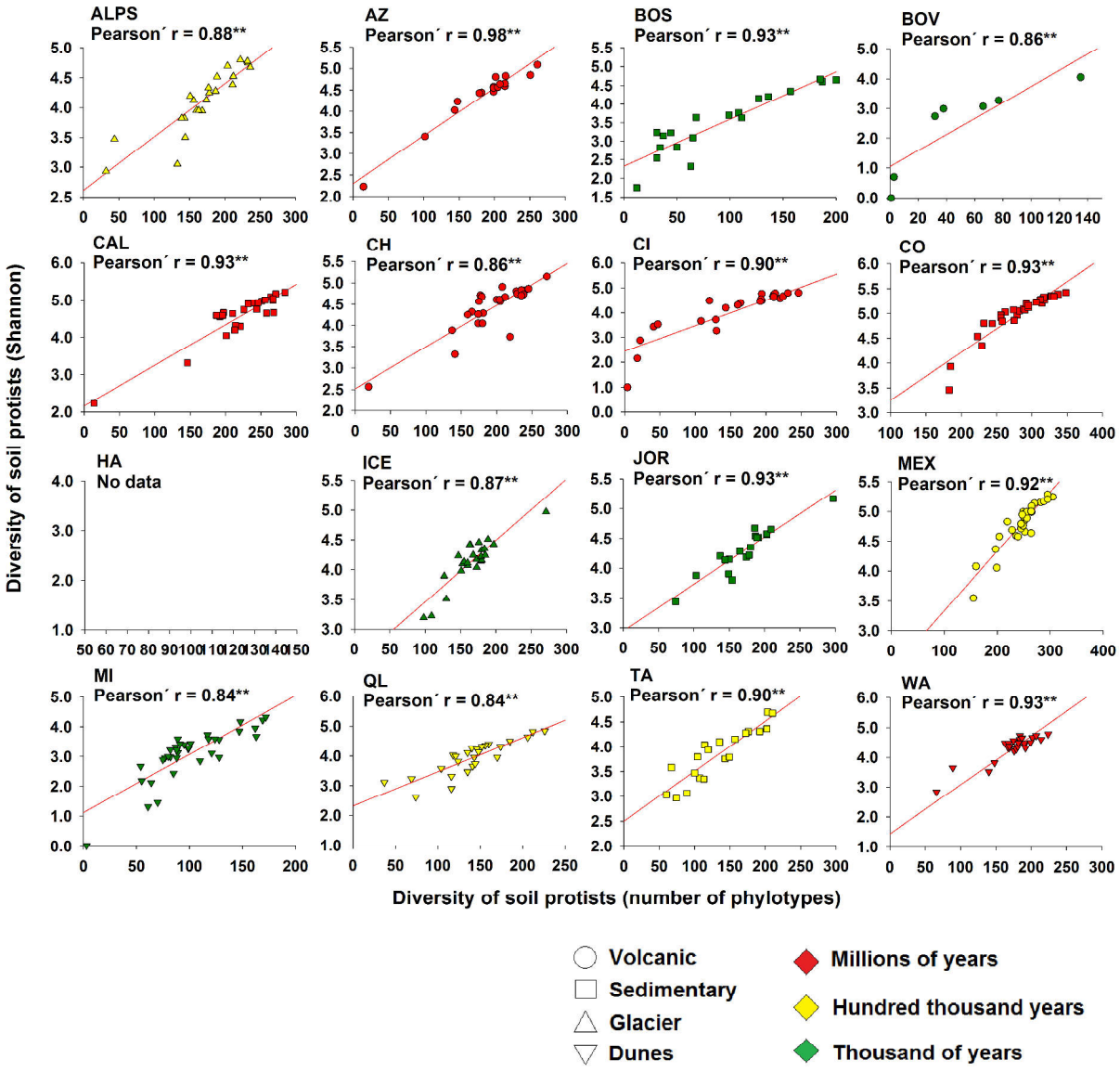

Figure S3. Relationships between number of phylotypes and Shannon diversity of soil protists in 16 globally distributed soil chronosequences.

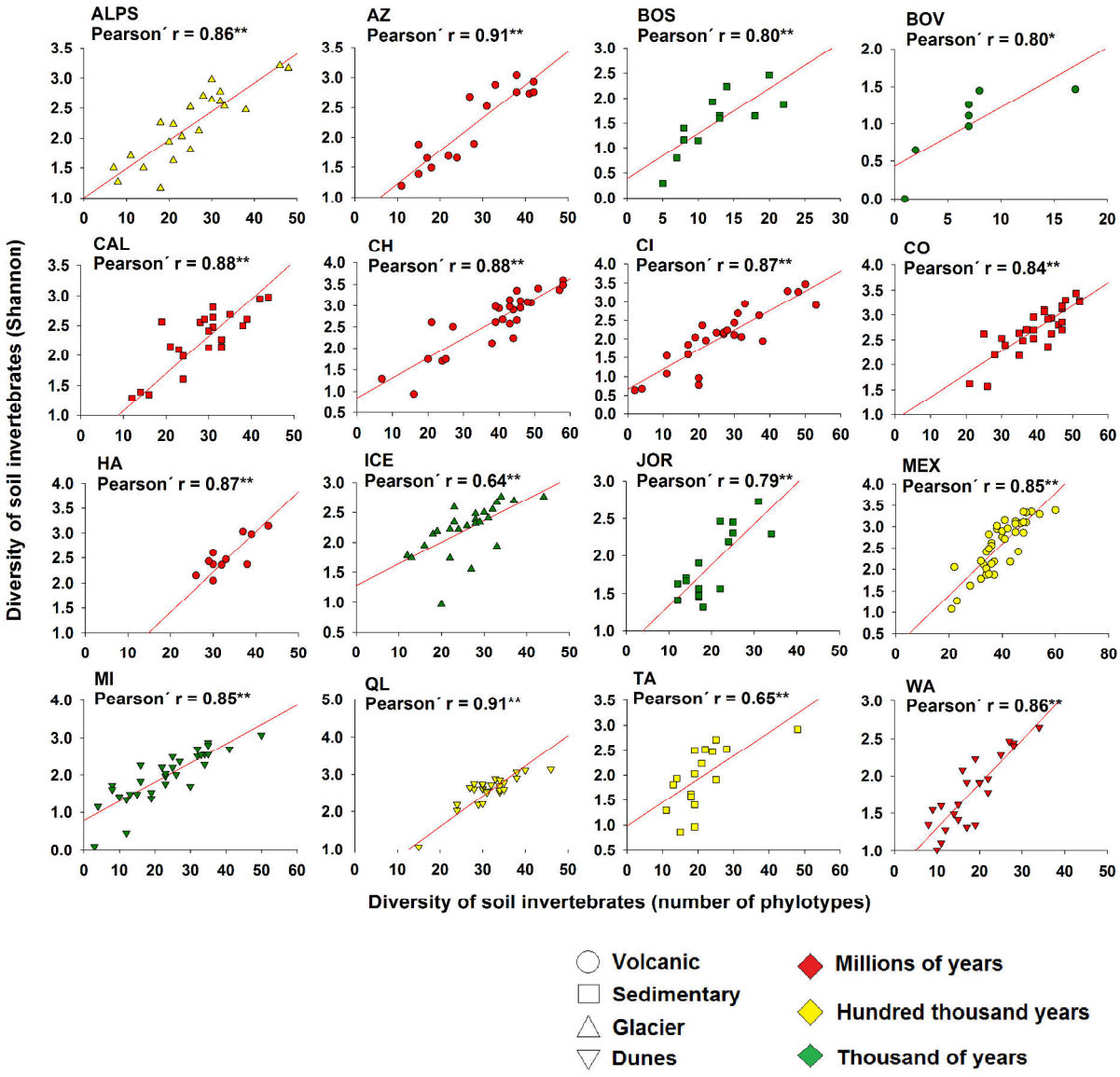

Figure S4. Relationships between number of phylotypes and Shannon diversity of soil invertebrates in 16 globally distributed soil chronosequences.

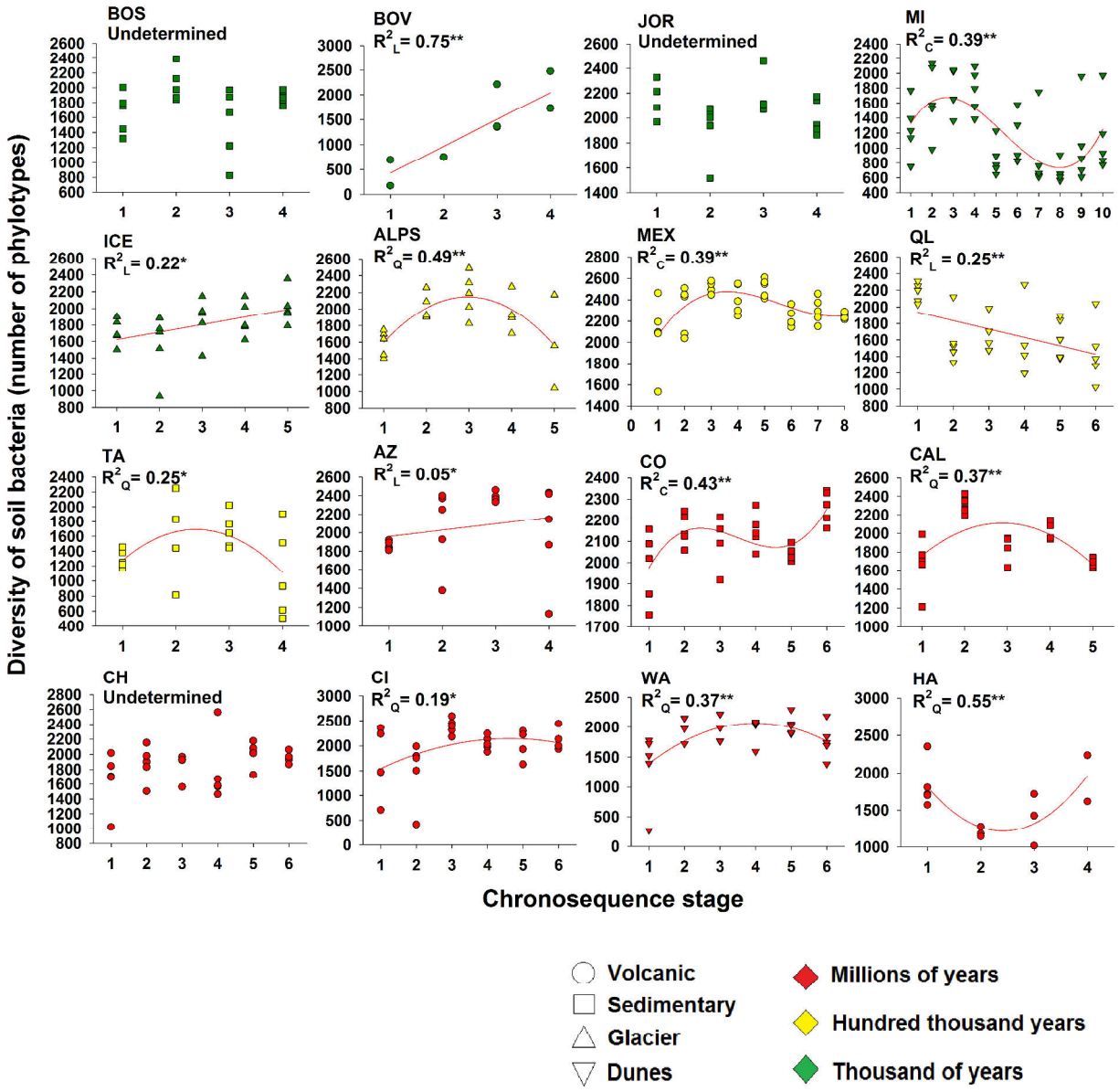

Figure S5. Relationships between chronosequence stage and the diversity of soil bacteria in 16 globally distributed soil chronosequences. No line indicates that a model could not be fitted to the data.

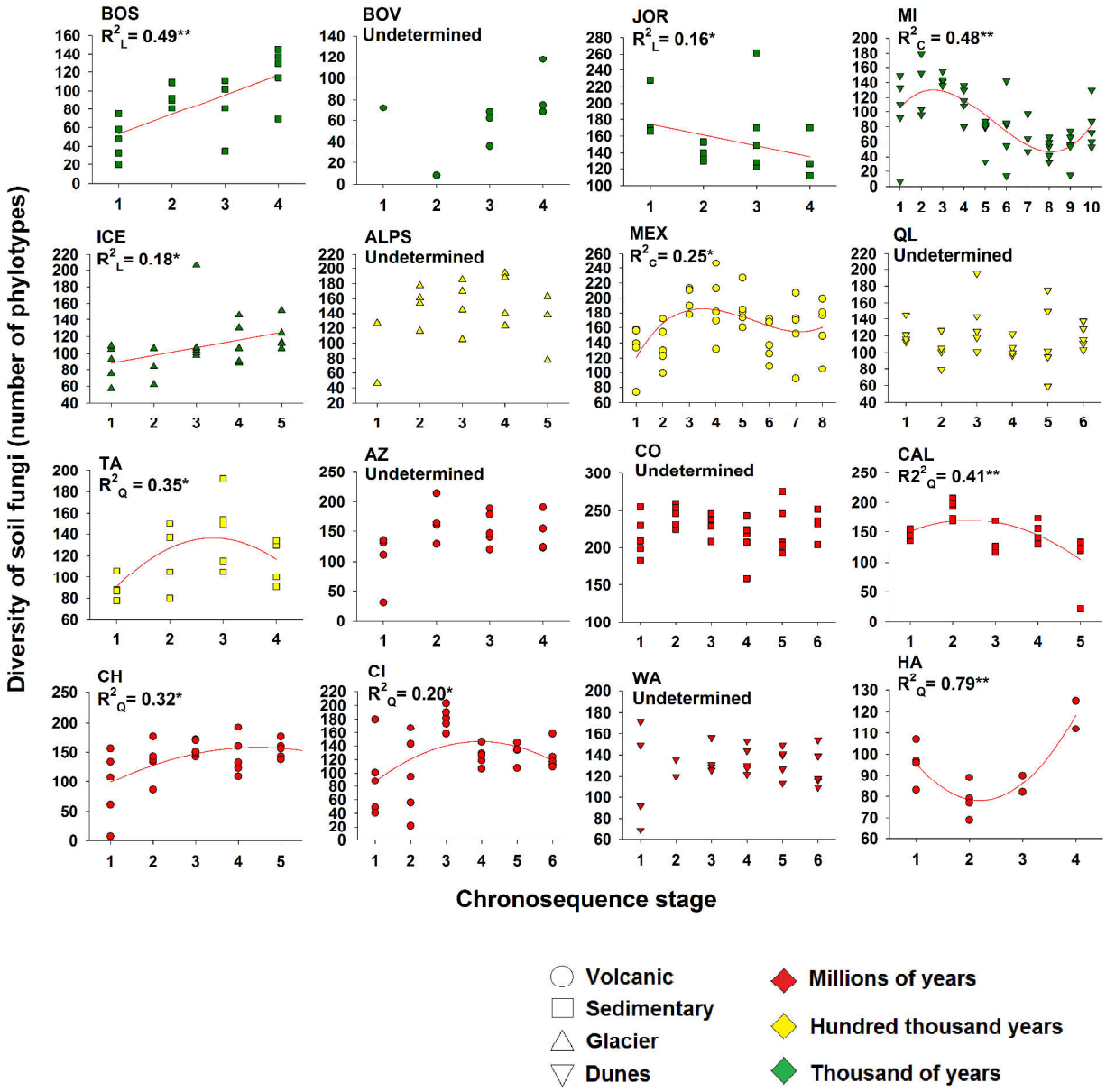

Figure S6. Relationships between chronosequence stage and the diversity of soil fungi in 16 globally distributed soil chronosequences. No line indicates that a model could not be fitted to the data.

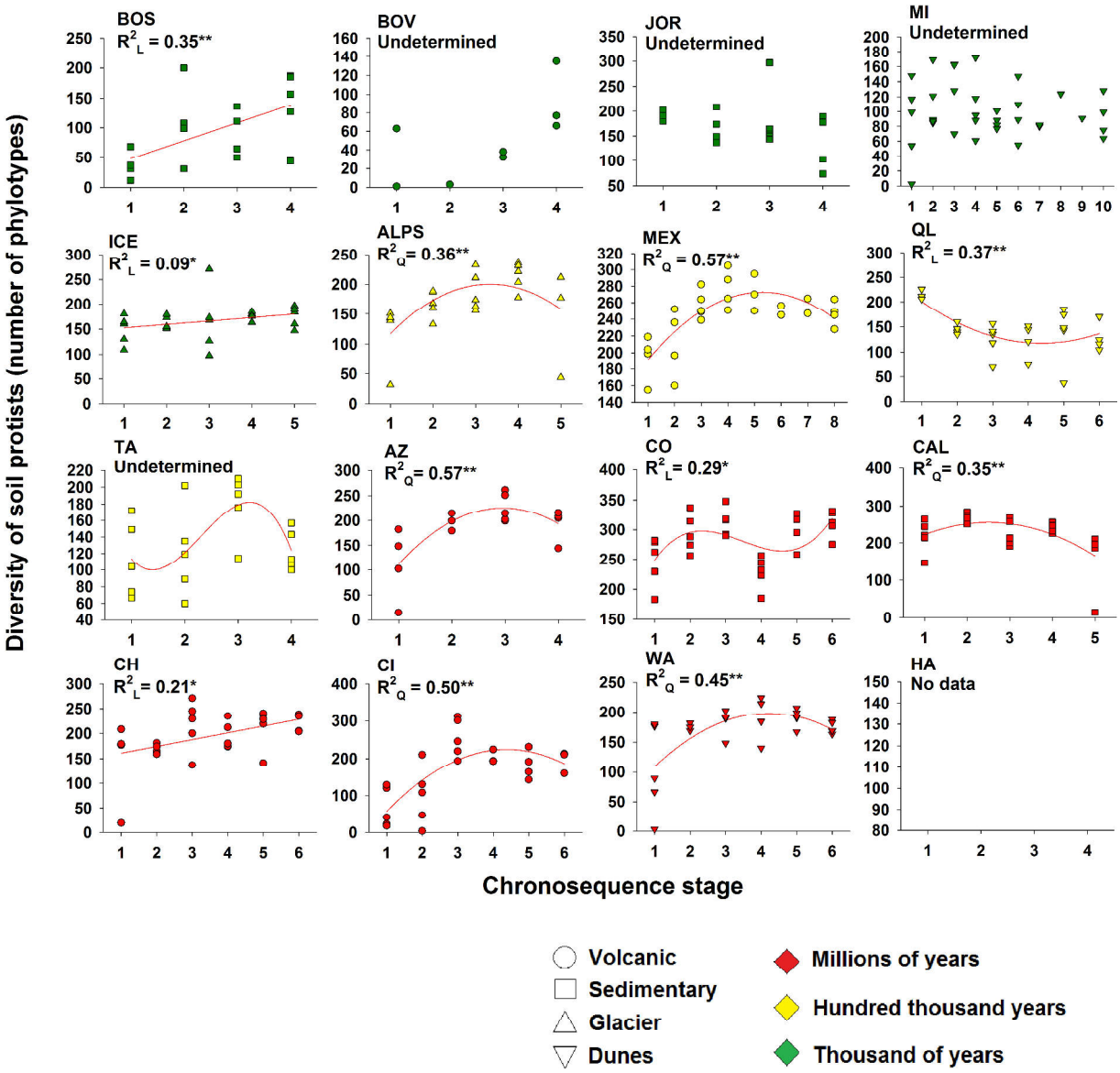

Figure S7. Relationships between chronosequence stage and the diversity of soil protists in 16 globally distributed soil chronosequences. No line indicates that a model could not be fitted to the data.

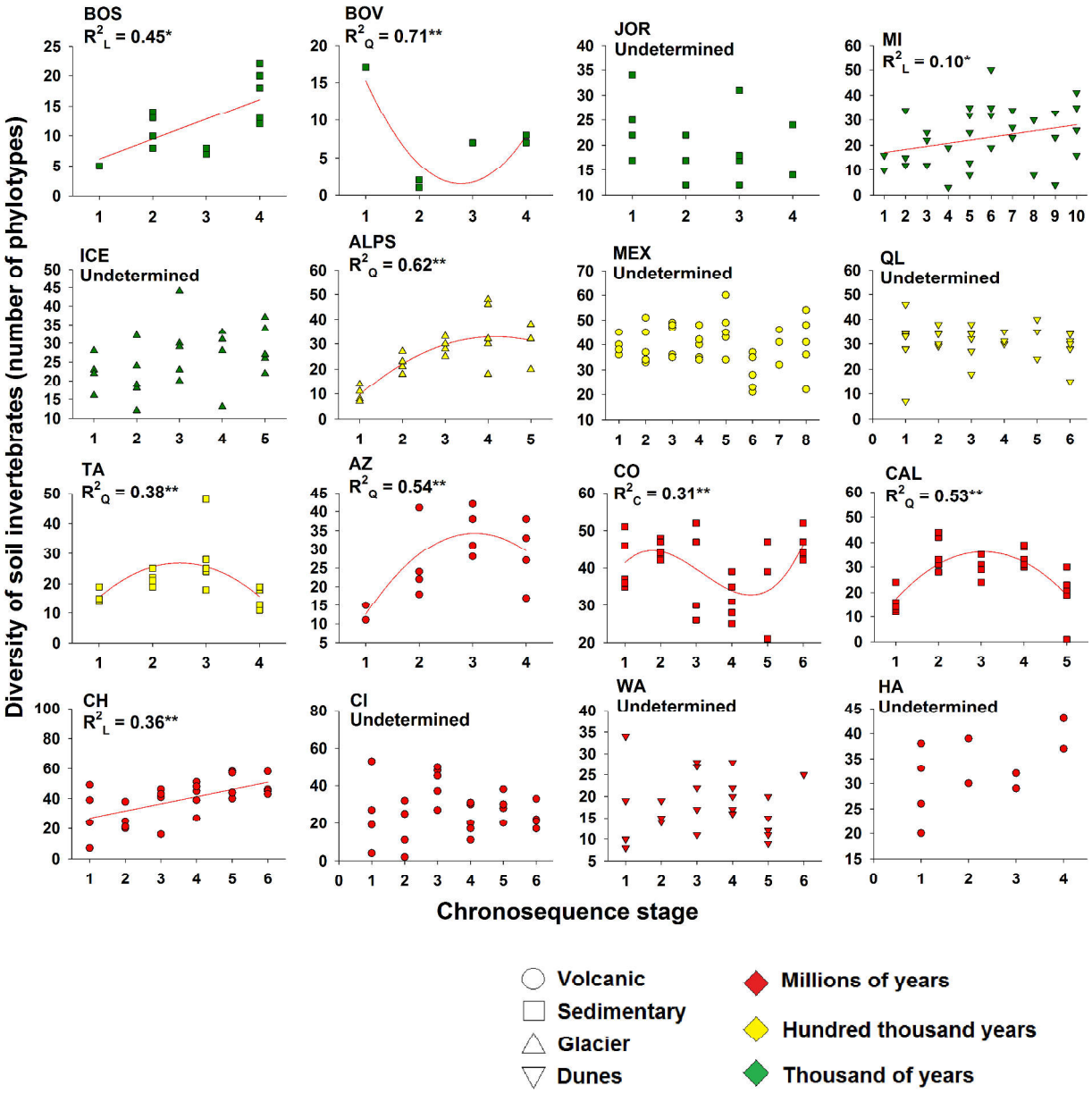

Figure S8. Relationships between chronosequence stage and the diversity of soil invertebrates in 16 globally distributed soil chronosequences. No line indicates that a model could not be fitted to the data.

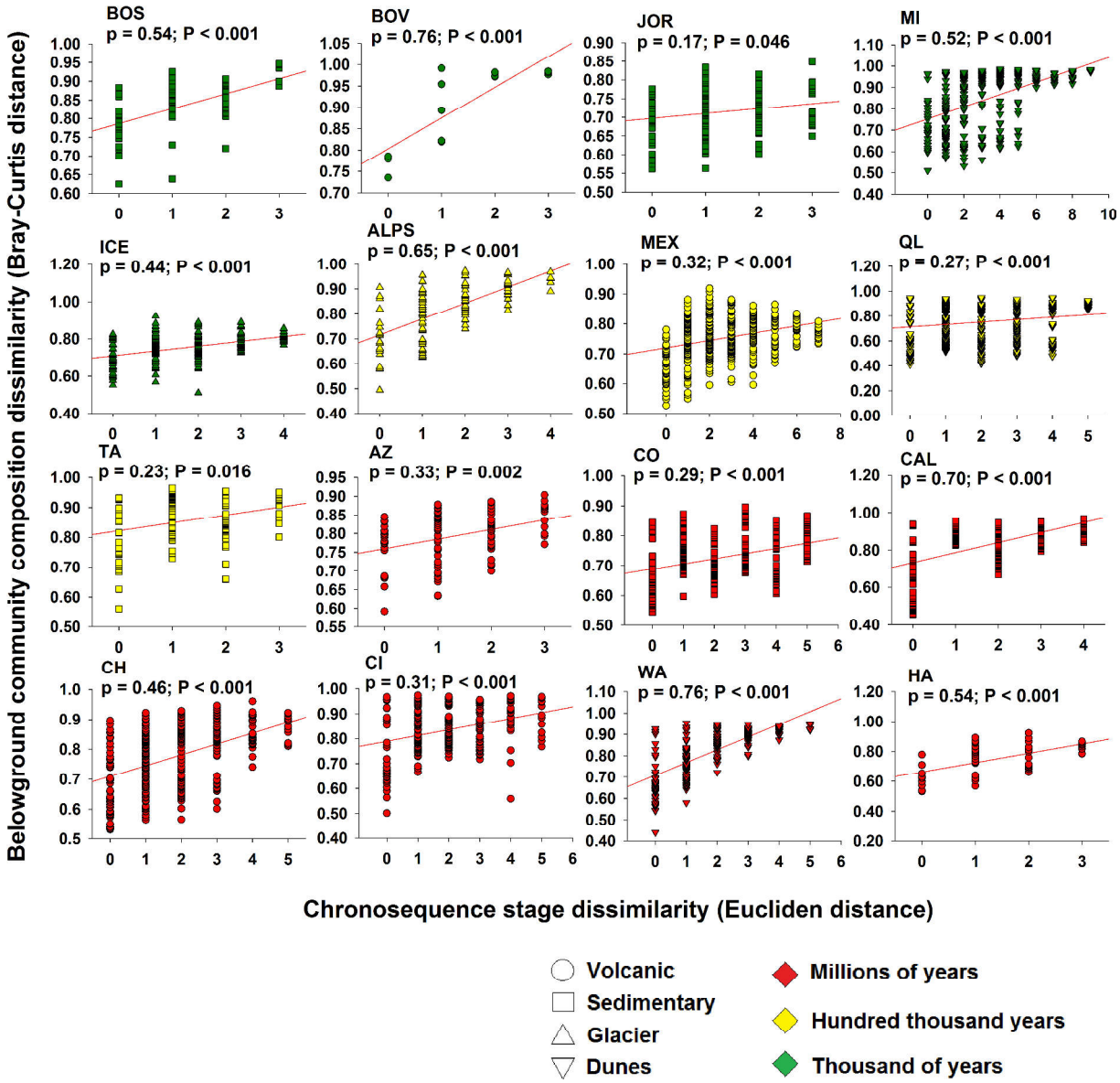

Figure S9. Mantel correlation (Spearman, p) between belowground community dissimilarity (bacteria, fungi, protists and invertebrates) (Bray-Curtis distance) and chronosequence stage dissimilarity (Euclidean matrix of distance that express the similarity pair to pair between two chronosequence stages) in the 16 soil chronosequences studied.

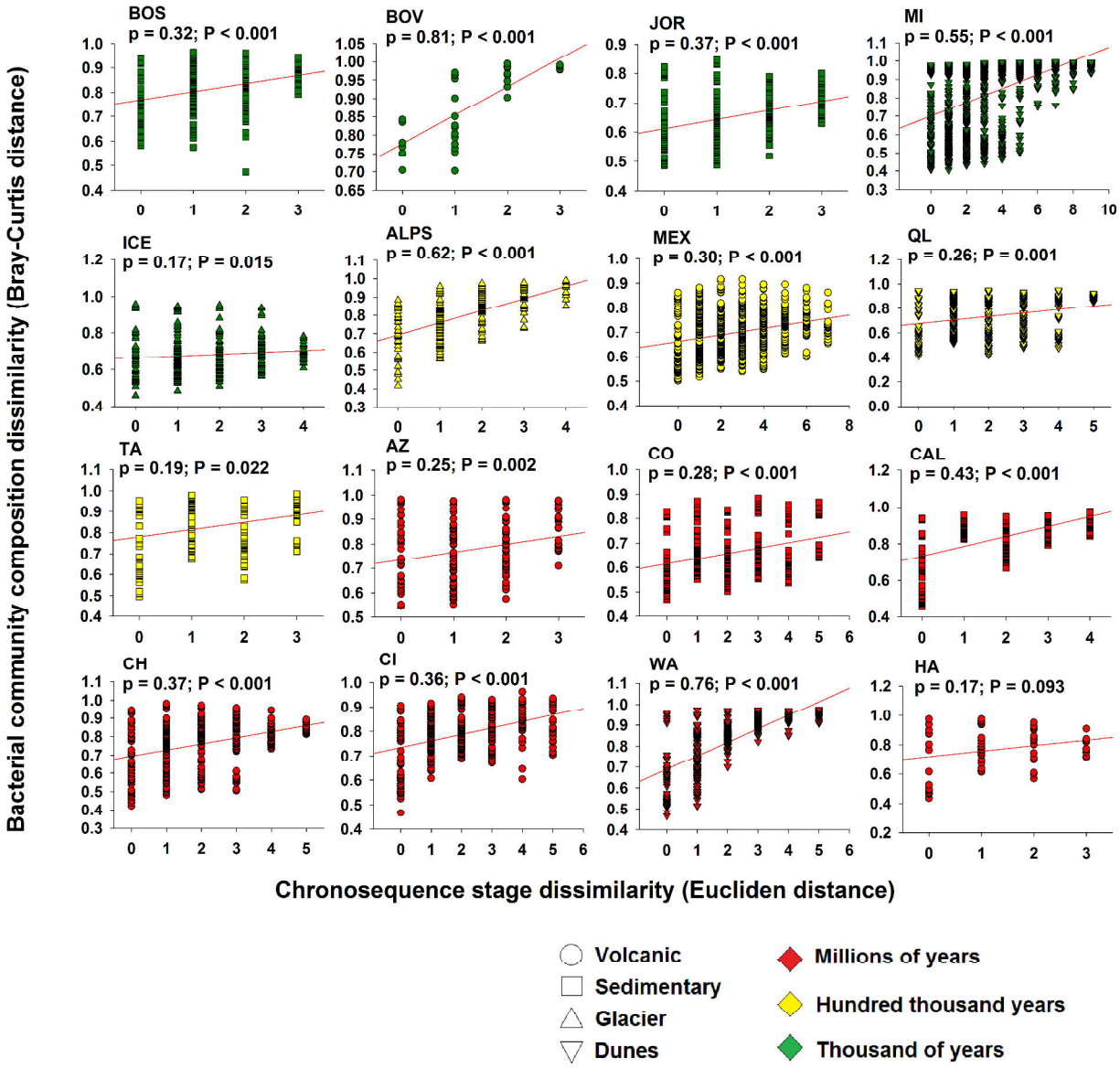

Figure S10. Mantel correlation (Spearman, p) between soil bacterial community dissimilarity (Bray-Curtis distance) and stage dissimilarity (Euclidean distance) in 16 globally distributed soil chronosequences.

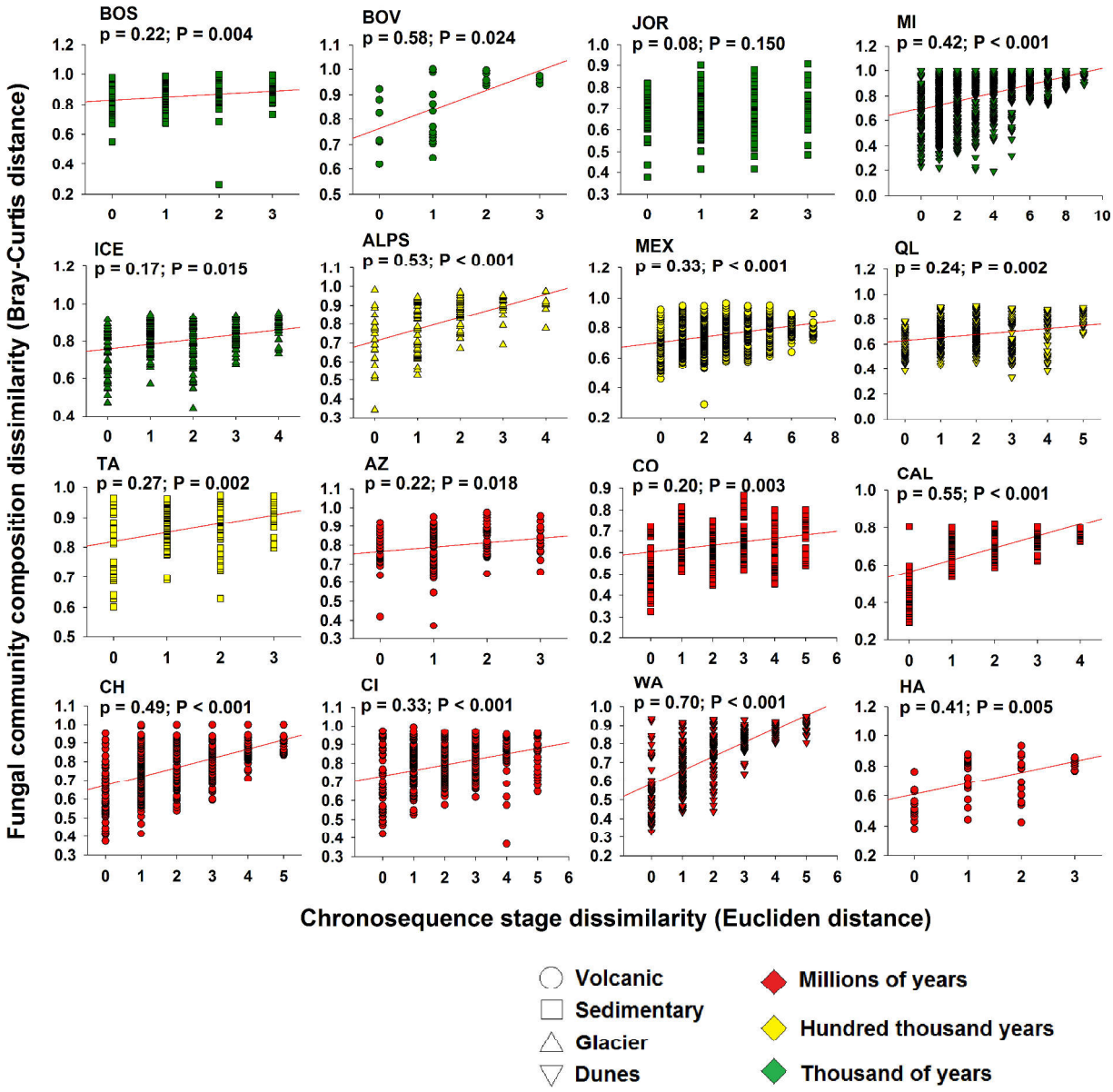

Figure S11. Mantel correlation (Spearman, p) between soil fungal community dissimilarity (Bray-Curtis distance) and stage dissimilarity (Euclidean distance) in 16 globally distributed soil chronosequences.

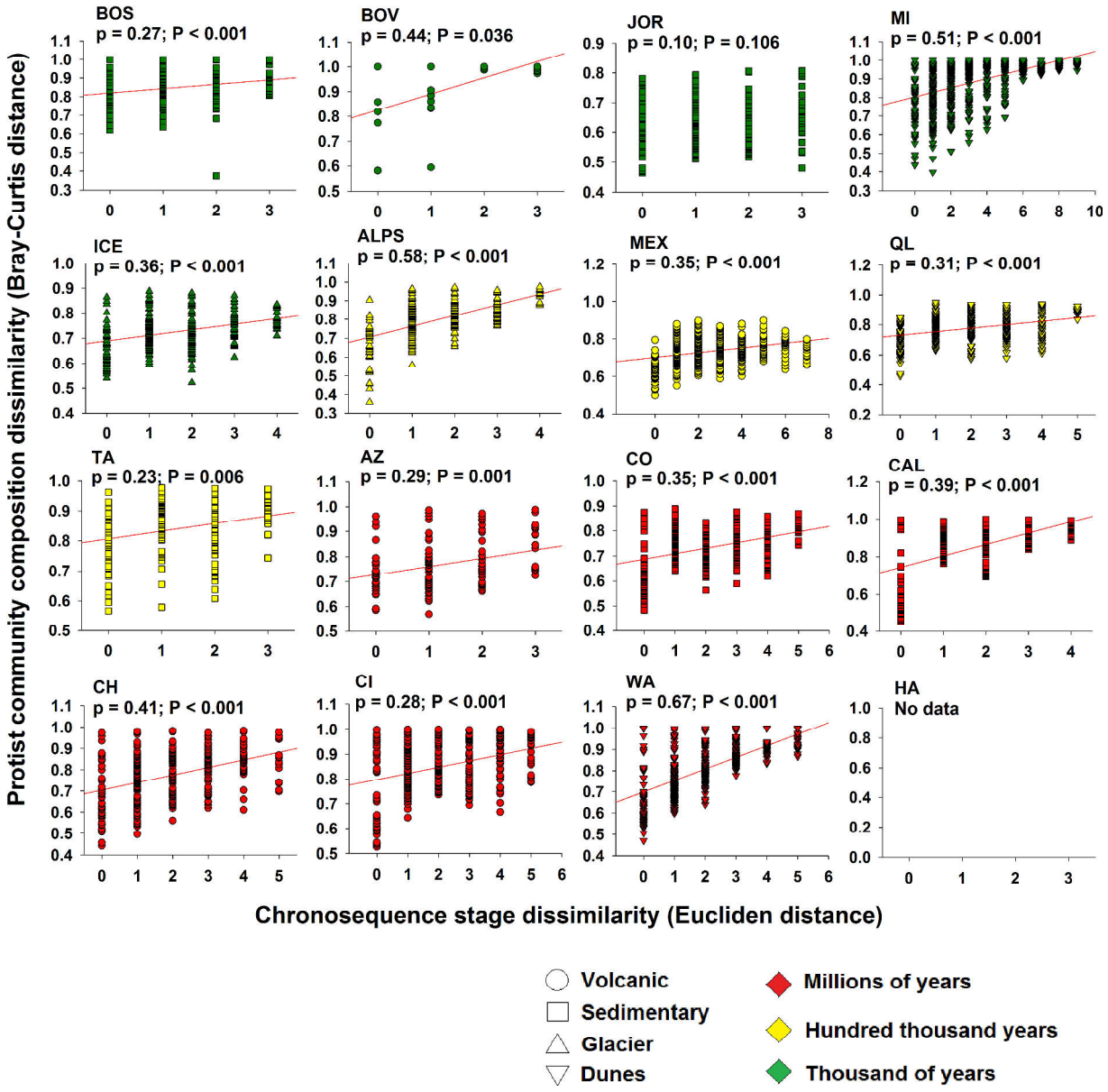

Figure S12. Mantel correlation (Spearman, p) between soil protist' community dissimilarity (Bray-Curtis distance) and stage dissimilarity (Euclidean distance) in 16 globally distributed soil chronosequences.

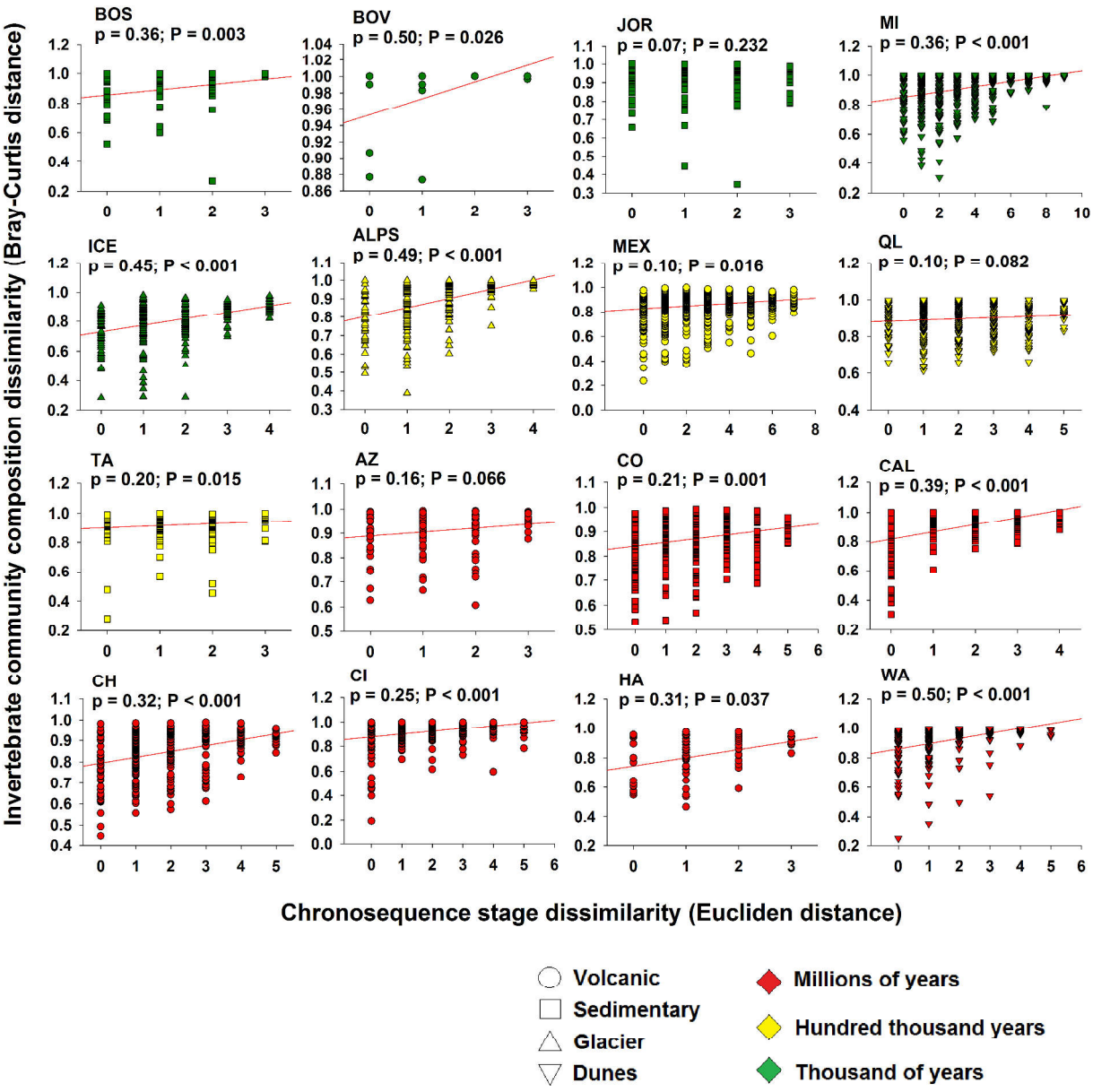

Figure S13. Mantel correlation (Spearman, p) between soil invertebrate' community dissimilarity (Bray-Curtis distance) and stage dissimilarity (Euclidean distance) in 16 globally distributed soil chronosequences.

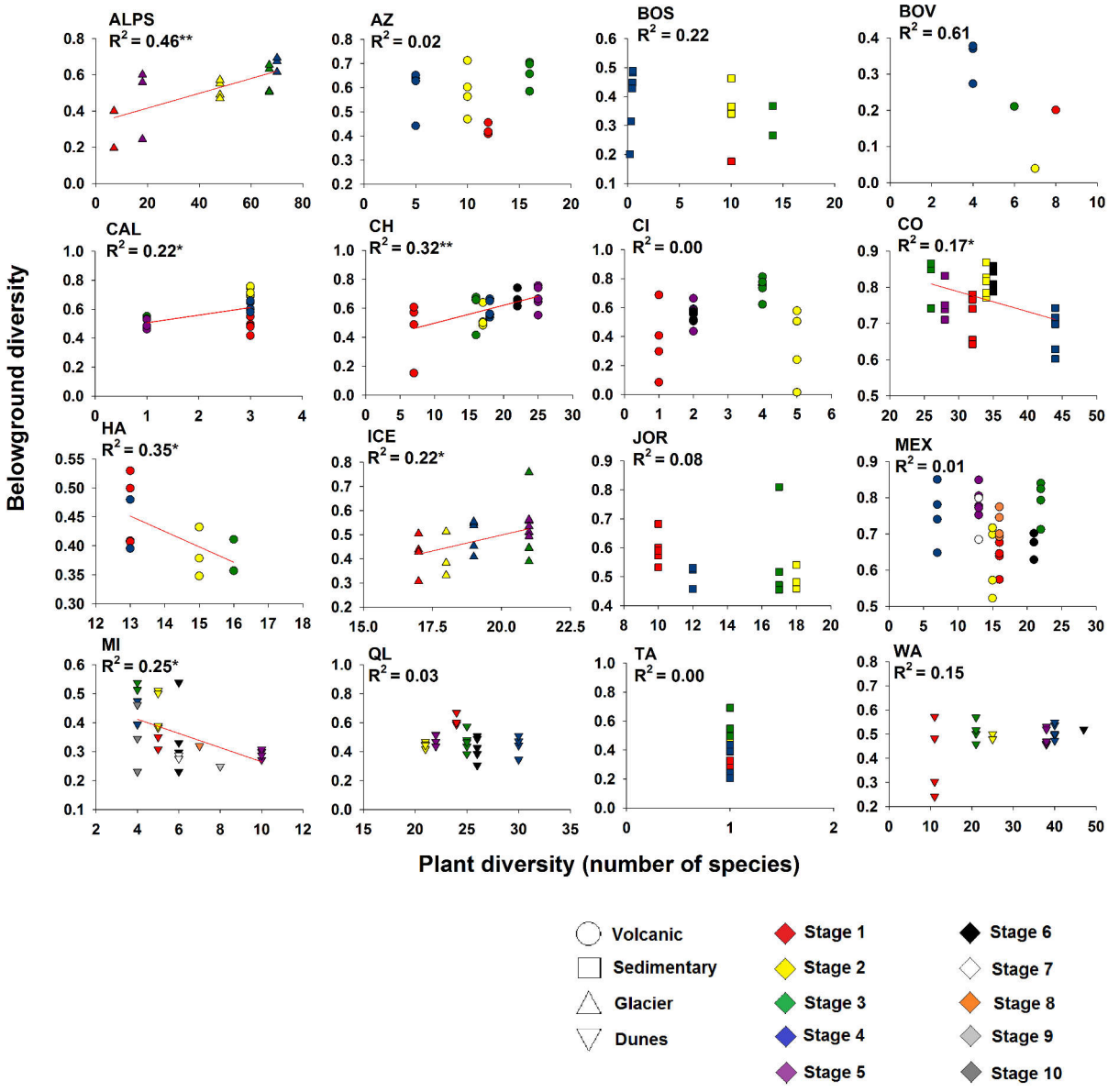

Figure S14. Relationships between belowground and plant diversity in 16 globally distributed soil chronosequences.

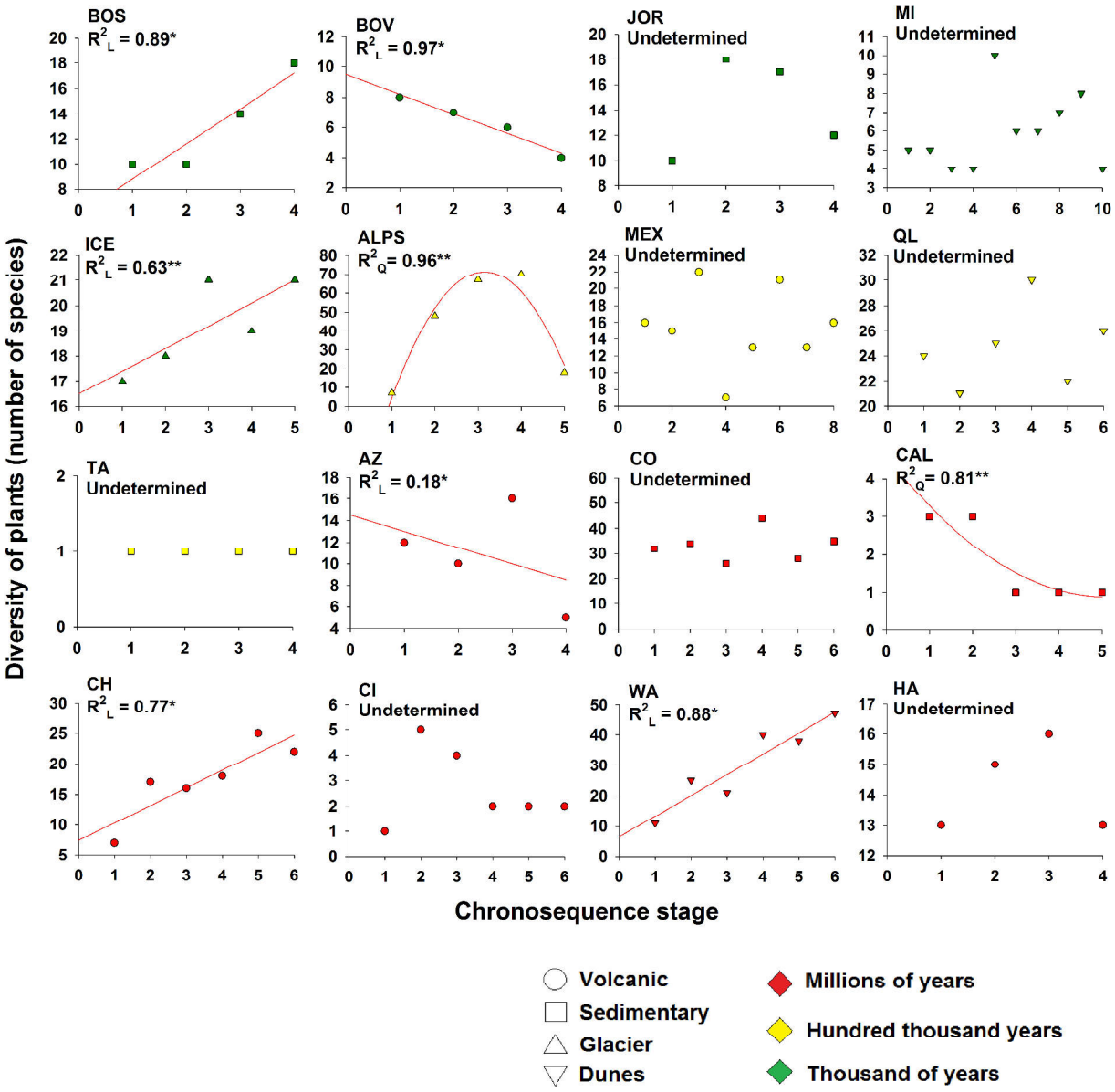

Figure S15. Relationships between chronosequence stage and plant diversity in 16 globally distributed soil chronosequences. Texture = % clay + silt.

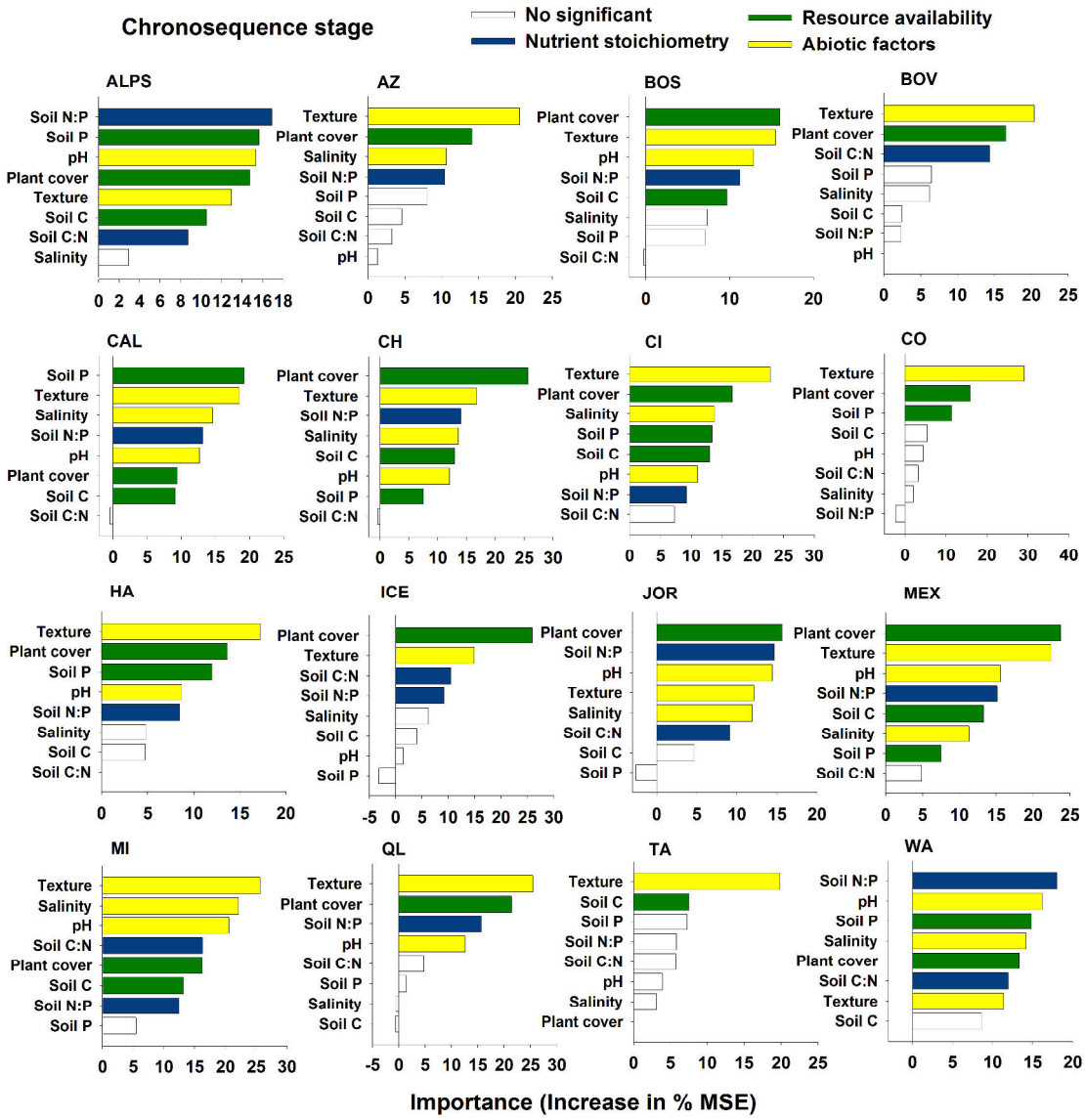

Figure S16. Important environmental predictors of age-based stage across 16 globally distributed soil chronosequences, identified using random forest modeling. MSE = Mean Square Error. No bar = 0. Texture = % clay + silt.

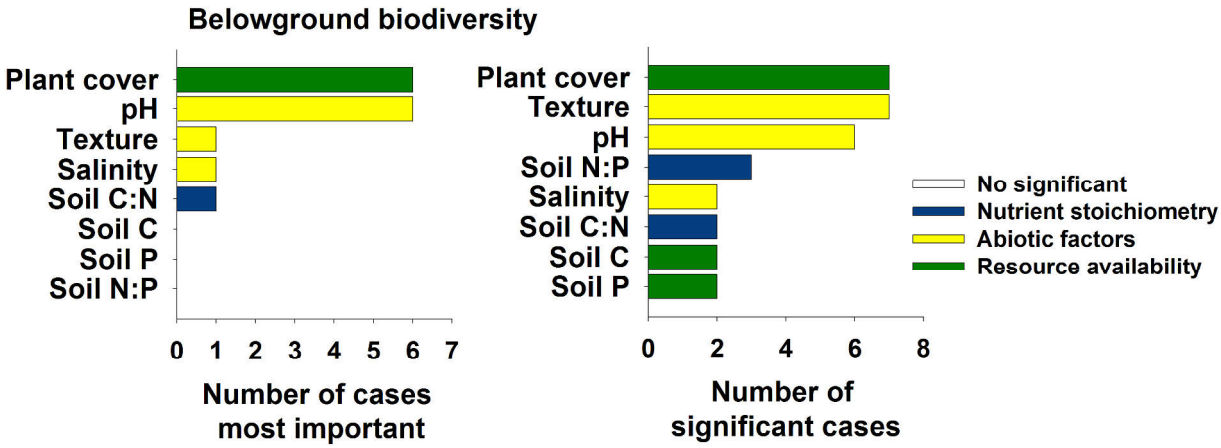

Figure S17. Ecological drivers of belowground biodiversity during pedogenesis. Summary for the most important predictors, from Random Forest modelling, of the diversity of belowground organisms across sixteen globally distributed soil chronosequences. A more detailed version of this figure can be found in Appendix S1, Fig. S18. Texture = % clay + silt.

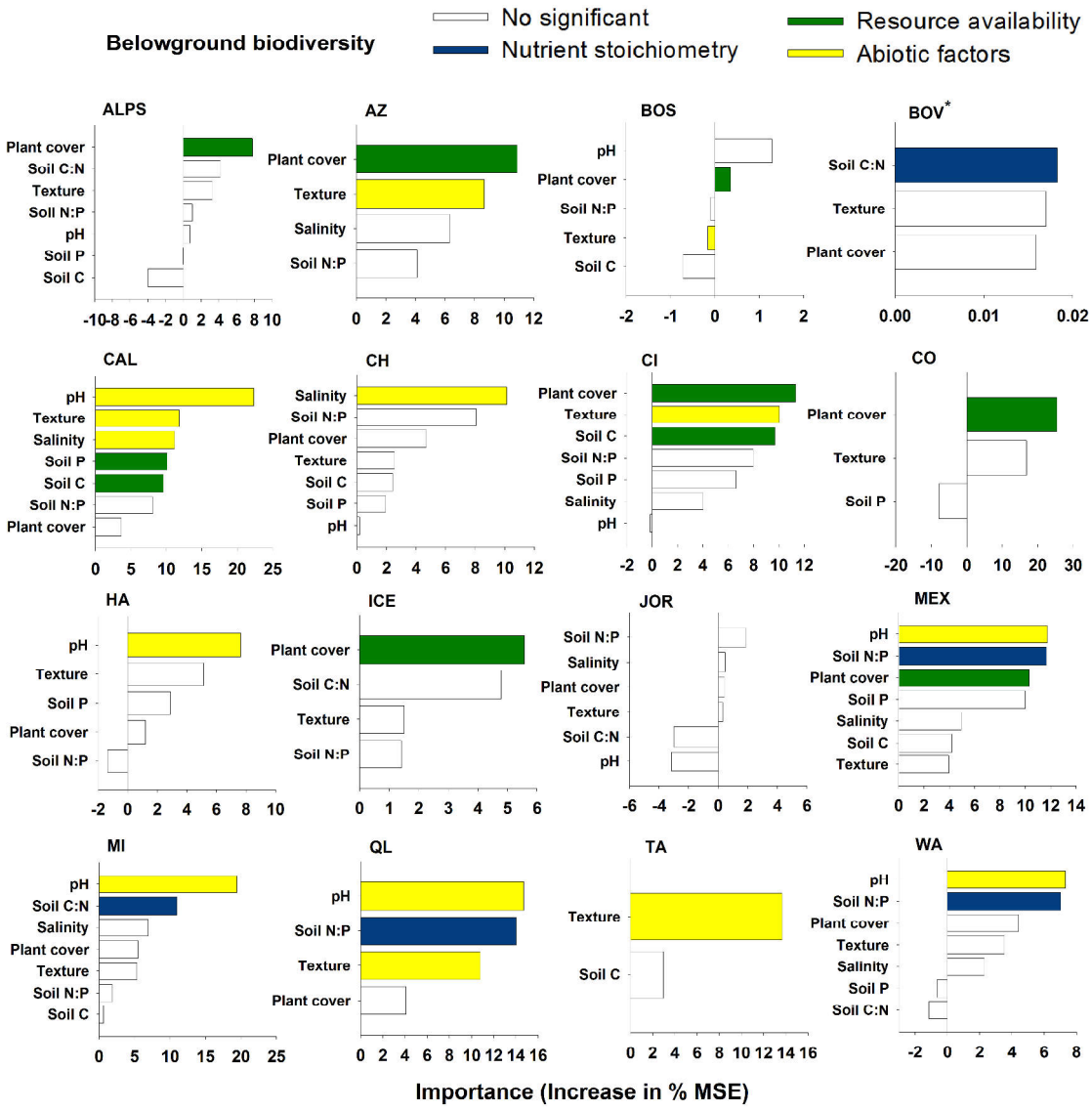

Figure S18. Important environmental predictors of belowground biodiversity across 16 globally distributed soil chronosequences, identified using random forest modeling. MSE = Mean Square Error. *Increase in Node Purity was used as an alternative importance metric for this analysis, as MSE did not work in this case. No bar = 0. No significant = $P > 0.05$. Colors highlight significant predictors. Texture = % clay + silt.

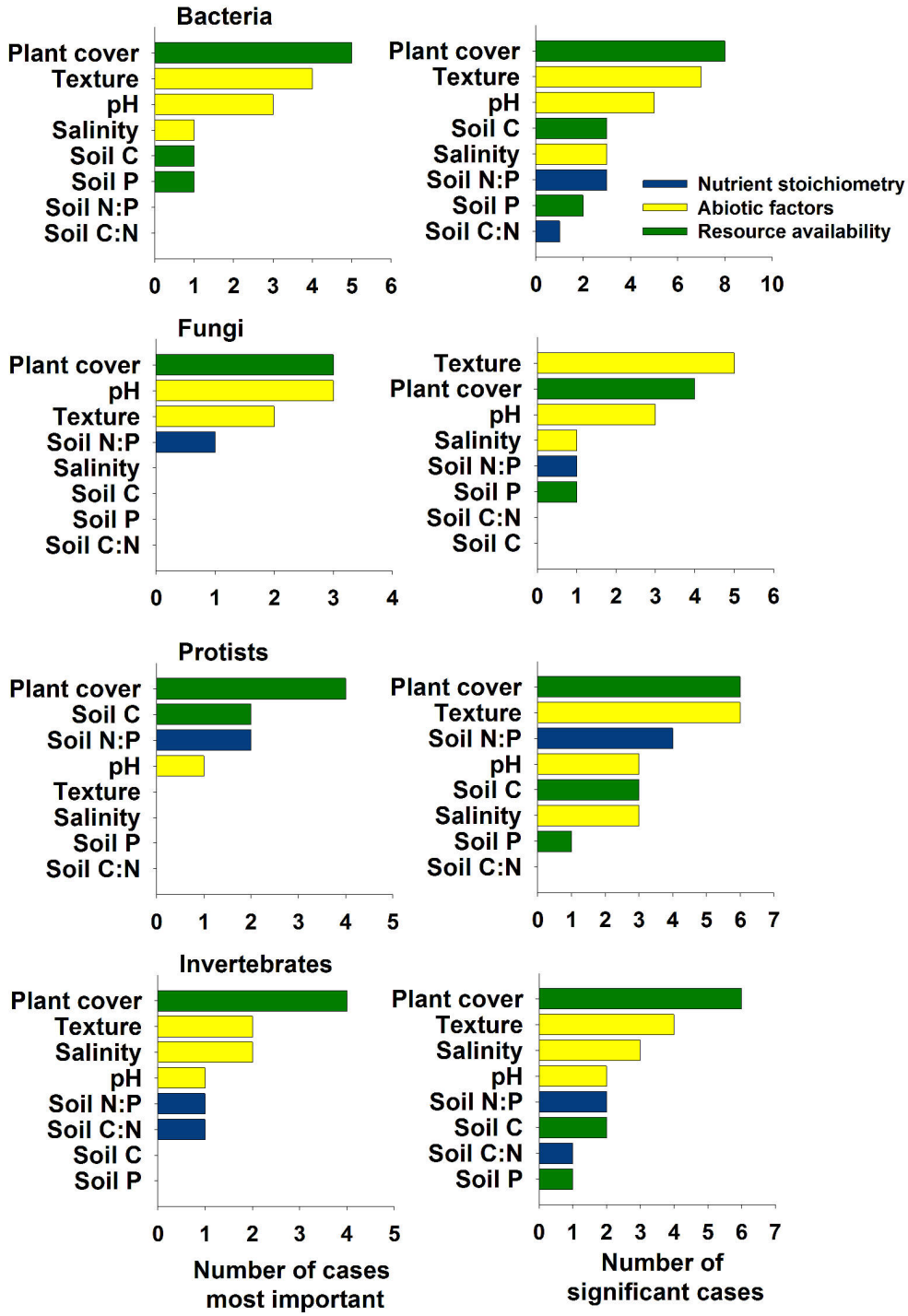

Figure S19. Summary for the most important predictors from Random Forest modeling of the diversity of soil bacteria, fungi, protists and invertebrates across 16 globally distributed soil chronosequences. MSE = Mean Square Error. No bar = 0 cases. Texture = % clay + silt.

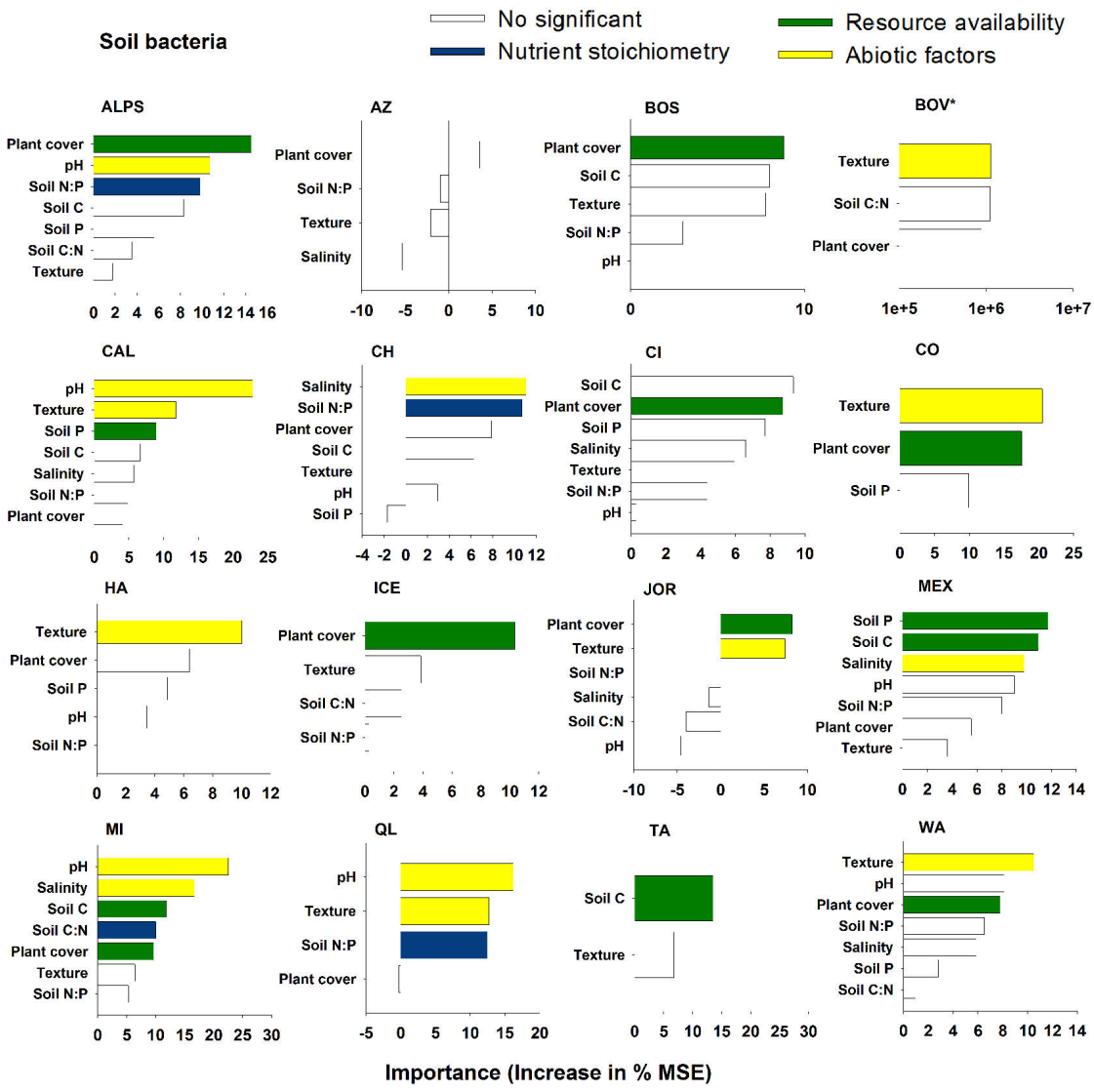

Figure S20. Important environmental predictors of soil bacterial diversity across 16 globally distributed soil chronosequences, identified using random forest modeling. MSE = Mean Square Error. *Increase in Node Purity was used as an alternative importance metric for this analysis, as MSE did not work in this case. No bar = 0. No significant = $P > 0.05$. Colors highlight significant predictors. Texture = % clay + silt.

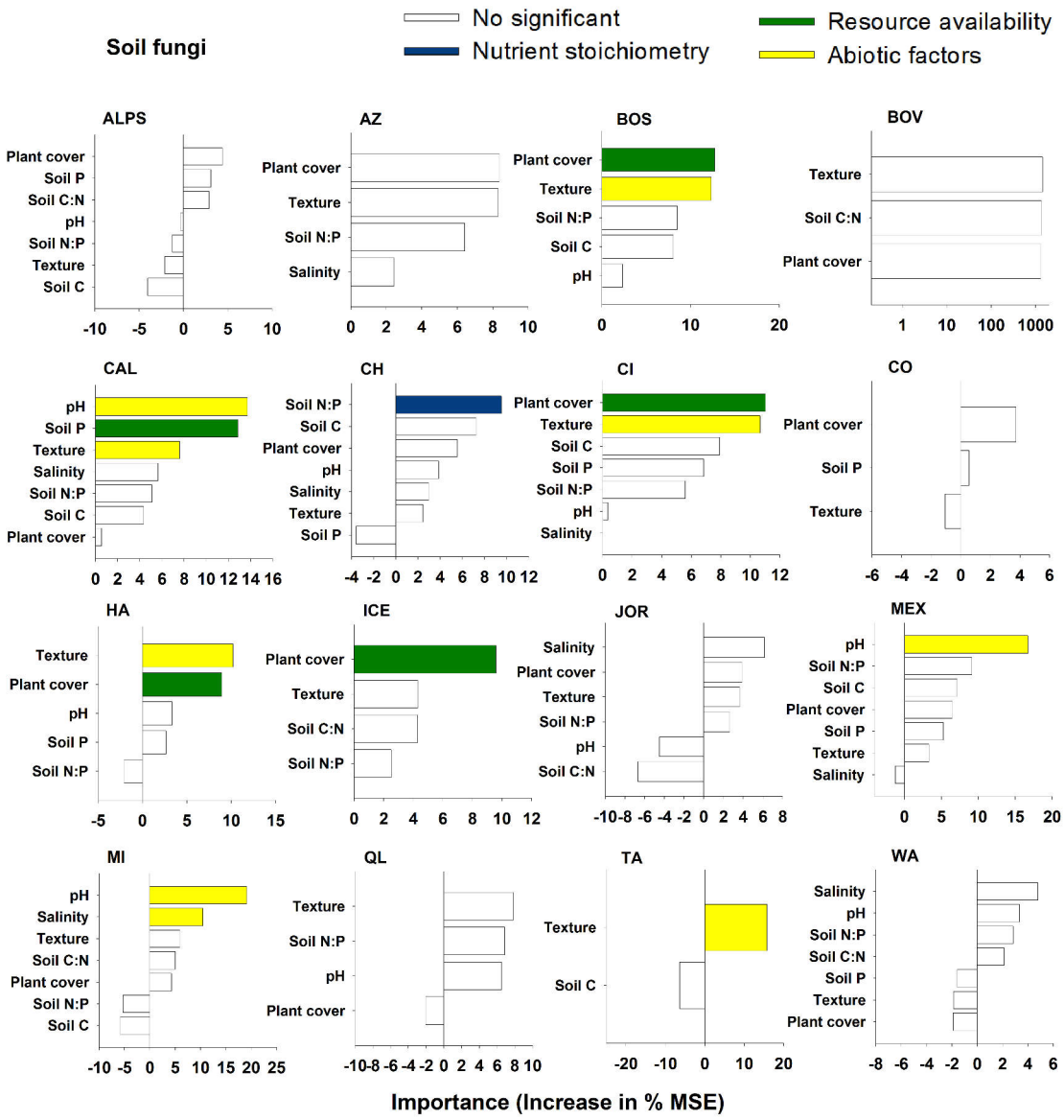

Figure S21. Important environmental predictors of soil fungal diversity across 16 globally distributed soil chronosequences, identified using random forest modeling. MSE = Mean Square Error. No bar = 0. No significant = $P > 0.05$. Colors highlight significant predictors. Texture = % clay + silt.

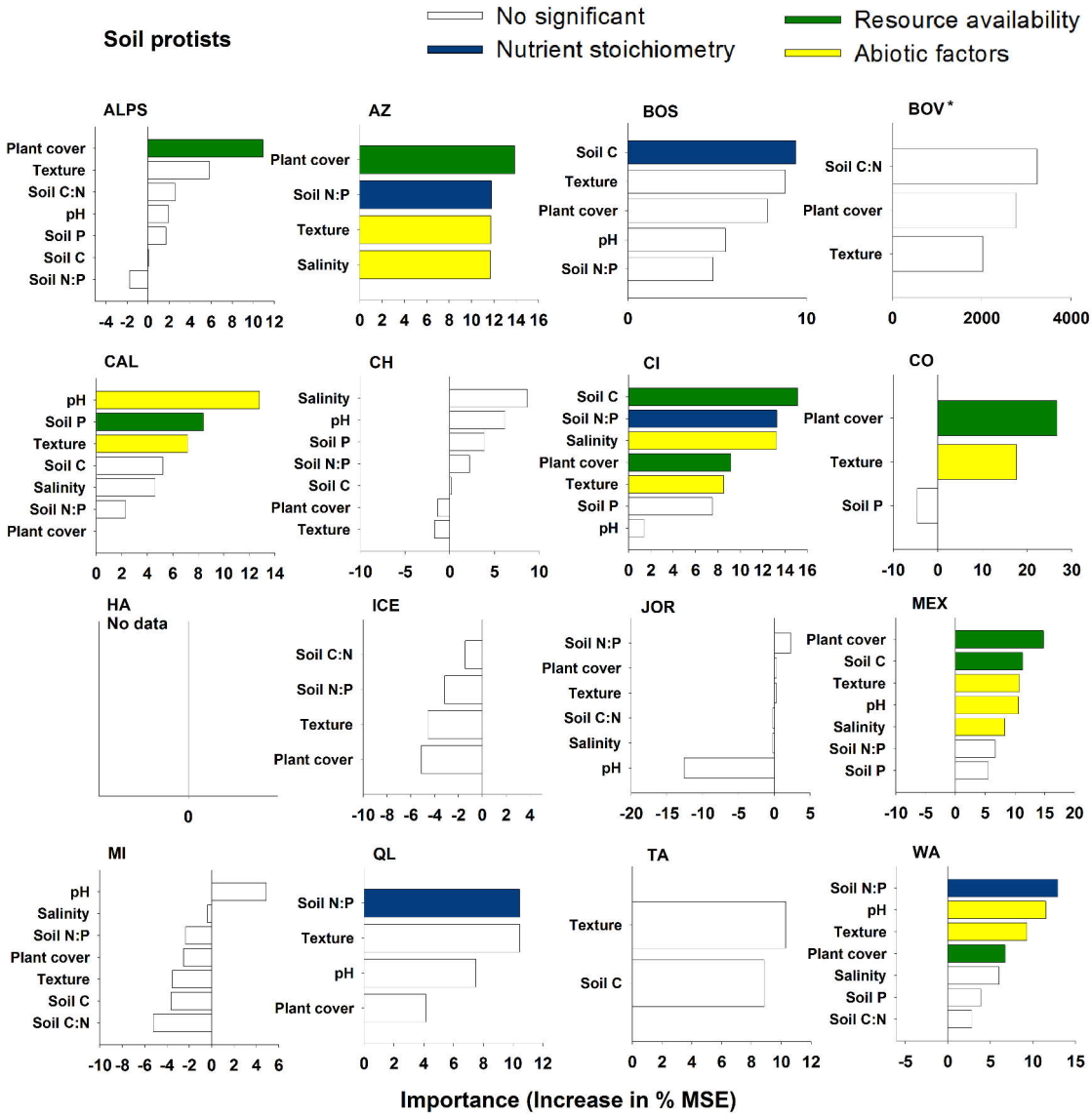

Figure S22. Important environmental predictors of soil protists diversity across 16 globally distributed soil chronosequences, identified using random forest modeling. MSE = Mean Square Error.*Increase in Node Purity was used as an alternative importance metric for this analysis, as MSE did not work in this case. No bar = 0. No significant = P > 0.05. Colors highlight significant predictors. Texture = % clay + silt.

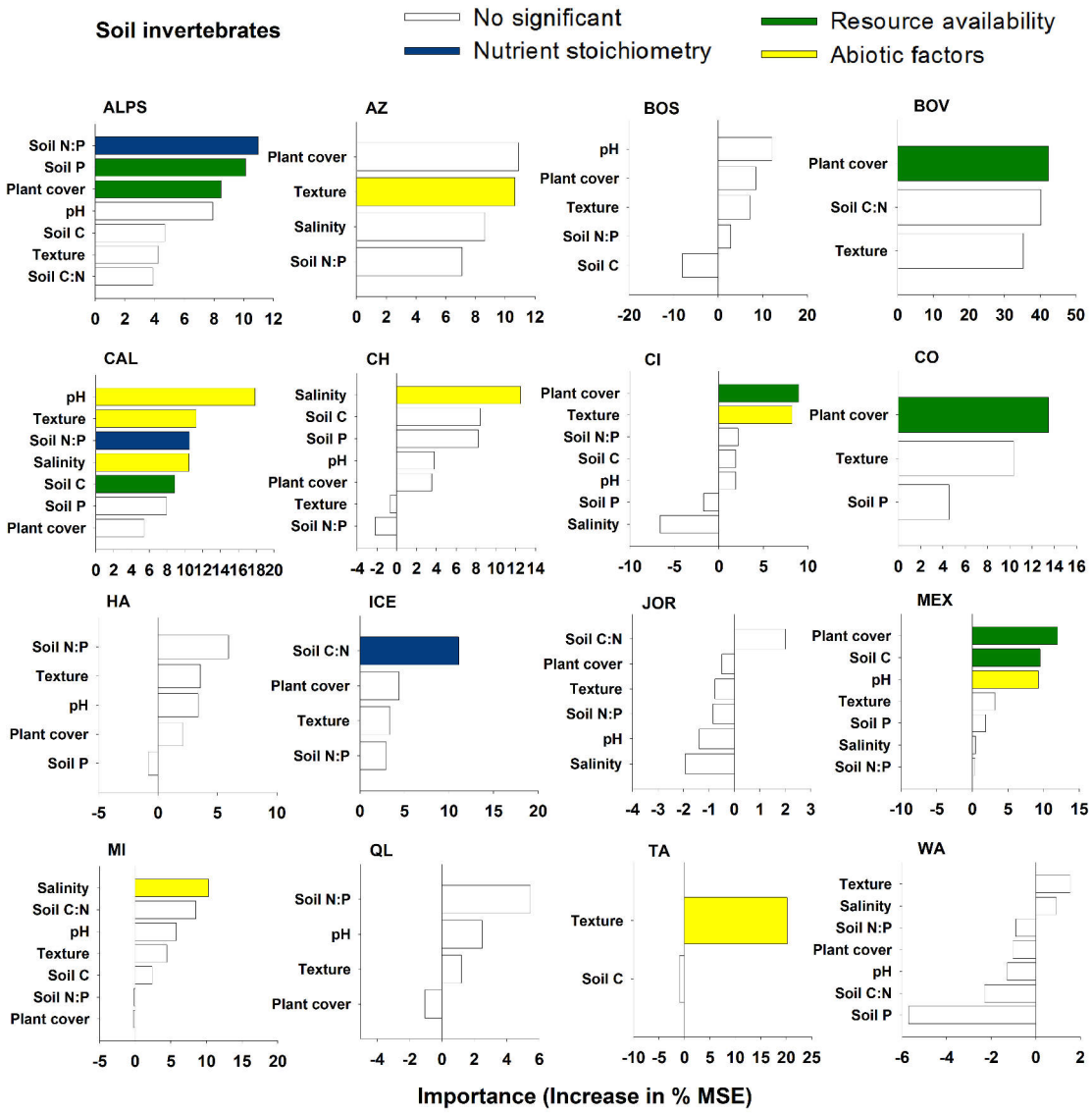

Figure S23. Important environmental predictors of soil invertebrate diversity across 16 globally distributed soil chronosequences, identified using random forest modeling. MSE = Mean Square Error. No bar = 0. No significant = $P > 0.05$. Colors highlight significant predictors. Texture = % clay + silt.

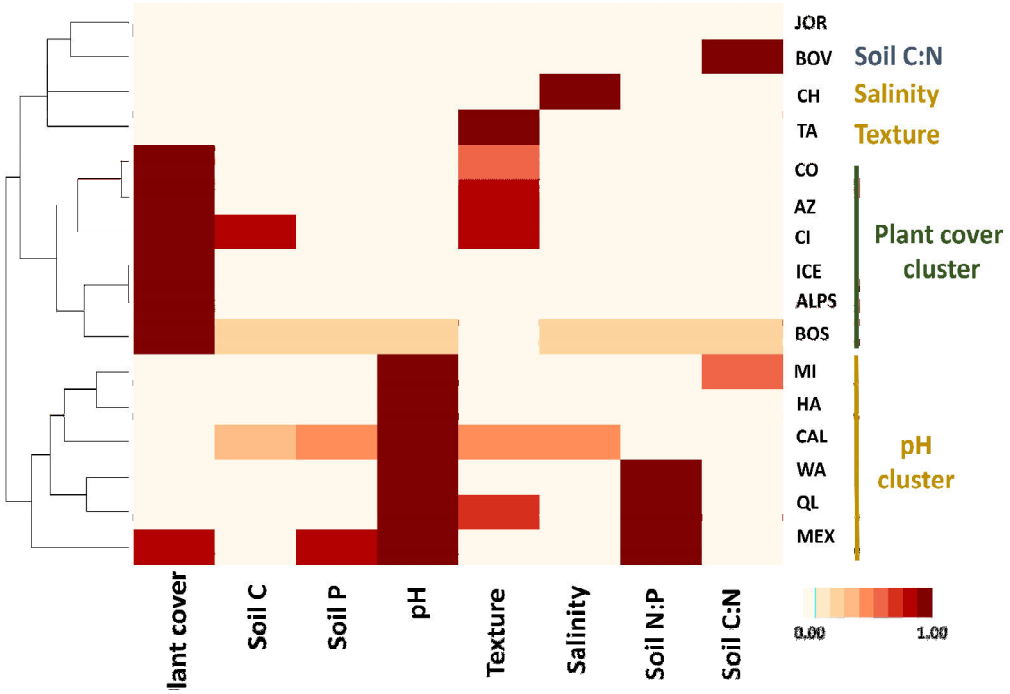

Figure S24. Hierarchical clustering using information on the importance of environmental factors in predicting belowground biodiversity (from Random Forest modeling) to identify the major ecological patterns driving the fate of belowground biodiversity during pedogenesis across 16 global distributed soil chronosequences.

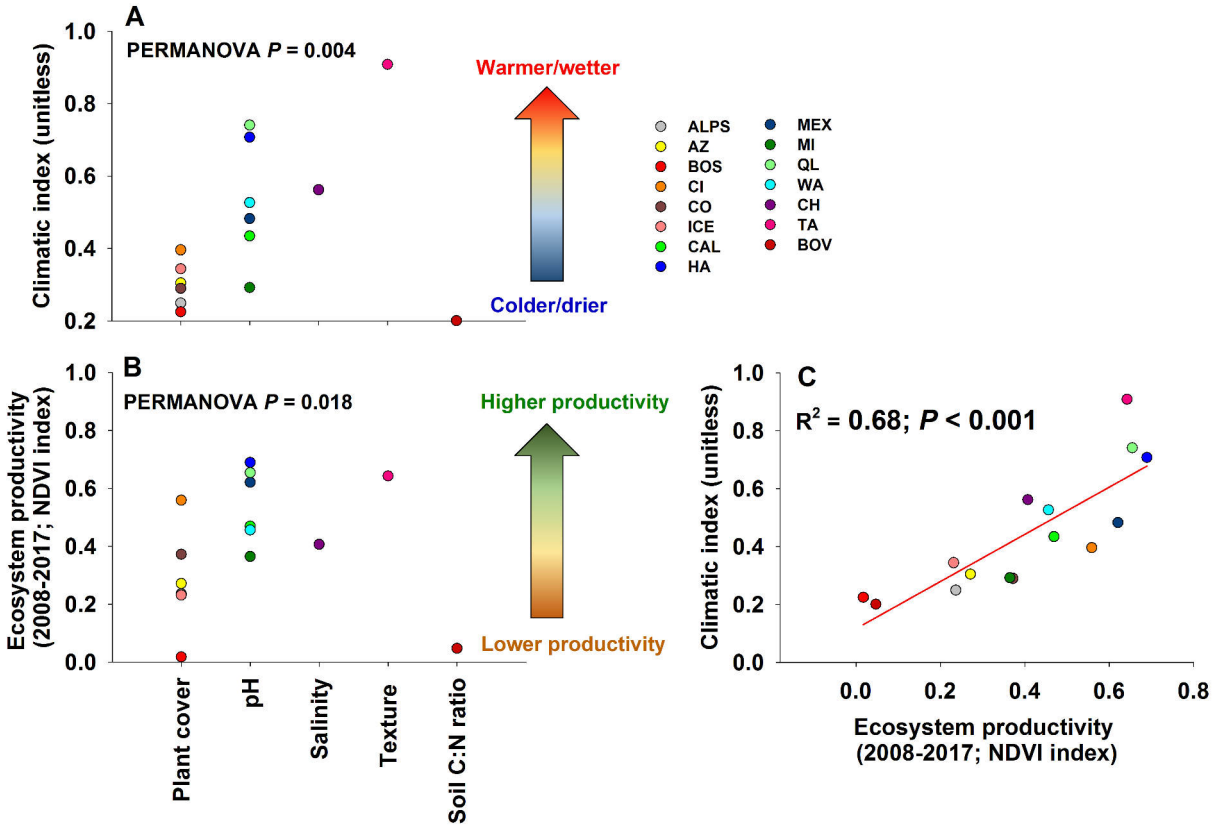

Figure S25. Mean ecosystem productivity and climatic index –standardized averaged for mean precipitation and temperature– in 16 globally distributed soil chronosequences. Low levels of climatic index represents colder and drier ecosystems. Chronosequences where belowground biodiversity is predicted by plant cover have significantly lower plant productivity and climatic index (temperature|precipitation) than those where soil biodiversity is predicted by soil pH. For ecosystem productivity, we used the monthly average value for Normalized Difference Vegetation Index (NDVI) for the 2008-2017 period (~10km resolution). Data was obtained from the Moderate Resolution Imaging Spectroradiometer (MODIS) aboard NASA's Terra satellites (http://neo.sci.gsfc.nasa.gov/).

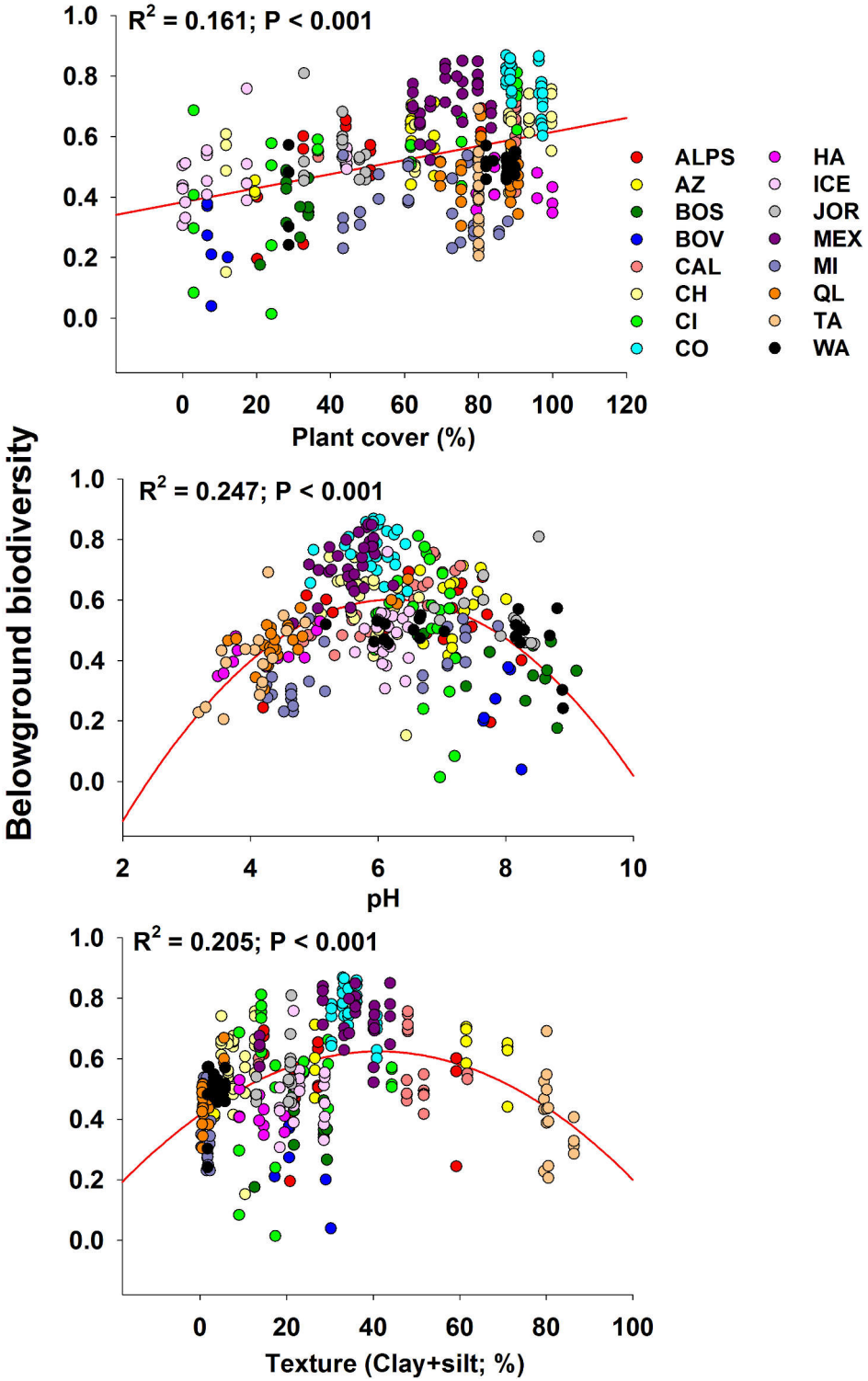

Figure S26. Relationships between % of plant cover, soil pH and % of soil clay+silt with the belowground biodiversity across all soil samples.

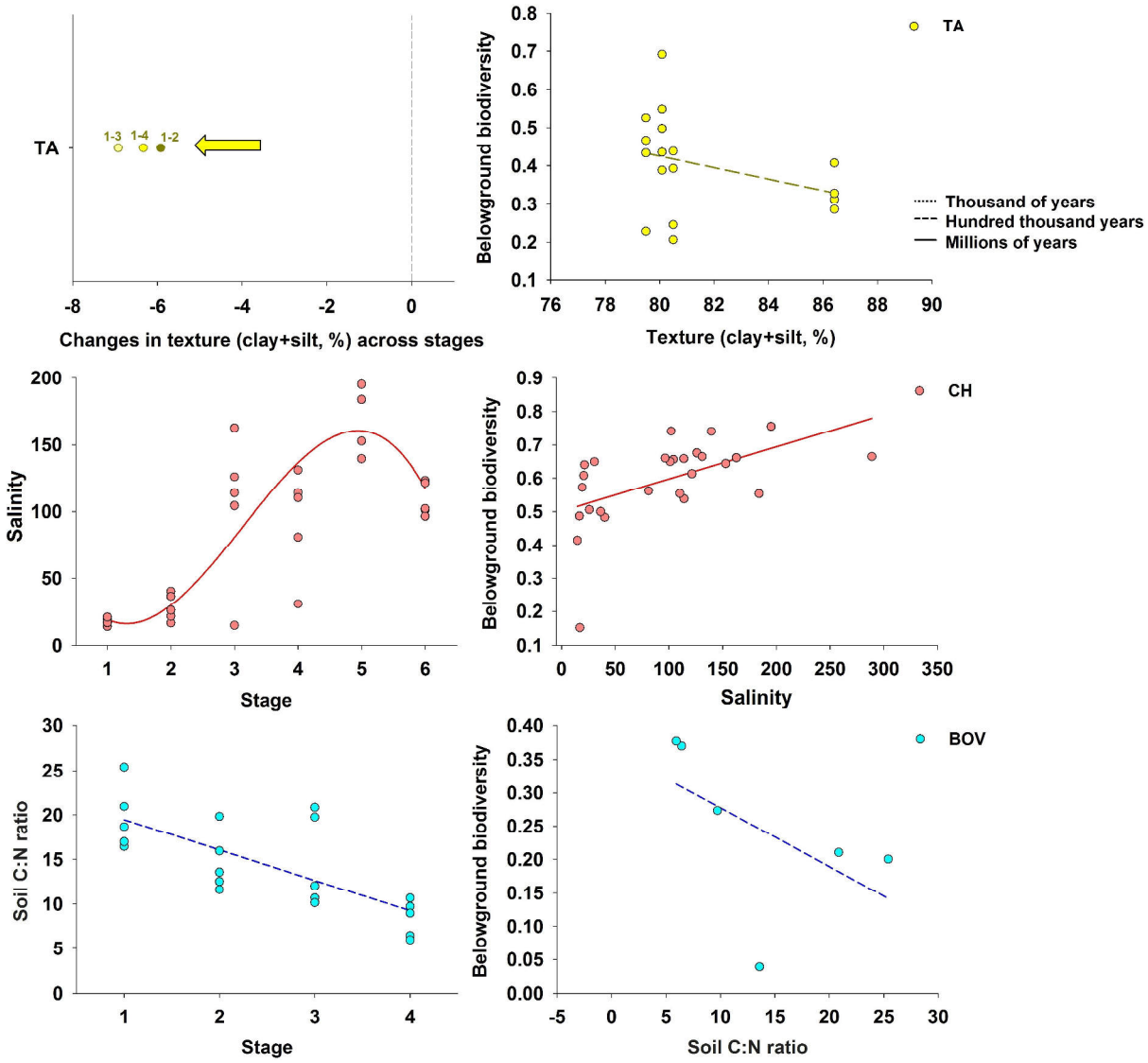

Figure S27. Less common ecological drivers of the fate of belowground biodiversity during pedogenesis. Reductions in % of fine texture (% of silt + clay in soil) during development correlated with increases in belowground biodiversity at the chronosequence at Taiwan (TA). Increases in salinity correlated with increases in belowground biodiversity at the chronosequence of Chile (CH). Decreases in soil C:N ratio during development correlated with increases in belowground biodiversity at the volcanic chronosequence of Bolivia (BOV). Numbers on the circles in the left upper panel indicate number of chronosequence stage. Changes in clay+silt across chronosequence stages are calculated from the stage 1 in this chronosequence. Arrows in this panel indicate the overall directions for the changes in clay+silt across stages.

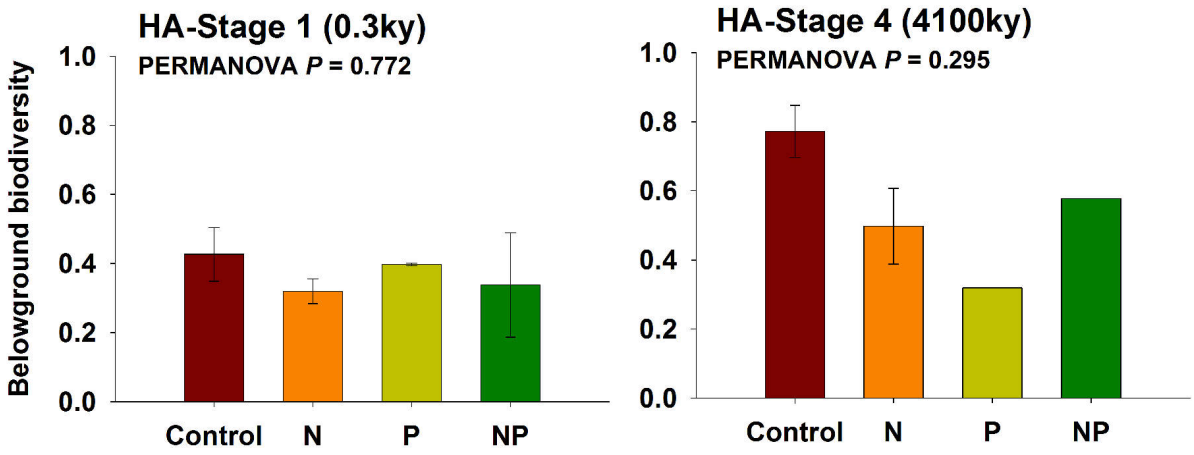

Figure S28. Mean (±SE) of belowground biodiversity in response to N, P and N+P additions in a 27 year experiment conducted over the youngest (0.3ky) and oldest (4100ky) soils from the chronosequence in HA (n = 3). Details on the experimental design can be found in refs. 27 and 45. Belowground biodiversity is defined as the standardized average of the diversity of soil bacteria, fungi and invertebrates.

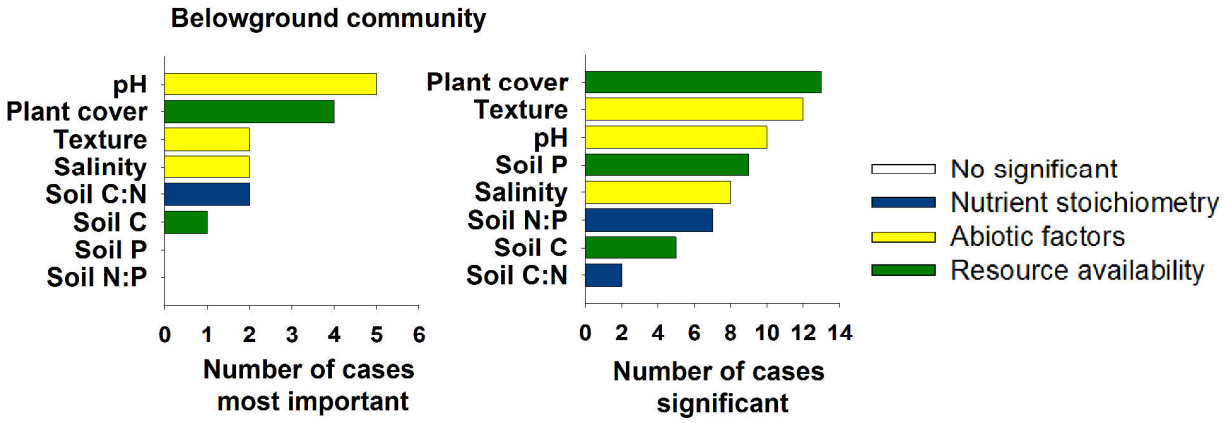

Figure S29. Summary for the most important predictors from Mantel test (Spearman) correlation of the community dissimilarity of belowground organisms, bacteria, fungi, protists and soil invertebrates across 16 globally distributed soil chronosequences. No bar = 0. See Extended Data Tables 12-13 for details.

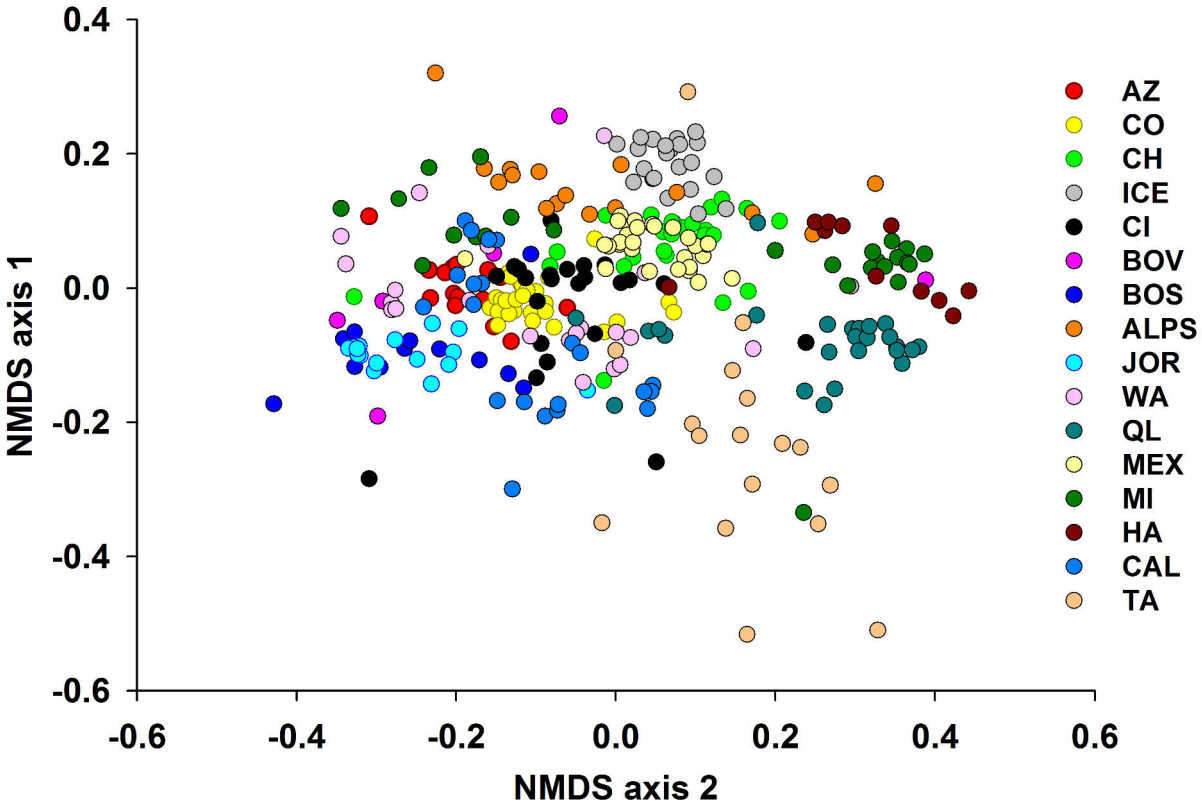

Figure S30. Nonmetric multidimensional scaling (NMDS) plots showing the belowground community composition across 16 soil chronosequences. Analyses are based on the averaged Bray-Curtis dissimilarity across samples for four matrices of distances (bacterial, fungal, protist and soil invertebrate communities). The number of samples included in this analysis is available in Appendix S1, Table S15.

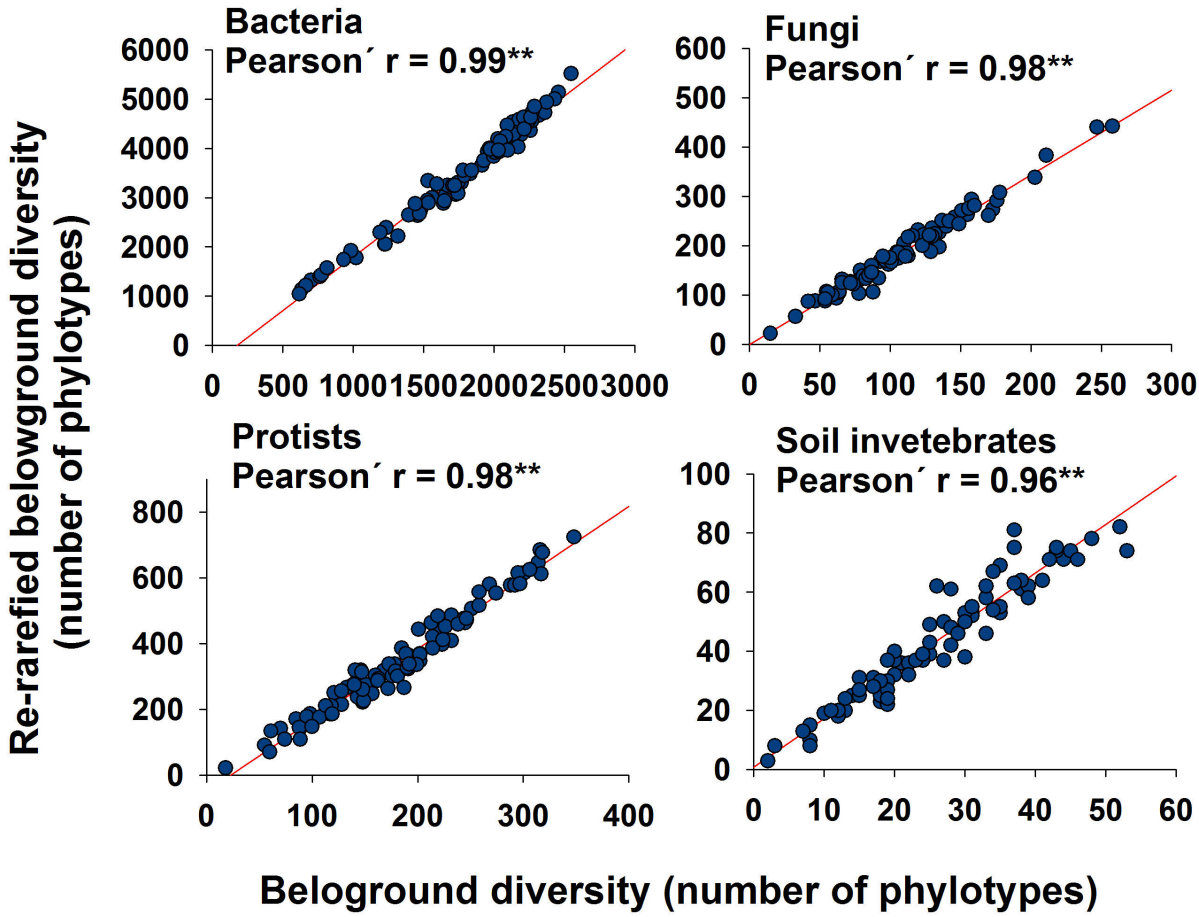

Figure S31. Relationships between diversity (number of phylotypes) of bacteria (rarefied at 5000 vs. 18000 sequences/sample), fungi (rarefied at 2000 vs. 10000 sequences/sample for fungi), protists (rarefied at 800 vs. 4000 sequences/sample) and soil invertebrates (rarefied at 300 vs. 1800 sequences/sample).

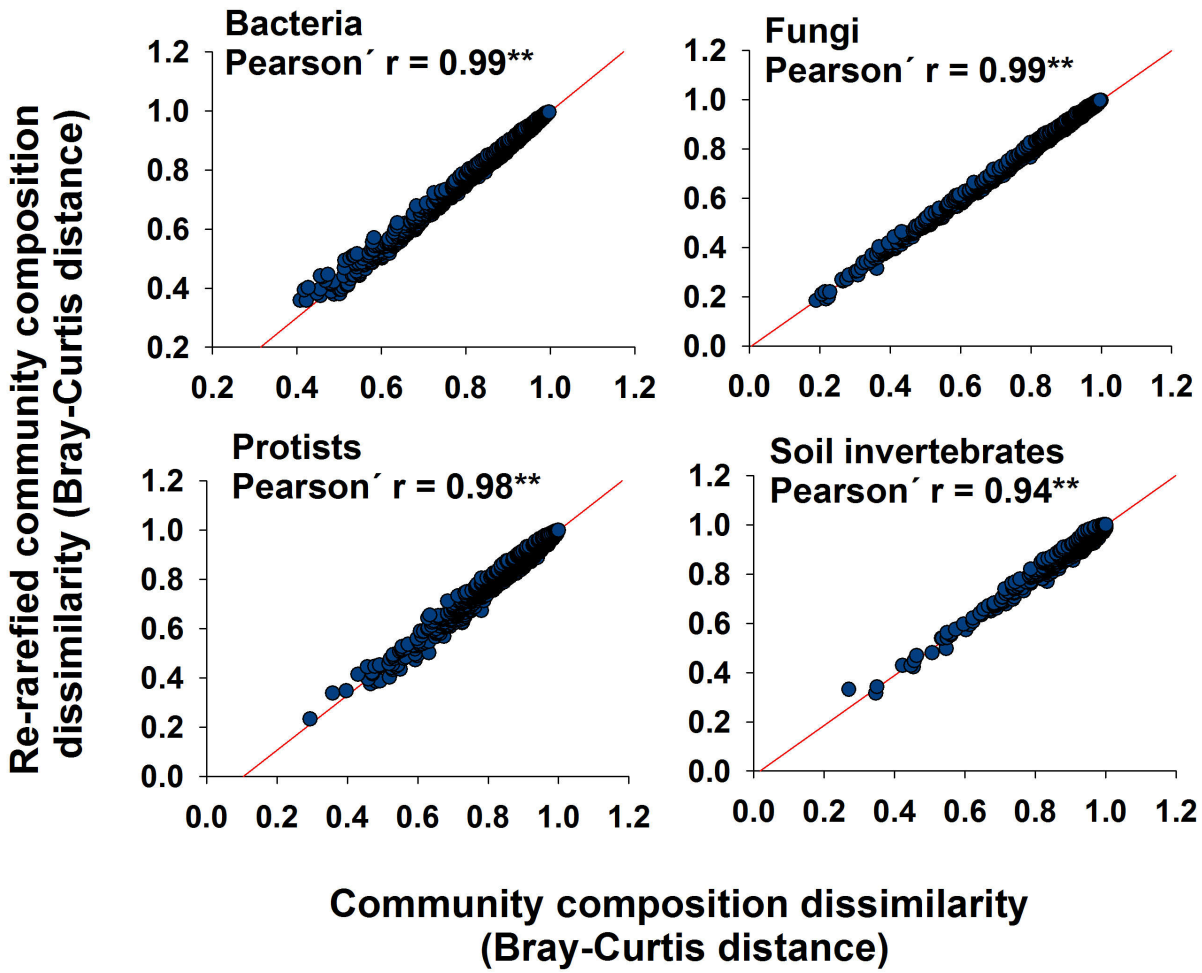

Figure S32. Mantel test correlation (Pearson) between community composition of bacteria (rarefied at 5000 vs. 18000 sequences/sample), fungi (rarefied at 2000 vs. 10000 sequences/sample for fungi), protists (rarefied at 800 vs. 4000 sequences/sample) and soil invertebrates (rarefied at 300 vs. 1800 sequences/sample).

References

1. Delgado-Baquerizo, M. et al. (2018) A global atlas of the dominant bacteria found in soil. Science **19,** 320-325.
2. Bulgarelli, D. et al. (2012) Revealing structure and assembly cues for Arabidopsis root-inhabiting bacterial microbiota. Nature **488,** 91–95.
3. Maestre, F.T. et al. (2012) Plant Species Richness and Ecosystem Multifunctionality in Global Drylands. Science **335,** 214-218.
4. Cade, B.S. (1997) Comparison of Tree Basal Area and Canopy Cover in Habitat Models: Subalpine Forest. J Wildl Manage **61,** 326-335.
5. Wardle, D.A. et al. (2004) Ecosystem properties and forest decline in contrasting long-term chronosequences. Science **305,** 509-513.
6. Wardle, D.A. et al. (2009) Among- and within-species variation in plant litter decomposition in contrasting long-term chronosequences. Funct. Ecol. **23,** 442–453.
7. Maestre, F.T. et al. (2015) Increasing aridity reduces soil microbial diversity and abundance in global drylands. Proc Natl Acad Sci U.S.A **112,** 15684–15689.
8. Tedersoo, L. et al. (2014) Fungal biogeography. Global diversity and geography of soil fungi. Science **346,** 1256688.
9. Carini, P. et al. (2018) Unraveling the effects of spatial variability and relic DNA on the temporal dynamics of soil microbial communities. bioRxiv doi: https://doi.org/10.1101/402438.
10. Delgado-Baquerizo, M. et al. (2018) Plant attributes explain the distribution of soil microbial communities in two contrasting regions of the globe. New Phytol. **219,** 574-587.
11. Fierer, N., Jackson, R.B. (2006) The diversity and biogeography of soil bacterial communities. Proc. Natl Acad. Sci. USA **103,** 626–631.
12. Lauber, C.L. et al. (2009) Soil pH as a predictor of soil bacterial community structure at the continental scale: a pyrosequencing-based assessment. Appl Environ Microbiol **75,** 5111-5120.
13. Alfaro, F.D. et al. (2017) Microbial communities in soil chronosequences with distinct parent material: the effect of soil pH and litter quality. Journal of Ecology **105**, 1709-1722.
14. Wardle, D.A. et al. (2006) Ecological Linkages Between Aboveground and Belowground Biota. Science **304,** 1629-1633.
15. Vitousek, P. et al. (2010) Terrestrial phosphoruslimitation: mechanisms, implications, and nitrogen-phosphorus interactions. Ecol Appl. **20,** 5–15.
16. Kettler, T.A. Doran, J.W., Gilbert, T.L. (2001) Simplified method for soil particle-size determination to accompany soil-quality analyses. Soil Sci. Soc. Am. J. **65,** 849.
17. Anderson, J. M., Ingramm, J.S.I. (1993) Eds., Tropical Soil Biology and Fertility: A Handbook of Methods (CABI, Wallingford, UK, ed. 2).
18. Olsen, S.R., Sommers, L.E. (1982) in Methods of Soil Analysis. Part 2. Chemical and Microbiological Properties, A. L. Page, R. H. Miller, D. R. Keeney, Eds. (American Society of Agronomy and Soil Science Society of America, Madison, WI).
19. Ramirez K.S. et al. (2014) Biogeographic patterns in below-ground diversity in New York City's Central Park are similar to those observed globally. Proc R Soc Lond B Biol Sci. **281,** 1795.

20. Caporaso, J.G. et al. (2010) QIIME allows analysis of high-throughput community sequencing data. Nat Method **7,** 335.
21. Edgar, R.G. (2013) UPARSE: highly accurate OTU sequences from microbial amplicon reads. Nature Methods **10,** 996-998.
22. Edgar, R.C. (2016) UNOISE2: Improved error-correction for Illumina 16S and ITS amplicon reads.http://dx.doi.org/10.1101/081257
23. Soliveres, S. et al. (2016) Biodiversity at multiple trophic levels is needed for ecosystem multifunctionality. Nature. **25,** 456-9.
24. Wardle, D.A. et al. (2008) The response of plant diversity to ecosystem retrogression: evidence from contrasting long-term chronosequences. Oikos **117,** 93-103.
25. Laliberte, E. et al. (2013) How does pedogenesis drive plant diversity? Trends in Ecology & Evolution **28**, 6.
26. Laliberté, E., Zemunik, G., Turner, B.L. (2014) Environmental filtering explains variation in plant diversity along resource gradients. Science **345,** 1602-1605.
27. Vitousek, P.M. (2004) Nutrient Cycling and Limitation: Hawai'i as a Model System (Princeton University Press, New Jersey, NY).
28. Andersen, R. (2008) Modern Methods for Robust Regression. Sage University Paper Series on Quantitative Applications in the Social Sciences, 07-152.
29. Yegorov, O. (2016) Robust Fitting of Linear Model. R package version 1.2.
30. Burnham, K.P., Anderson, D.R. (2002) Model Selection and Multimodel Inference: a Practical Information-Theoretic Approach (Springer, New York, ed. 2).
31. Burnham, K.P., Anderson, D.R., Huyvaert, K.P. (2011) AIC model selection and multimodel inference in behavioral ecology: some background, observations, and comparisons. Behav Ecol Sociobiol **65,** 23–35.
32. Turner B.L. et al. (2018) A climosequence of chronosequences in southwestern Australia. *European Journal of Soil Science* 69, 69-85
33. Barton, K. (2018) Multi-Model Inference R package version 1.40.4.
34. Delgado-Baquerizo, M. et al. (2015) Differences in thallus chemistry are related to species-specific effects of biocrust-forming lichens on soil nutrients and microbial communities. Funct Ecol **29,** 1087–1098.
35. Archer, E. (2016) rfPermute: Estimate Permutation p-Values for Random Forest Importance Metrics. R package version 1.5.2.
36. Anderson, M.J. (2001) A new method for non-parametric multivariate analysis of variance. Austral Ecology **26,** 32-46.
37. Hooper, D.U. et al. (2000) Interactions between aboveground and belowground biodiversity in terrestrial ecosystems: patterns, mechanisms, and feedbacks. BioScience **50,** 1049-1061
38. Waldrop, M.P. et al. (2006) Resource availability controls fungal diversity across a plant diversity gradient. Ecology Letters **9,** 1127–1135.
39. Jangid, K. et al. (2013). Progressive and retrogressive ecosystem development coincide with soil bacterial community change in a dune system under lowland temperate rainforest in New Zealand. Plant Soil **367,** 235–247.
40. Walker, T.W., Syers, J.K. The fate of phosphorus during pedogenesis. Geoderma **15,** 1–19 (1976).

41. Finzi, A.C. et al. (2011) Coupled biochemical cycles: Responses and feedbacks of coupled biogeochemical cycles to climate change: examples from terrestrial ecosystems. Front. Ecol. Environ. **9,** 61–67.
42. Robertson, G.P. & Groffman, P. (2007) Soil microbiology and biochemistry (Ecology Springer, New York).
43. Delgado-Baquerizo, M. et al. (2017) It is elemental: soil nutrient stoichiometry drives bacterial diversity. Environmental Microbiology **19,** 1176-1188.
44. Tripathi, B.M. et al. (2018) Soil pH mediates the balance between stochastic and deterministic assembly of bacteria. ISME J. **12,** 1072-1083.
45. Hobbie, S.E., P. Vitousek (2000) Nutrient limitation of decomposition in Hawaiian forests. Ecology **81,** 1765-2059.